Thoughts on Forces in Physics

2025

Jeroen van Engelshoven

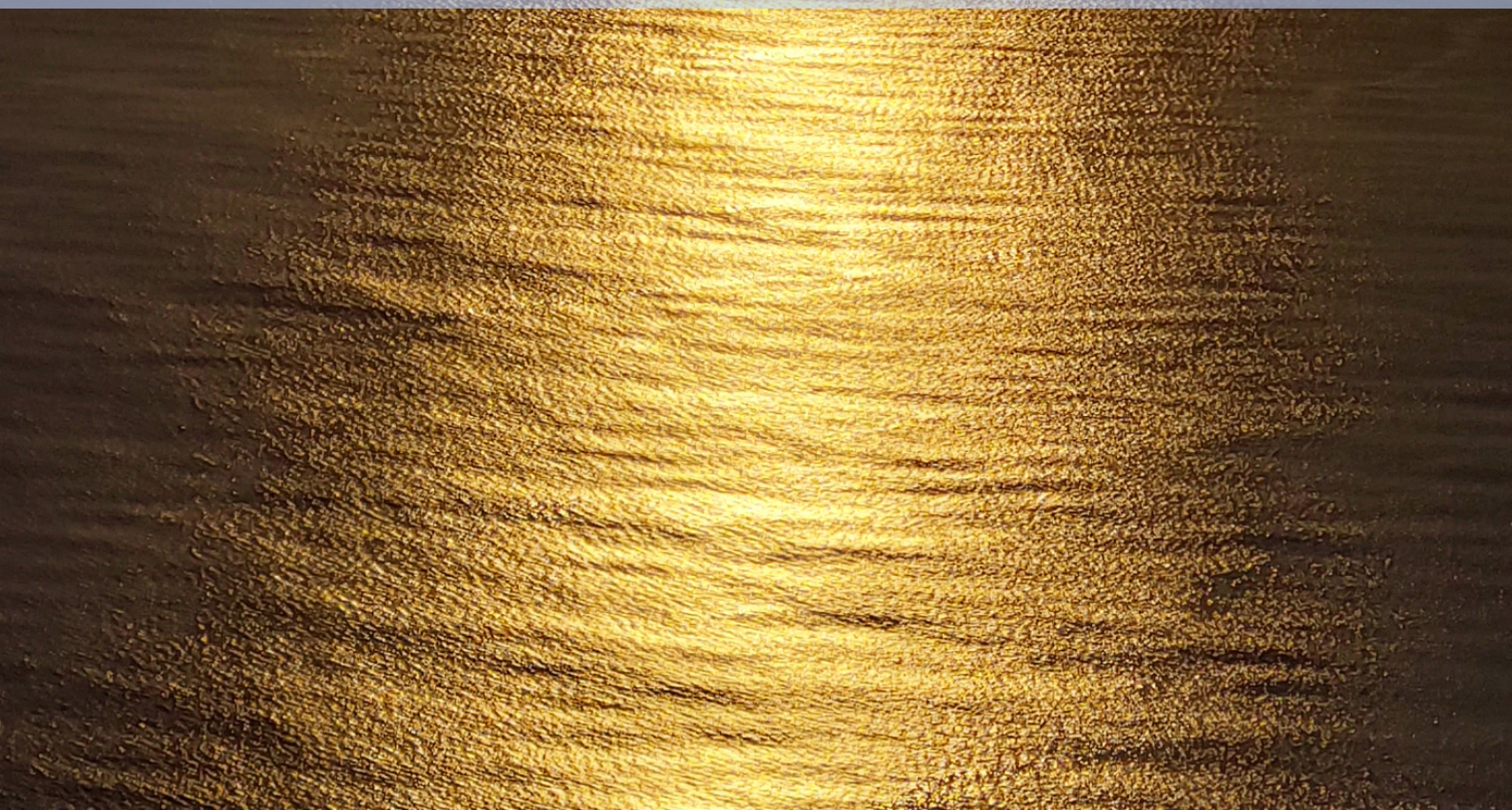

Editor: H.M.A. van Engelshoven-Reijnier

e-mail: f25@tophysics.com

Published on-line: www.tophysics.com

PUBLISHED BY AUTHOR

PAPERBACK PRINTED BY EXPRESTA - SLOVAKIA

PAPERBACK ISBN 978-989-33-7604-1 ON-LINE ISBN 978-989-33-7619-5

LATEX BOOK-TEMPLATE-WEBSITE.COM
Generated with LATEX with MiKTeX, using the Legrand-orange-book template, created by Mathias Legrand and Vel. Color optimization (RGB to CMYK) by PDF24 Creator

First edition (V1.1)
May 25, 2025

Contents

Figure 1: Nasa James Webb telescope [90],
deep field image of galaxy cluster SMACS 0723,
located about 4 billion lightyear from earth.

1. Prologue

"Did the Creator first take a course in tensor calculus,
before He invented the universe?"

This is one of the guiding thoughts behind this book: Are the fundamentals of the forces in physics (notably gravity) really as complicated as currently thought? Or can we simplify these, while still properly describing/predicting the known observables, such as gravitational light bending?

We will attempt to create a self-consistent theory linking gravity to the other fundamental forces, as we currently know them: strong & weak nuclear force and electro-magnetism. It will start from various fundamental observations, translating these to mathematical language and aims to find quantitative relations between the observables. In some cases full quantitative results will be obtained. In other cases only qualitative indications can be given. The reader is then encouraged to proceed with the, mathematical, evaluations and publish the results. These will then be referenced (and/or included) in future versions of this book.

We hope this document will inspire the reader to further studies on the topics that are touched upon in this book.

Madeira, May 25, 2025

"The task is not to see what has never been seen before, but to think what has never been thought before, about what you see everyday."

Erwin Schrödinger

2. Introduction

2.1 Some history

The earliest mention of a force 'at a distance' is attributed to the magnetic force, as early as 5th century BC, in both Greek and Chinese literature [67, page 281]. Newton created the concept of a gravitational (vector) field by the end of 17th century AD. Following a series of experiments (by Coulomb, Ampère and others), Maxwelll defined the laws of electro-magnetism by the late 19th century. Early 20th century, Einstein created the special relativity (including electro-magnetism) and General Relativity (gravity) [53]. During the 20th century, nuclear physics progressed with the advent of large particle accelerators, leading to the 'strong & weak' nuclear force concepts. For the description of the smallest (atomic [57] and nuclear [56, 74]) scale quantum mechanics was conceived. The weak and electro-dynamical forces have a unified description: electroweak interaction [93]. In 2017 it was found that gravitational waves travel with the speed of light [1].

A further force concept that has received attention is inertia. Its origins have been discussed by Mach , Einstein and others but are still poorly understood [13, 69].

We can therefore recognize following forces in nature (see table 2.1):

force	**range**	**macroscopic static force [r]**	**velocity**
strong nuclear	nuclear	/	??
weak nuclear	*nuclear*	/	*??*
electro-dynamic	infinite	$1/r^2$	speed of light
gravity	infinite	$1/r^2$	speed of light
inertia	??	/	? ∞ ?

Table 2.1: Some properties of fundamental forces

2.2 Action at a distance

The concepts of force have always attracted some controversy. Notably the 'action at a distance' idea was thought to be bewildering, starting with Newton [81]. A concept of touching was assumed to be necessary in order to transmit forces.

However, when evaluating 'touching' on a microscopic scale, modern electron-microscopes routinely reveal (see fig. 2.1 [6]) that 'touching' only means that the electron clouds of the 'touching' objects start interacting. The 'touching' action remains an 'action at a distance', albeit at nanometer scale.

Apparently, the 'action at a distance' concept for force interactions holds true at all length scales. From the nanometer range in atomic forces, to gravitational interaction taking place at light-year distance scales. Therefore, in this book we accept the 'action at a distance' as a starting point, and will express forces as vectors.

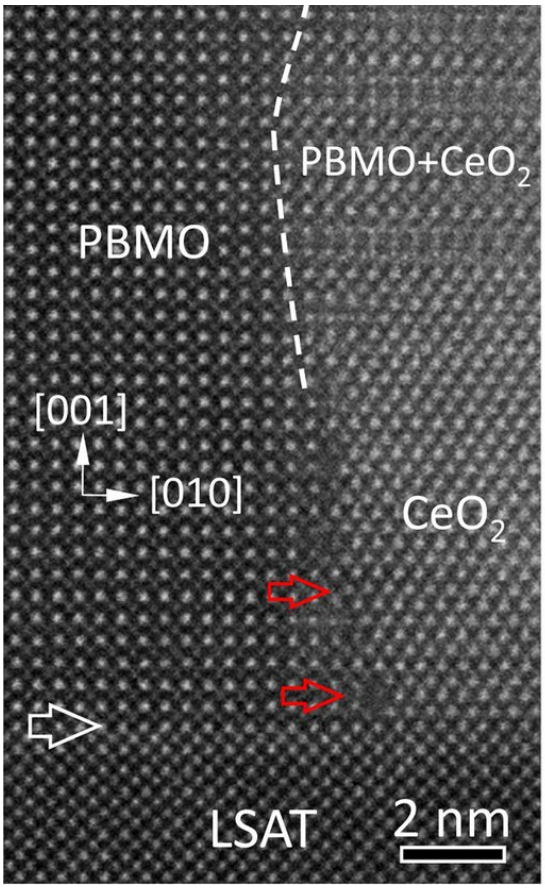

Figure 2.1: action at a distance: nanometers!

2.3 Build-up of book

We first touch upon known foundations of theoretical physics (electro-dynamics, standard model, quantum mechanics and model of universe). We state the most important elements of these theories, which impact our new concepts.

Then we proceed with the derivation of gravity as an electro-dynamically induced effect. Building on these new suggestions for gravity, we aim to compute various test results that are known from General Relativity (GR) [53, 65, 68, 69], such as gravitational bending of light and Shapiro time delay. To further test our suggestions, we study the atomic mass of various (low mass) isotopes.

Further we study inertia as a gravity induced effect, inspired by Sciama [37]. Then we proceed with orbit and gravitational wave analysis.

We end the book by touching upon some, as of yet not resolved, topics that need further attention. The reader is invited to study these questions. The author will also continue his pursuit for answers and publish (or even better: reference) these studies in future versions of this book.

3. Foundations

3.1 Introduction

This book is based on known physics, such as theories on electro-dynamical forces, quantum-mechanics and elementary particle physics. In this chapter we indicate the most important concepts and guide the reader to available literature.

3.2 Special Relativity

Special Relativity originated early 20th century [53, pages 35–65] with the publications of Einstein. By postulating the constancy of the velocity of light in vacuum, he changed our concepts of space and time, which lead to changes in velocity addition (see §3.7), Doppler effects and the concept that intrinsic energy (E_{int}) and mass of an object (m_{obj}) are interlinked, via the well known:

$$E_{int} = m_{obj}\, c^2 \tag{3.1}$$

with c representing the speed of light. This law was deduced [53, page 56] based on a 2-quanta thought experiment in which the 2 quanta are emitted in opposite directions from a static box (see fig. 3.1). When evaluating the energy content before and after the emission of the 2 quanta and demanding constancy of energy, Eq. (3.1) is found.

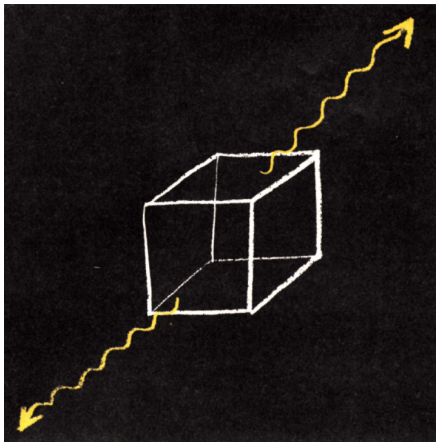

Figure 3.1: 2-Quanta thought experiment by Einstein [30].

The relativistic Doppler law gives the observed frequency (ν) or wavelength of light, emitted by a moving source (with velocity v_z, under an angle θ (see fig. 7.3) as [53, pages 67–71], [65, page 121], [69, page 109], [70, page 79] :

$$\nu_{obs} = \nu_{original}\, \frac{\sqrt{1-(v_z/c)^2}}{1+(v_z/c)\,Cos[\theta]} \tag{3.2}$$

Therefore, the observed frequency of light (and thus its energy, via $E = h\nu$, see §3.4.1) is directly influenced by the movement state of the light emitting source, as visualized in fig. 3.2.

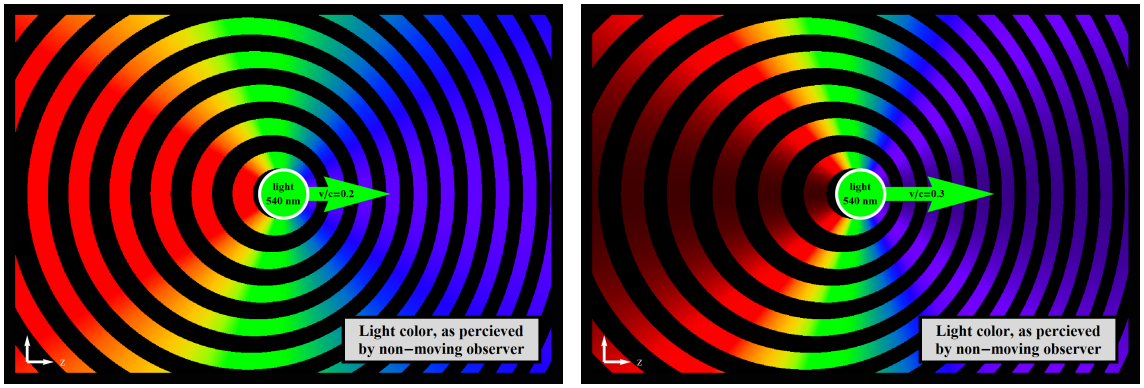

(a) Doppler for v/c=0.2 (b) Doppler for v/c=0.3

Figure 3.2: Doppler effect on light (color and wavelength) as function of location around a moving source, emitting monochromatic light of 540 nm. The light color turns (infra-)red when the source recedes from the observer at sufficient velocity.

3.3 Standard model

The study of nuclear phenomena has lead to the Standard Model [56, 74], which describes neutrons and protons to consist of 3 (point-size) moving quarks, carrying parts of elementary charge, as shown in fig. 3.3a. The 'up' quarks carry +2/3 of elementary charge, whereas 'down' quarks carry -1/3 of elementary charge.

3.4 Quantum mechanics

3.4.1 Quanta

The essence of quantum physics is the realization that energy is only transmitted in discrete amounts: quanta. Planck found that the electro-magnetic properties of light and quantum energy E are linked by frequency (ν) and the Planck constant $h \approx 6.63 \times 10^{-34}\, kg\, m^2\, /\, s$) as:

$$E = h\nu \tag{3.3}$$

Every quant of electro-magnetic radiation contains this amount of energy.

3.4.2 Quantum mechanics in atoms and nuclei

Quantum mechanical theory [57, pages 26, 130] prescribes that a contained particle has a finite (kinetic) energy in its ground state, as shown in fig. 3.3b. This key result will be explicitely used when identifying the key driving factors behind gravity, in chapter 4.

We need to determine 'ball-park' figures of the velocity of the quarks inside the neutron, and use classical mechanical elements. The energy of the ground state [57, pages 26, 130] of a quark moving inside a neutron ($E_{kin} = h^2/(8\, m_0\, r_n^2)$) can expressed in relation to the relativistic 'rest'-energy: $m_0\, c^2$ and the velocity of the involved particle.

$$E_{kin} = \frac{m_0\, c^2}{\sqrt{1-(v/c)^2}} - m_0\, c^2 = m_0\, c^2 \left(\frac{1}{\sqrt{1-(v/c)^2}} - 1 \right) \Rightarrow \tag{3.4}$$

$$v/c = \sqrt{1 - \frac{1}{\left(\frac{E_{kin}}{m_0\, c^2} + 1\right)^2}} = \sqrt{1 - \frac{1}{\left(\frac{h^2}{8\, m_0^2\, c^2\, r_n^2} + 1\right)^2}}$$

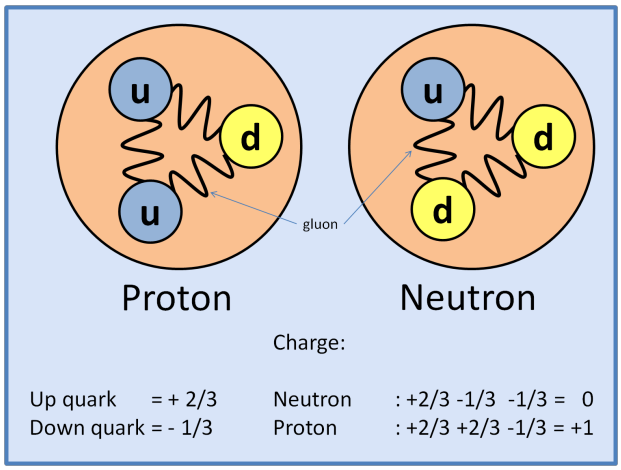

(a) Proton and neutron, quark composition.

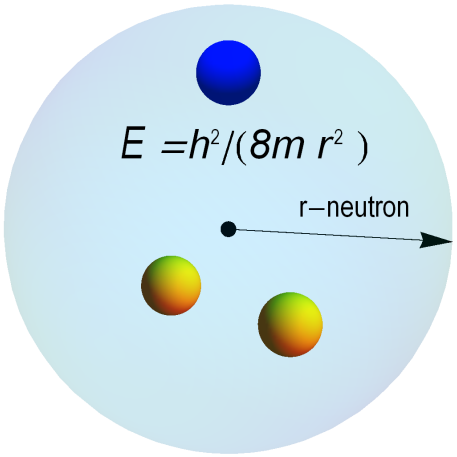

(b) Quantum ground state energy, as function of the dimension of the nucleus.

Figure 3.3: Moving quarks inside the nucleus.

Using following parameters [56, 57, 74] for the properties of quark and neutron (size: $r_n = 0.8 \times 10^{-15}\, m$; $m_n = 2.0\, MeV/c^2 = 2.0 \times 10^6 * 1.6 \times 10^{-19}/(3 \times 10^8)^2\, kg = 3.5 \times 10^{-30}\, kg$. From these values, we find:

$$\frac{E_{kin}}{m_0\, c^2} \approx 75.000 \qquad \Rightarrow \qquad v/c \approx 1 \tag{3.5}$$

In conclusion: the velocity of a quark inside a neutron is close to that of the speed of light.

As a side note: the dual-nature (particle-wave) of quantum mechanics, is partly shown in the figure at the heading of this chapter: water can act both as a wave [rocking a boat] or as individual droplets [making you wet]. It remains the same water. The difference (particle or wave) is determined by the interaction with the object.

3.5 Electro-dynamical force

The electro-dynamical force concept originated from investigations by Coulomb on static electrical forces. He found that a rotational symmetric charge creates a rotational symmetric force field, with the static force reducing with distance (r) as $1/r^2$, see fig. 3.4a. The Gauss flux law expresses mathematically that the number of mathematical Euclidean space dimensions is 1 higher than the (negative) power of physical force reduction with distance (in spherical symmetric forces). Therefore, it can be concluded (as done by I. Kant [17]) that we live in a physical universe that can be described mathematically by 2+1 =3 space dimensions !

It is also known that the static (=non-moving) electrical force does not change with time (t): $1/t^0$. Therefore, (same as for the variation with distance): the dimensionality of time is 0+1=1!

In short: **Static electrical force interactions spread evenly over (3D) space and (1D) time.**

As a thought experiment, we can change the locations of the charged particles, and re-execute the static force experiment. We will then find a change in strength and (vector) direction of the static electric force. This change means that the electric field can change with time. It propagates: has a velocity!

This time variation was studied by Maxwell, who included magnetic fields as well.

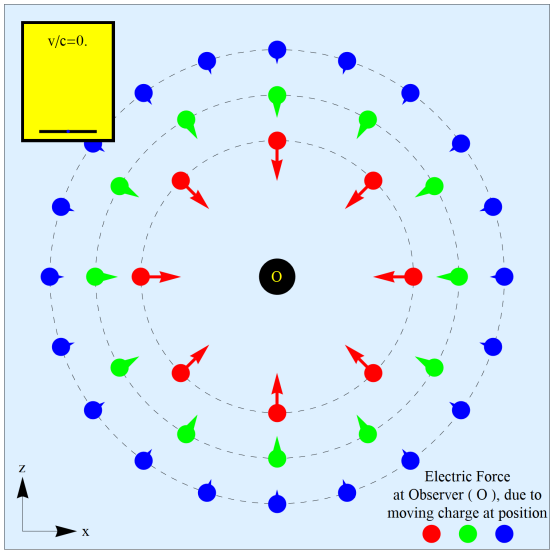

(a) Electric force field plot of a static charge (v/c=0), as experienced by the observer in the center.

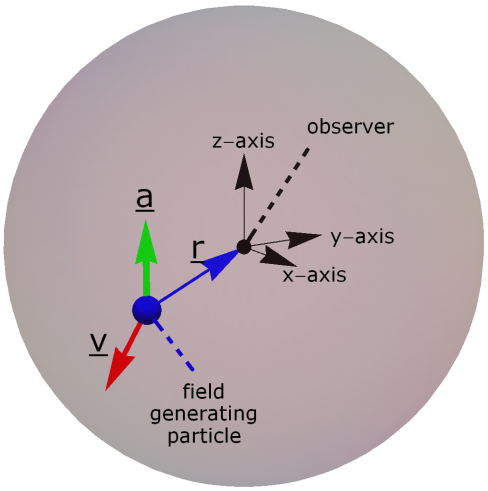

(b) Co-ordinate definitions. Observer is in the center.

Figure 3.4: Static electric field and co-ordinate definition of Eq. (3.6).

$\vec{F}$	Electro-dynamical interaction force between particle and observer (= 3D vector)
$\vec{E}$ $\vec{B}$	field vectors to arrive at the interaction force vector
$\vec{r}$	position of field generating particle $\overrightarrow{r_{part}}$ compared to observer $\overrightarrow{r_{obs}}$, in direction particle to observer: $\vec{r} = \overrightarrow{r_{obs}} - \overrightarrow{r_{part}}$. We use $\overrightarrow{r_{obs}} = \vec{0}$: observer in center.
$\vec{v}$ $\vec{a}$	velocity $\vec{v} = d\overrightarrow{r_{part}}/dt$ and acceleration $\vec{a} = d\vec{v}/dt$ vectors of particle relative to the observer
r v	vector norm of $\vec{r}$ and $\vec{v}$
c	velocity of electro-magnetic fields in vacuum = speed of light (≈299 792 km/s)
s	r - ($\vec{r}$ • $\vec{v}$) / c
ϵ_0	vacuum permittivity ≈ $8.854 \times 10^{-12} F/m$
q_{obs}	charge of the observer, located at the origin $(x, y, z) = (0, 0, 0)$
q_{part}	charge of the field generating particle
• *	represent the vector dot product and vector cross product

Table 3.1: Explanation of terms in Eq. (3.6).

This resulted in the Maxwell equations, describing the interaction between electric and magnetic fields as function of charge and current densities, which propagate with the speed of light. These fields can also be described (in SI units, see appendix G) for point charges by means of the Liénard-Wiechert (LW) fields [58, pages 459–460], [64, pages 173–176], [69, pages 142–148]:

$$\vec{F} = q_{obs}\,(\vec{E} + \vec{v} * \vec{B}) \tag{3.6}$$

$$\vec{E} = \frac{q_{part}}{4\pi\epsilon_0\, s^3}\,(\,(1-(v/c)^2)\,(\vec{r} - r\,\vec{v}/c)\; + \vec{r} * ((\vec{r} - r\,\vec{v}/c) * \vec{a})\,/c^2\,)$$

$$\vec{B} = \vec{r} * \vec{E}/(r\,c)$$

For details of the orientation of the coordinates in Eq. (3.6), see fig. 3.4b. The formula abbreviations are given in table 3.1, where the position is to be taken as the observer identifies it: the 'retarded' position. The static Coulomb law re-appears, when $\vec{v} = \vec{0}$ and $\vec{a} = \vec{0}$. For $\vec{r} = (x, y, z) = (0, 0, r)$ the resulting electrostatic force: $\vec{F} = \frac{q_{obs}\, q_{part}}{4\pi\epsilon_0\, r^2}\,(0, 0, -1)$ is repulsive for equally signed charges q_{obs} and q_{part}.

Einstein studied the propagation of an electric field, under the assumption of constant speed of electrical phenomena [53, pages 35–65], and proved the Maxwell equations to hold true. As, such, it has been pointed out by various authors that the magnetic field arises from the static electric field, when motion is added (in combination with the finite speed of light). The magnetic field is an extremely important concept for engineering, with examples such as a compass, electro-motors, Magnetic Resonance Imaging (MRI) and electron microscopes. However, as can be seen from Eq. (3.6), the magnetic force field of one moving point charge can be expressed as a direct function proportional to the electric field, via $\overrightarrow{F_{magnetic}} = q_{obs}\,\vec{v} * (\vec{r} * \vec{E})\,/(r\,c)$. Therefore [80, page 42]:

For fundamental physics,
the magnetic field is a superfluous concept!

We can reformulate the Liénard-Wiechert force from Eq. (3.6) to:

$$\frac{\vec{F}}{q_{obs}} = \vec{E} + \frac{\vec{v}}{c} * (\frac{\vec{r}}{r} * \vec{E}) \tag{3.7}$$

We immediately recognize the velocity (v/c) term, indicating that the 'magnetic' force of a moving charge is smaller than the electric field and disappears for the static $(\vec{v} = \vec{0})$ case.

3.5.1 Fields from a charge moving with constant velocity

Here we study the fields that arise from a moving charge with constant velocity, in the positive z-direction. The charge is located at position $\vec{x} = (r\,Cos[\phi]\,Sin[\theta],\ r\,Sin[\phi]\,Sin[\theta],\ r\,Cos[\theta])$ (see fig. C.1a), with velocity $\vec{v} = (0, 0, v_z)$, with $0 \leq v_z < c$. This gives for the E-field:

$$\vec{E} = \frac{q}{4\pi\epsilon_0 r^2}\,\frac{1-(v_z/c)^2}{(1+(v_z/c)\,Cos[\theta])^3}\,(Cos[\phi]\,Sin[\theta],\ Sin[\phi]\,Sin[\theta],\ (v_z/c)+Cos[\theta]) \tag{3.8}$$

As this problem statement is symmetric in the (x,y) plane we evaluate Eq. (3.6), for y=0 (or $\phi = 0$). A visualization of the electric field as given by Eq. (3.8), with $\phi = 0$, for various values of v_z, can be found in fig. 3.4a, 3.5a and 3.5b.

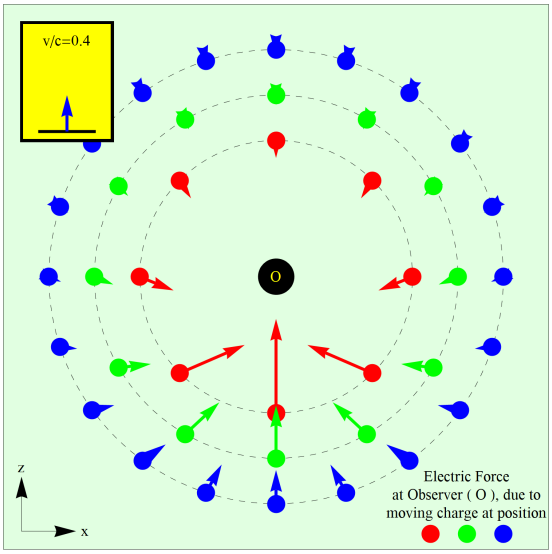

(a) Electric force field plot of a uniformly moving charge (v/c=0.4)

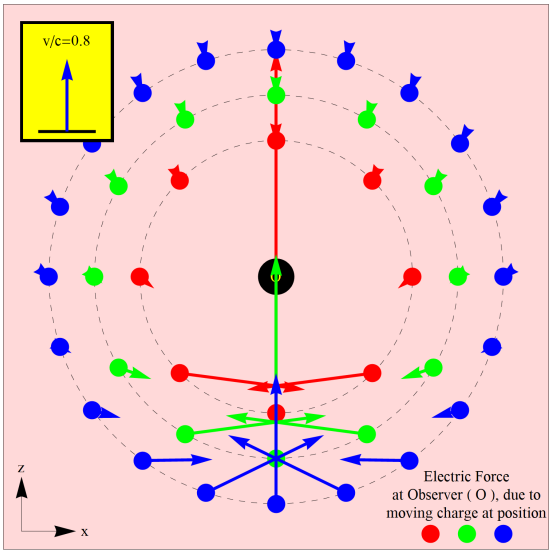

(b) Electric force field plot of a uniformly moving charge (v/c=0.8)

Figure 3.5: Electric field of a uniformly moving charge for various velocities

The direction of the (opposite of) the E-field points into the direction of the non-retarded position of the moving charge [64, 69] , as this 'instantaneous position' is given by:
$\overrightarrow{x_{inst}} = \vec{x} + (0,0,v_z)\,(r/c) = r\,(\,Cos[\phi]\,Sin[\theta]\,,\ Sin[\phi]\,Sin[\theta]\,,\ (v_z/c) + Cos[\theta]\,)$, which has a vector direction which is identical to the (opposite of) the E-field, as given by Eq. (3.8). For low velocities ($v/c \ll 1$), the magnetic term drops from the force equation Eq. (3.7). We find that the total electro-dynamical force of a constant moving charge points to the same direction as the electric field, and thus towards the 'instantaneous' position of the moving charge.

For high values of v/c we find a concentration of the electric field in the direction from where the uniformly moving charge is coming.

3.5.2 Electric field flux

The flux of any vector field is given as the surface integral of the dot-product of the vector field with the normal on the surface of the integral, as stated in Eq. (3.9),

$$\text{flux} = \oiint \overrightarrow{field[\vec{r}]} \bullet \left(\frac{\vec{r}}{r}\right) dA \tag{3.9}$$

where the dot product of the field vector and the normalized position is integrated over a closed surface. For the static electric field, this is known [64, 69] to be the total enclosed charge (as per Gauss law and described by the static Maxwell equation $\nabla \bullet \vec{E} = \rho/\epsilon_0$). We now evaluate the integrand of Eq. (3.9), for the case of an arbitrarily moving charge with velocity $\vec{v} = (0, 0, v_z)$ and acceleration $\vec{a}$, based on Eq. (3.6) and integrate over a sphere (radius r) around the moving charge.

We notice that the Electric field $\vec{E}$, as given by Eq. (3.6), consists of two parts: a velocity and position dependent part and an acceleration part. We first study the impact of the electric flux for the acceleration term. For this we make use of well known vector identities as found in appendix G, like: $(\vec{a} \bullet \vec{b}) = (\vec{b} \bullet \vec{a})$, $\vec{a} \bullet (\vec{b} * \vec{c}) = \vec{c} \bullet (\vec{a} * \vec{b}) = \vec{b} \bullet (\vec{c} * \vec{a})$ and $\vec{a} * \vec{a} = \vec{0}$. When calculating the flux contribution of the acceleration term (flux_a) in Eq. (3.6), we find:

$$\text{flux}_a = \left(\vec{r} * ((\vec{r} - r\,\vec{v}/c) * \vec{a})/c^2\right) \bullet (\frac{\vec{r}}{r}) = \frac{1}{r\,c^2}\left((\vec{r} - r\,\vec{v}/c) * \vec{a}\right) \bullet (\vec{r} * \vec{r}) = 0 \tag{3.10}$$

Therefore, we conclude that the acceleration term in Eq. (3.6) does not contribute to the electric field flux. We can therefore concentrate on the velocity term, for a moving charged particle, as expressed by Eq. (3.8). This yields for the electric flux (E_{flux}), with $dA = r^2\,Sin[\theta]\,d\phi d\theta$:

$$\begin{aligned} E_{flux} &= \oiint \vec{E} \bullet \left(\frac{\vec{r}}{r}\right) dA = \int_0^{\pi}\int_0^{2\pi} r^2\,Sin[\theta]\,(\vec{E} \bullet \frac{\vec{r}}{r})\,d\phi d\theta \\ &= \frac{q_{part}}{4\pi\epsilon_0}\int_0^{\pi}\int_0^{2\pi} \frac{(1-(v_z/c)^2)\,Sin[\theta]}{(1+(v_z/c)\,Cos[\theta])^2}\,d\phi d\theta = \frac{q_{part}}{\epsilon_0} \end{aligned} \tag{3.11}$$

by virtue of [85] :

$$\int_0^{\pi}\int_0^{2\pi} \frac{(1-(v_z/c)^2)\,Sin[\theta]}{(1+(v_z/c)\,Cos[\theta])^2}\,d\phi d\theta = 4\pi \tag{3.12}$$

Therefore the Gauss theorem of preserved electric flux is proven valid also for moving charges (as was to be expected from Maxwell's equations).

3.5.3 Magnetic field flux

The flux of the magnetic field is expected to be zero, given the Maxwell equation $\nabla \bullet \vec{B} = 0$. This can also be directly deduced from the Liénard-Wiechert formula Eq. (3.6), where we find the magnetic field to be: $\vec{B} = \vec{r} * \vec{E}/(r\,c)$. The magnetic field flux is the dot-product of the position $\vec{r}$ and the magnetic field vector $\vec{B}$. Using the general vector identities of appendix G again, we find that the magnetic flux (M_{flux}) is given by:

$$M_{flux} = \oiint \vec{B} \bullet \left(\frac{\vec{r}}{r}\right) dA = \oiint \frac{\vec{r} * \vec{E}}{r\,c} \bullet \left(\frac{\vec{r}}{r}\right) dA = \frac{1}{r^2\,c} \oiint \vec{E} \bullet (\vec{r} * \vec{r})\, dA = 0 \tag{3.13}$$

Therefore, for any magnetic field, we find the magnetic flux for a closed surface to be zero.

3.5.4 Electro-dynamical force flux

Now we study the electro-dynamical force flux of a uniformly moving charge, where the total force is given as Eq. (3.6): $\vec{F} = (q_{obs}/4\pi\epsilon_0)(\vec{E} + \vec{v} * (\vec{r} * \vec{E})/(r\,c))$. The 'magnetic' force component $\vec{v} * (\vec{r} * \vec{E})/(r\,c)$ contains the cross product with velocity, and therefore the arguments that helped to null the magnetic field flux do not apply. In fig. 3.6a, the 'magnetic' force is visualized, with the force perpendicular to the movement in z-direction.

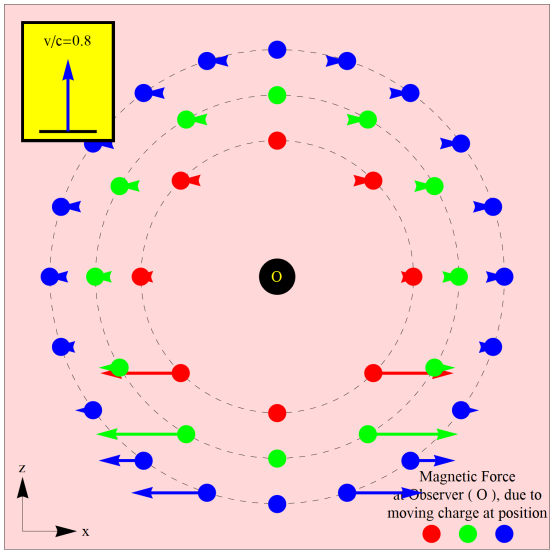

(a) Magnetic force field plot of a uniformly moving charge (v/c=0.8).

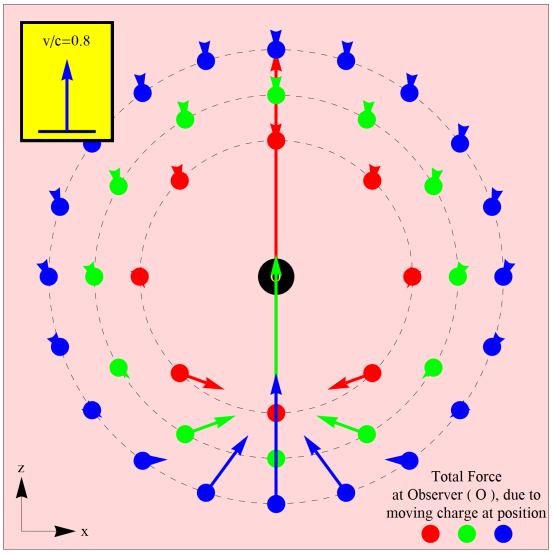

(b) Total force field plot of a uniformly moving charge (v/c=0.8), which is the summation of the forces as shown in fig. 3.5b and 3.6a.

Figure 3.6: Magnetic and total force field of uniformly moving charge, for v/c=0.8.

The total force, which is the summation of the electrical part and the 'magnetic' part of the force, is shown in fig. 3.6b. Therefore we have to perform the total computation for the force flux (F_{flux}) of a charge, moving uniformly in the z-direction, leading to [85]:

$$F_{flux} = \oiint \vec{F} \bullet \left(\frac{\vec{r}}{r}\right) dA = q_{obs} \oiint \left(\frac{\vec{r}}{r}\right) \bullet (\vec{E} + \vec{v} * (\vec{r} * \vec{E})/(r\,c)\,)\, dA \tag{3.14}$$

$$= q_{obs} \int_0^{\pi} \int_0^{2\pi} r^2\, Sin[\theta] \left(\frac{\vec{r}}{r}\right) \bullet \left(\vec{E} + \vec{v} * (\vec{r} * \vec{E})/(r\,c)\,\right) d\phi d\theta$$

$$= \frac{q_{part}\, q_{obs}\, (1 - (v_z/c)^2)}{4\pi\epsilon_0} \ldots$$

$$\ldots \int_0^{\pi} \int_0^{2\pi} \frac{(2 - (v_z/c)^2 + 2\,(v_z/c)\, Cos[\theta] + (v_z/c)^2\, Cos[2\theta])}{2\,(1 + (v_z/c)\, Cos[\theta])^3}\, Sin[\theta]\, d\phi d\theta$$

$$= \frac{q_{part}\, q_{obs}}{\epsilon_0} \frac{(1 - (v_z/c)^2)\, ArcTanh[\,v_z/c\,]}{(v_z/c)}$$

The function $F_{flux}[\,v_z/c\,] = (1 - (v_z/c)^2)\, ArcTan[\,v_z/c\,]/(v_z/c)$ is shown in fig. 3.7, which shows that the total electro-dynamical force flux reduces strongly towards zero as the charged particle moves at velocities close to the speed of light[1].

It must be realized that the only 'physics' property of the moving charge is how it interacts with its surrounding, which is only the total force, and not the electric or magnetic fields alone. Therefore the conservation of the total electrical flux and the absence of a magnetic flux are mathematical constructs only. The true relevant factor is only the total force. The total force flux is NOT a constant property as function of the velocity of the moving charge!

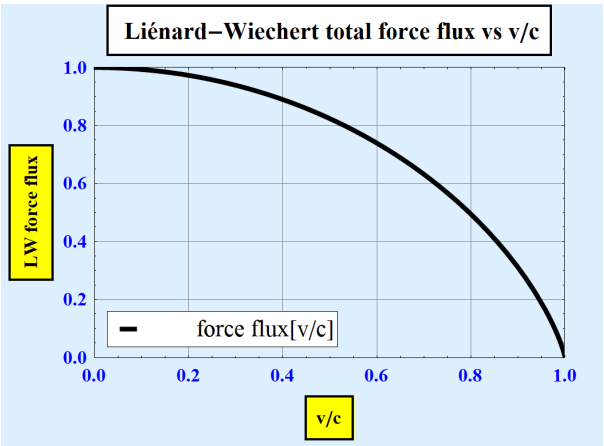

Figure 3.7: Electro-dynamic force flux of a uniformly moving charge, as function of v/c relative to static charge.

3.5.5 Energy of LW field

We have seen that the LW force is given by $\vec{F_{LW}} = q(\vec{E} + \vec{v} * \vec{B})$. Energy is defined as: $W = \int_{\vec{s_0}}^{\vec{s_{max}}} \vec{F} \bullet d\vec{s}$, which can be calculated via velocity (and time) via: $W = \int_{t_0}^{t_{max}} \vec{F} \bullet \vec{v}\, dt$. Inserting the general force low, and realizing the vector dot-product rule $(\vec{a} * \vec{b}) \bullet \vec{a} = 0$, gives: $W = \int_{t_0}^{t_{max}} q(\vec{E} + \vec{v} * \vec{B}) \bullet \vec{v}\, dt = \int_{t_0}^{t_{max}} q\vec{E} \bullet \vec{v}\, dt$. In short: the magnetic field component does not play a role in energy considerations.

Therefore, in fields of physics where only energy (delta's) are involved, like quantum physics, the analysis of electric fields (or potentials) suffices.

[1] In all relativistic formulas, we find the impact of velocity to scale with the speed of light. A lot of visual formula simplification can be obtained by scaling the velocity v_z to the speed of light directly. To clearly keep dimensions of formulas intact, we have chosen not to do this here.

3.5.6 Radiated electro-dynamical energy: Poynting vector

The radiated energy per time per opening angle can be calculated by means of the Poynting vector ($\overrightarrow{P_{LW}}$) [64, 69, 70], which is defined as (using the vacuum magnetic permeability μ_0) :

$$\overrightarrow{P_{LW}} = \frac{1}{\mu_0}\,\vec{E} * \vec{B} = \epsilon_0\, c^2\, \vec{E} * \vec{B} = \epsilon_0\, c^2\, \vec{E} * (\vec{r} * \vec{E})\,/\,(r\,c) = \epsilon_0\, c\,(\vec{E} * (\frac{\vec{r}}{r} * \vec{E})\,) \tag{3.15}$$

where we used $c^2 = 1\,/\,(\mu_0\,\epsilon_0)$ and the LW fields, as given in Eq. (3.6). For the non-relativistic case ($v\,/\,c \ll 1$), we find for the radiated power per time unit per opening angle, for an electrical particle (with charge q) accelerated in the z-direction ($\vec{a} = (0, 0, a_z)$):

$$\overrightarrow{P_{LW}} = \frac{a_z^2\, q^2}{16\,\pi^2\,\epsilon_0\, c^3\, r^2}\, Sin^2[\theta]\, \left(\frac{\vec{r}}{r}\right) \tag{3.16}$$

When integrating over the total surface with arbitrary radius, we find the Larmor emitted power formula [58, 69] for an accelerated charge:

$$\text{Energy} = \oiint \overrightarrow{P_{LW}} \bullet \left(\frac{\vec{r}}{r}\right) dA \tag{3.17}$$

$$= \epsilon_0\, c \int_0^{\pi} \int_0^{2\pi} \left(\vec{E} * (\frac{\vec{r}}{r} * \vec{E})\right) \bullet \left(\frac{\vec{r}}{r}\right) r^2\, Sin[\theta]\, d\phi\, d\theta = \frac{a_z^2\, q^2}{6\,\pi\,\epsilon_0\, c^3}$$

From Eq. (3.6), we find that the electric field ($\vec{E}$) consist of two parts, that are proportional to $1/r^2$ and $1/r$. These two parts contain terms that are functions of position and velocity ($1/r^2$ -term) and additionally acceleration ($1/r$). We use these terms in the (dot- and cross-product) multiplications for the total energy flux integration of Eq. (3.17). Then we find that only the terms containing the double multiplication of the acceleration term produce a non-vanishing result. The other terms of the Poyting vector integration end with terms of $1/r$ or $1/r^2$. These terms give a zero contribution to the total energy flux, at large distances from the radiation source. Therefore [69, page 146], [64, page 176], only the part of the electric field $\vec{E}$ containing acceleration contributes to the total radiated power, as observed from a large distance from the radiating source.

3.6 General Relativity

Gravity is properly described (not **explained**) by General Relativity [53, pages 109–164]. It is known since 1918 [23, 40], [48, pages 91–109], [65, pages 490–492], [70, §15.5], [4, 36] that the general relativity can be linearized to equations (like the Maxwell equations) under conditions of:

1. **low field strength** : distances that are much larger than the Schwarzschild radius $r_s = 2\,G\,M\,/\,c^2$, with G being the gravitational constant [$G \approx 6.67 \times 10^{-11}\, m^3\, kg^{-1}\, s^{-2}$] and M representing the central mass
2. **low velocities** : much smaller than the speed of light.

Under these conditions, the gravitational field can therefore be expressed directly via the Liénard-Wiechert field equations, as given by Eq. (3.6), with appropriate reversal for vector force direction, substitution of charge by gravitational mass and $1/4\pi\,\epsilon_0$ by the gravitational constant G.

3.7 Relativistic velocity addition

For use in chapters 4.1 and 7.4.3, we now review relativistic velocity addition. Both 1D and full 3D addition will be studied, focusing on oscillatory movements, that are to be added.

3.7.1 Relativistic 1D velocity addition

The 1D (one dimensional) velocity addition is known since the start of Special Relativity [53] and given as:

$$v_{13}/c = \frac{(v_{12}+v_{23})/c}{1+v_{12}\,v_{23}/c^2} \tag{3.18}$$

where v_{12} is the velocity of particle 2 as observed by particle 1 and v_{23} is the velocity of particle 3 as observed by particle 2. The relativistic addition leads to velocity v_{13}, which is the velocity of particle 3 as observed by particle 1, which we also label as $v_{rel-1D}[\delta v_1, \delta v_2]$.
From fig. 3.8 we notice the non-relativistic limit for $v_{12}/c \ll 1$ & $v_{23}/c \ll 1$. When one of the velocities (v_{12} or v_{23}) is close to the speed of light any positive velocity addition hardly increases the total relativistic velocity.

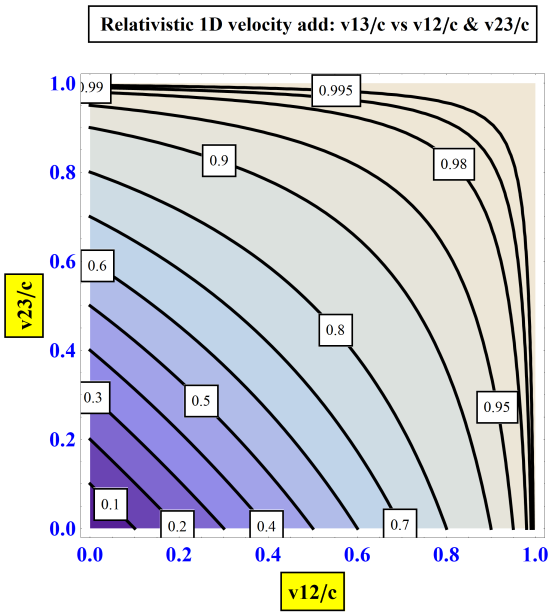

Figure 3.8: 1D velocity addition.

3.7.2 Relativistic 3D velocity addition

The 3D (three dimensional) velocity addition was developed later in Special Relativity studies and is described as [73, 45]:

$$\vec{v_{13}} = \overrightarrow{v_{rel-3D}}[\vec{v_{12}}, \vec{v_{23}}] = \vec{v_{12}} \oplus \vec{v_{23}} = \tag{3.19}$$
$$\frac{1}{1+(\vec{v_{12}}.\vec{v_{23}})/c^2}\left(\vec{v_{12}}+\vec{v_{23}}+\frac{\gamma_{12}}{1+\gamma_{12}}\left(\frac{1}{c^2}\right)(\vec{v_{12}}*(\vec{v_{12}}*\vec{v_{23}}))\right)$$

with $\gamma_{12} = \gamma[v_{12}/c] = 1/\sqrt{1-(v_{12}/c)^2}$. We now study the relativistic 3D velocity addition of oscillatory behavior of 2 particles, with spherical symmetrical distribution with radial velocity δv. Therefore we use: $\vec{v_{12}} = \delta v_1\,(Cos[\phi_1]\,Sin[\theta_1], Sin[\phi_1]\,Sin[\theta_1], Cos[\theta_1])$ and similarly for $\vec{v_{23}}$. When using fixed values for δv_1 & δv_2 and randomly selecting the spherical angles (ϕ and θ), we calculate the resulting $\overrightarrow{v_{rel-3D}}$, to find a spherical symmetrical velocity distribution, as shown in fig. 3.9. The maximum resulting radial velocity is then given by Eq. (3.18) $v_{rel-1D}[\delta v_1, \delta v_2]$. For high values of resulting relativistic velocities, we find (from the histograms) that the radial component in the velocity distribution ($Đ[v, \delta v_1, \delta v_2]$) can be approximated by:

$$Đ[v, \delta v_1, \delta v_2] = e^{\left(\frac{v - v_{rel-1D}[\delta v_1, \delta v_2]}{c - v_{rel-1D}[\delta v_1, \delta v_2]}\right)} \qquad \text{for } |\delta v_1 - \delta v_2| < v < v_{rel-1D}[\delta v_1, \delta v_2] \tag{3.20}$$

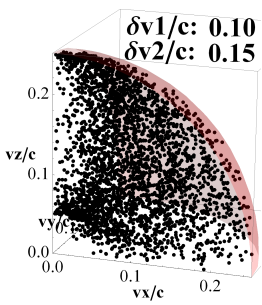

(a) 3D velocity addition for $\delta v_1/c = 0.10$ & $\delta v_2/c = 0.15$.

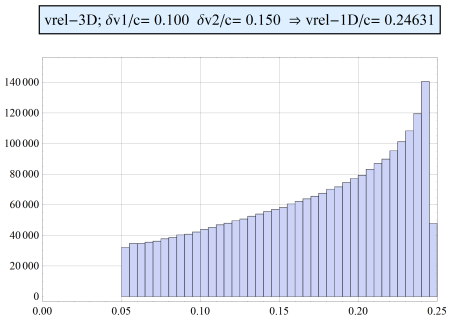

(b) Histogram for 3D velocity addition for $\delta v_1/c = 0.10$ & $\delta v_2/c = 0.15$.

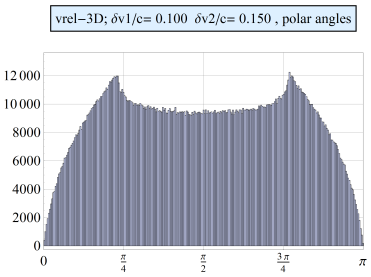

(c) Polar angle distribution for 3D velocity addition for $\delta v_1/c = 0.10$ & $\delta v_2/c = 0.15$.

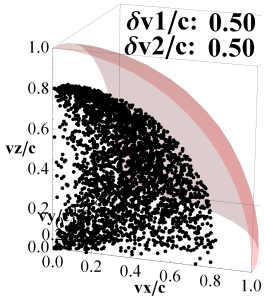

(d) 3D velocity addition for $\delta v_1/c = 0.50$ & $\delta v_2/c = 0.50$.

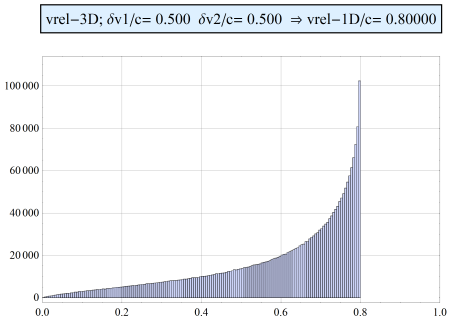

(e) Histogram for 3D velocity addition for $\delta v_1/c = 0.50$ & $\delta v_2/c = 0.50$.

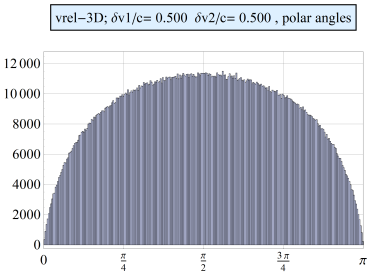

(f) Polar angle distribution for 3D velocity addition for $\delta v_1/c = 0.50$ & $\delta v_2/c = 0.50$.

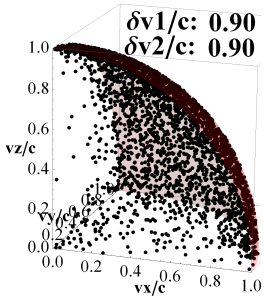

(g) 3D velocity addition for $\delta v_1/c = 0.90$ & $\delta v_2/c = 0.90$.

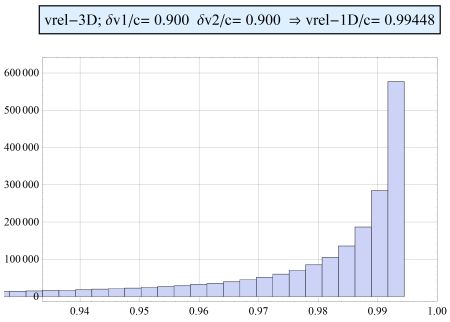

(h) Histogram for 3D velocity addition for $\delta v_1/c = 0.90$ & $\delta v_2/c = 0.90$.

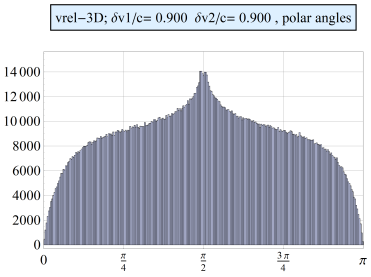

(i) Polar angle distribution for 3D velocity addition for $\delta v_1/c = 0.90$ & $\delta v_2/c = 0.90$.

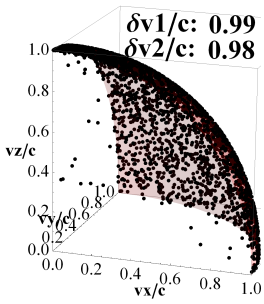

(j) 3D velocity addition for $\delta v_1/c = 0.99$ & $\delta v_2/c = 0.98$.

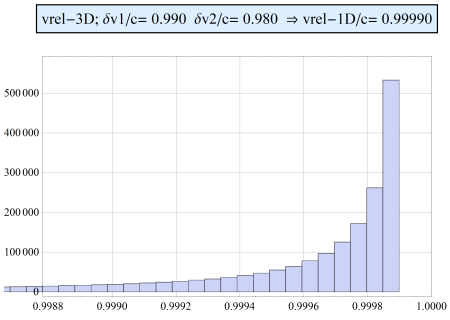

(k) Histogram for 3D velocity addition for $\delta v_1/c = 0.99$ & $\delta v_2/c = 0.98$.

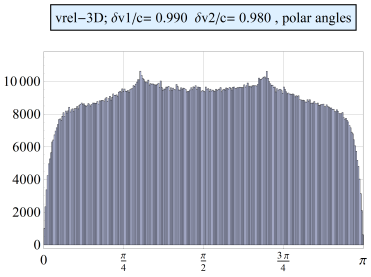

(l) Polar angle distribution for 3D velocity addition for $\delta v_1/c = 0.99$ & $\delta v_2/c = 0.98$.

Figure 3.9: 3D Velocity addition. The left graphs only give 1 % of the total relativistic 3D velocity distribution, starting from n = 2 500 000 random start conditions for $\vec{v}_1$ and $\vec{v}_2$. The orange sphere has radius $\delta v_1/c + \delta v_2/c$ or 1.

3.8 Model of universe

During the 20th century our model of the universe has changed. During the first 25 years, the concept of the universe was limited to the Milky Way, with discussions whether Andromeda was a part of it [68, page 758], [91]. This view changed when Hubble [69, 70] discovered the relation of red-shift and distance, leading to the expanding universe model.
This expansion is a contributor to the darkness of the night-sky, popularized as 'Olber's paradox' [12, 72], [68, page 756], see appendix B.

Figure 3.10: Andromeda galaxy, (image by NASA).

Satelite supported observations, as made by WMAP [89, 39], Planck [77], Hubble [88], James Webb [90] and others, showed the vastness of the universe. They proved that the universe, at large, has a uniform galaxy distribution [31] and no intrinsic space curvature [77, 89, 39].

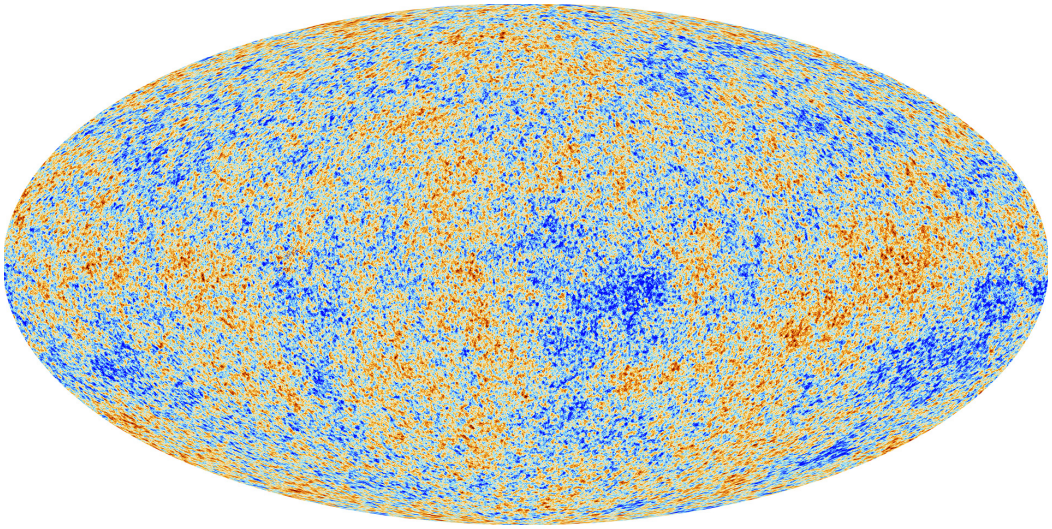

Figure 3.11: ©ESA: Planck image of the temperature fluctuations of the early universe [77].

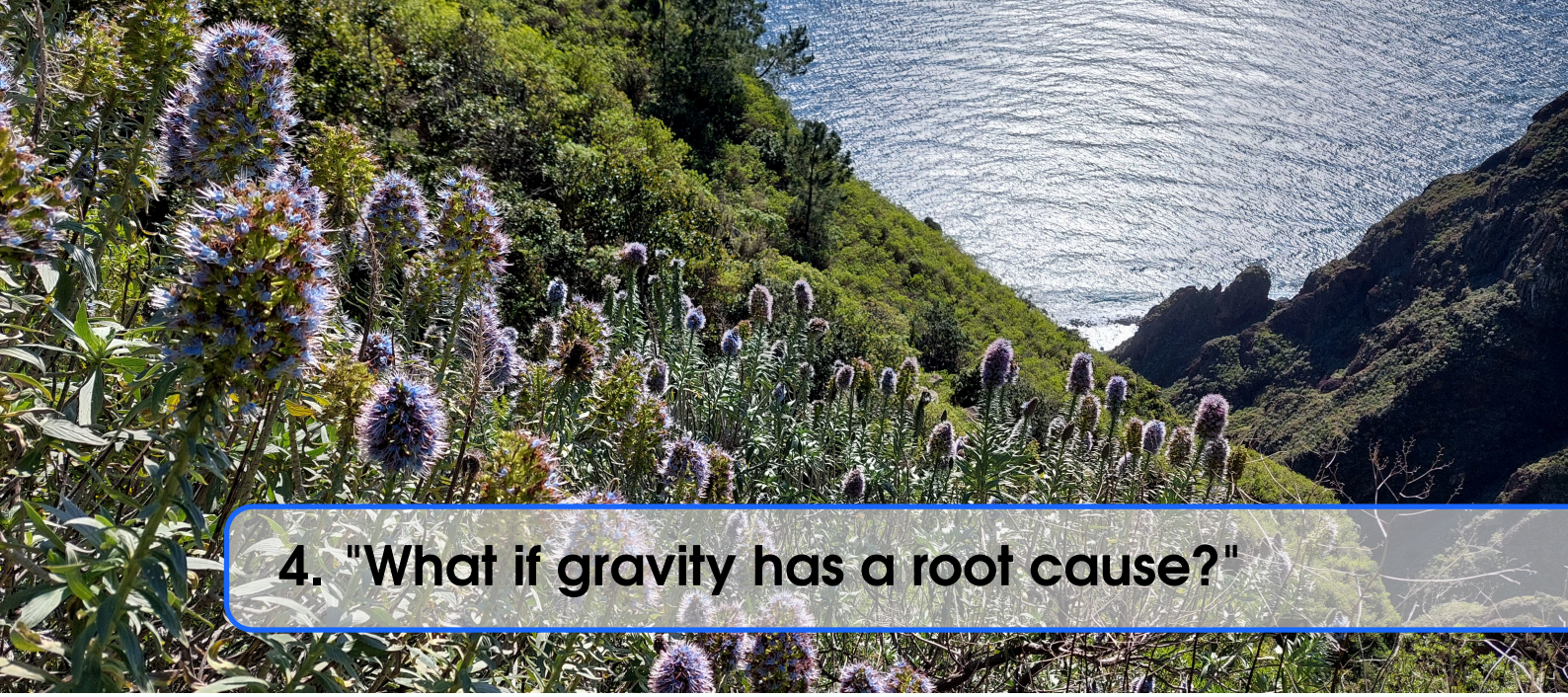

4. "What if gravity has a root cause?"

4.1 Introduction

The source of gravity, as well as its expansion mechanism, have been subject to controversy since the concepts of gravity were formulated [59, 21, 46]: *"Is gravity an intrinsic or an induced property?"* The 'action at a distance' concept was perceived as strange, as all interactions between macroscopic objects require physical contact. However, even physical contact, when evaluated at atomic scale, only involves electro-dynamical effects 'at a distance' from the electron clouds orbiting the nuclei, as seen in §2.2. General Relativity [53, 65, 68, 69] is considered to describe best the gravitational interactions. It must be noted that although General Relativity properly *describes* gravity, it does not *explain* it.

The main interactions in nature are best described, via the Standard model [56, 74], via 4 fundamental forces (see table 4.1)[1]. Recently, it was verified by astronomical observations, that the speed of gravity equals the speed of light [1]. Therefore, if the long-range force of gravity is to be *explained*, it must be deduce-able from the strong (and weak) nuclear force in combination with the electro-dynamical force.

force	**range**	**macroscopic static force [r]**	**velocity**
strong nuclear	nuclear	/	??
weak nuclear	*nuclear*	/	*??*
electro-dynamic	infinite	$1/r^2$	speed of light
gravity	infinite	$1/r^2$	speed of light

Table 4.1: Some properties of fundamental forces

If gravity is deduce-able from other forces, the range and velocity of those forces must be equal to those of gravitaty. Therefore, the experimentally proven equality of range and speed for gravity and electro-dynamical forces triggers the thought process to attempt to explain gravity as an electro-dynamically induced effect. We aim to determine the electro-dynamical force of two macroscopically separated static neutrons and need to prove that this force is attractive and drops with distance as $1/r^2$. Further, we need to prove that this electro-dynamically induced gravity bends light near large masses, and creates (Shapiro) time delay.

[1] The weak and electro-dynamical forces have a unified description: electro-weak interaction [93]

In §3.3 [56, 74] we found that a neutron consists of various charged sub-particles (quarks). These quarks are assumed to be moving in their quantum mechanical ground state [57]. We will study the induced electro-dynamical forces of *moving* charged quarks inside the neutrons. Then, we repeat this analysis for a proton-proton pair and a proton-neutron pair. A simplified, non-quantum mechanical, approach is used to maintain focus on the underlying physics.

4.2 Electro-dynamical forces and quark movements

Electro-dynamical force interactions are described by the linear Maxwell equations, which can also be expressed via the Liénard-Wiechert fields [64, 69] for a point charge, as given by Eq. (3.6), in §3.5. The total electrical field is then the addition of all electrical fields of all (charged) field generating particles. Usually the field generating particles are assumed to be point sources of infinitely small size, leading to a spherical symmetrical field distribution around a static particle. However, in this article we will not assume a point size of nuclear particles (like protons or neutrons). The Standard Model [56, 74] describes neutrons and protons to consist of 3 (point-size) moving quarks, carrying parts of elementary charge, as shown in fig. 3.3a. The 'up' quarks carry +2/3 of elementary charge, whereas 'down' quarks carry -1/3 of elementary charge.

Quantum theory [57], see §3.4, prescribes that if a particle is confined to a limited space, it can only obtain various distinct energy (movement) states, where the lowest energy state still gives rise to a non-zero energy (=movement) state. Therefore, we may assume that the quarks in a proton or neutron are in permanent movement, confined to the nucleus by the strong nuclear forces.

In this chapter, we will study the resulting electro-dynamical forces due to this permanent movement of the quarks in a neutron and proton. For simplicity, we will not use full quantum mechanical formulations, but limit the evaluations to the forces arising amongst the quarks of distant neutrons evaluated by the Liénard-Wiechert fields, using macroscopic concepts of classical mechanics such as velocity and acceleration.

4.3 The electro-dynamical force between 2 quarks

We aim to calculate the static force between two static neutrons which are at macroscopic distances from each other. We will treat the neutron-neutron interaction as a 6-body interaction, as each of the 3 quarks of each neutron is in interaction with the 3 quarks of the other neutron. This results in 3x3=9 force interactions, as seen in fig. 4.1. We assume that all quarks are in permanent movement, and calculate the resulting force via Eq. (3.6). We realize that:

- the quarks are confined to the static neutrons and thus have as time average: zero velocity and zero acceleration,
- the frequency of the movements of the confined quarks [57] is extremely high and thus only time averaged forces are important,
- the quark movements of the 2 separated neutrons can be taken to be independent.

We study the forces between two *moving* charges $(m\,q_0,\ n\,q_0)$, with the field generating particle, located at space co-ordinates $\vec{x} = (0,0,r)$. We indicate the elementary proton charge with q_0. The pre-factors $(m\ \&\ n)$ indicate the partial charges of quarks (+2/3 & -1/3). These quarks are assumed to be in a stable, minimum energy state, and thus do not emit any radiation. This means that the emissive part of the Liénard-Wiechert fields (containing the acceleration) as given in Eq. (3.6) can be omitted, see §3.5.6 [64, page 176], [69, page 146].

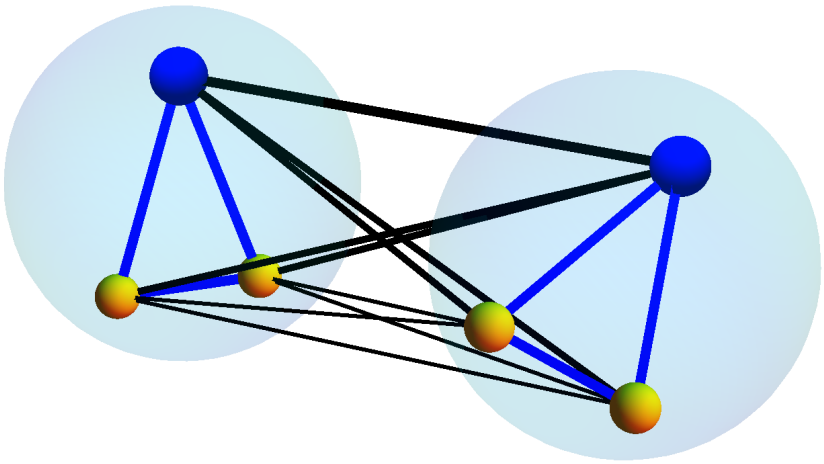

Figure 4.1: The 2 neutrons each contain 3 *moving* charged quarks, leading to a total of 9 electro-dynamical forces between the quarks.

The resulting force vector can be expressed as the time integral of:

$$\overrightarrow{F_{q_1 \leftrightarrow q_2}[t]} = (F_x, F_y, F_z) = -\frac{m\,n\,q_0^2}{4\pi\epsilon_0\,r^2}\;(1-(\delta v/c)^2)\,... \tag{4.1}$$

$$... \left(\frac{(\delta v/c)\,Cos[\phi_v]\,Sin[\theta_v]}{(1+(\delta v/c)\,Cos[\theta_v])^2}\,,\; \frac{(\delta v/c)\,Sin[\phi_v]\,Sin[\theta_v]}{(1+(\delta v/c)\,Cos[\theta_v])^2}\,,\; \frac{2-(\delta v/c)^2+2\,(\delta v/c)\,Cos[\theta_v]+(\delta v/c)^2\,Cos[2\theta_v]}{2\,(1+(\delta v/c)\,Cos[\theta_v])^3} \right)$$

For the velocity difference between the 2 moving quarks, we use spherical coordinates $(v_x, v_y, v_z) = \delta v\,(Cos[\phi_v]\,Sin[\theta_v]\,,\, Sin[\phi_v]\,Sin[\theta_v]\,,\, Cos[\theta_v])$. The time averaging operation can be regarded as integrating Eq. (4.1) over all angles and the (normalized) velocity distribution, using spherical integration. The total static force is then found from integration as given in Eq. (4.2).

$$\overrightarrow{F^{\,tot}_{q_1 \leftrightarrow q_2}} = \frac{\int_0^c \int_0^\pi \int_0^{2\pi} \overrightarrow{F_{q_1 \leftrightarrow q_2}[t]}\; Đ[\delta v]\;\delta v^2\,Sin[\theta_v]\;d\phi_v\,d\theta_v\,d\delta v}{\int_0^c \int_0^\pi \int_0^{2\pi} Đ[\delta v]\;\delta v^2\,Sin[\theta_v]\;d\phi_v\,d\theta_v\,d\delta v} \tag{4.2}$$

The function $Đ[\delta v]$ is a - yet undetermined - distribution function of δv, defined only for $0 \le \delta v < c$. For **one** moving charge (with one radial velocity δv_0) we can take the distribution function $Đ[\delta v]$ to be a Dirac delta function around δv_0. Integration of Eq. (4.2) can now be performed, yielding:

$$\overrightarrow{F^{\,tot}_{q_1 \leftrightarrow q_2}} = -\frac{m\,n\,q_0^2}{4\pi\epsilon_0\,r^2}\left(0\,,0\,,\frac{1-(\delta v_0/c)^2}{\delta v_0/c}\,ArcTanh[\delta v_0/c]\right) \tag{4.3}$$

This is identical to the force flux, as given by Eq. (3.14), apart from the 4π surface integration factor. We find the resulting force to drop with distance as $1/r^2$. When dropping the pre-factor $\frac{-m\,n\,q_0^2}{4\pi\epsilon_0\,r^2}$, we visualize the velocity dependence in fig. 4.2, under the name 'Dirac' distribution. For $\delta v_0 = 0$ we find the repulsive static force between 2 equally signed static charges.

Further, we calculate the force between **two** moving charges, each assumed to move with a single radial velocity, but with random spherical angles. In §3.7.2, we found the resulting radial velocity distribution to be of exponential shape in Eq. (3.20). Calculating the resulting electro-dynamical force via Eq. (4.2), we find a lengthy expression [85], which we label as $\chi[\delta v_0/c]$. The results are visualized in fig. 4.2, where δv_0 is to be interpreted as $v_{rel}[\delta v_1\,,\delta v_2]$ as given in Eq. (3.18). For $\delta v_0 = 0$ we find the repulsive static force between 2 equally signed static charges. This force drops over distance as $1/r^2$ which is equal for the static gravitational force.

4.4 Total inter-neutron force

For the full interaction force between 2 neutrons, we need to assess the summation of the 3x3=9 interactions forces between the quarks, as given by Eq. (4.3). We distinguish between the 3 types of velocity delta's between the types of quarks of the 2 neutrons (up-up δv^{nn}_{uu}, up-down δv^{nn}_{ud} and down-down δv^{nn}_{dd}) and notice that we take into account the different partial charges of these quarks (+2/3 and -1/3). We arrive at (assuming fully non-correlated velocities of the quarks inside each neutron):

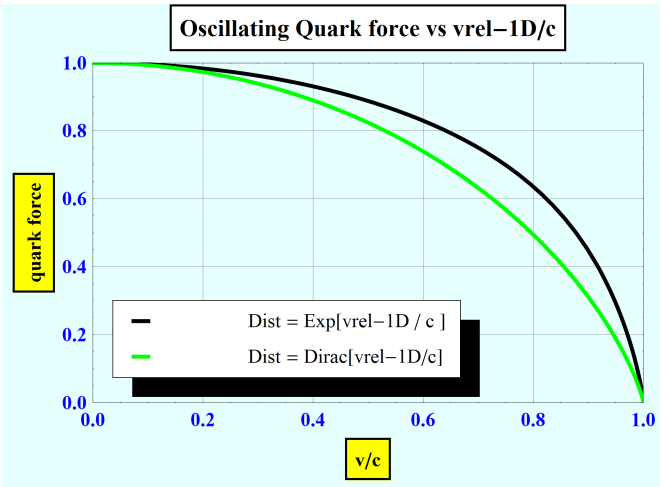

Figure 4.2: Static Force functions.
For **one** moving charge: 'Dirac' distribution.
For **two** moving charges: 'Exp' distribution $\chi[\delta v_0]$

$$\overrightarrow{F_{n\leftrightarrow n}} = \sum_{i=1}^{3}\sum_{j=1}^{3}\overrightarrow{F_{q_i\leftrightarrow q_j}} = \left(\frac{-q_0^2}{4\pi\epsilon_0 r^2}\right)\left(\frac{1}{9}\right)\left(0,0,4\chi[\delta v^{nn}_{uu}/c]-8\chi[\delta v^{nn}_{ud}/c]+4\chi[\delta v^{nn}_{dd}/c]\right) \quad (4.4)$$

Its magnitude is determined by the velocity difference (distribution) of the various quark types in the 2 neutrons ($\delta v^{nn}_{uu}, \delta v^{nn}_{ud}, \delta v^{nn}_{dd}$) [2]. The exact inter-quark velocity distributions will need to follow from more detailed assessments, based on relativistic (full 3D) velocity additions of the individual quark velocities, correlated within each neutron. Alternatively a full (relativistic) quantum mechanical assessment is to be employed. Here, we will limit ourselves to the impact of Eq. 4.4 for the exponential velocity distribution. We assume the quarks inside each neutron to be in totally independent movement, and can thus evaluate the total neutron-neutron force, as expressed by Eq. 4.4, by evaluating the electro-dynamical forces arising from the various (relativistically added, see §3.7.2) inter-quark velocities (between the 2 neutrons): $\delta v^{nn}_{uu} = vrel[v^n_{up}, v^n_{up}]$, $\delta v^{nn}_{ud} = vrel[v^n_{up}, v^n_{down}]$, $\delta v^{nn}_{dd} = vrel[v^n_{down}, v^n_{down}]$, where v^n_{up} and v^n_{down} indicate the velocities of the up- and down- quarks (scaled to the speed of light c) of the 2 involved neutrons. We evaluate Eq. (4.2) for the exponential velocity distribution (Eq. 3.20) , to arrive a lengthy expression [85], which can be inserted into Eq. (4.4) and represented graphically as shown in fig. 4.3a.

From fig. 4.3a, it becomes clear that the 2 neutrons have an attractive force ($F<0$) when the radial velocities of the up- and down- quarks are limited to: $v^n_{up}/c + v^n_{down}/c < 0.8$. This observation is not supported by the conclusions on the quantum mechanical movement of the quarks inside a neutron, as stated in §3.4. We will come back to this topic in §4.6.

[2] In the notation δv^{xy}_{ab},we indicate with $a\ b$ the type of quark (up or down) and with $x\ y$ the atomic particle (p=proton or n=neutron) in which the quark resides

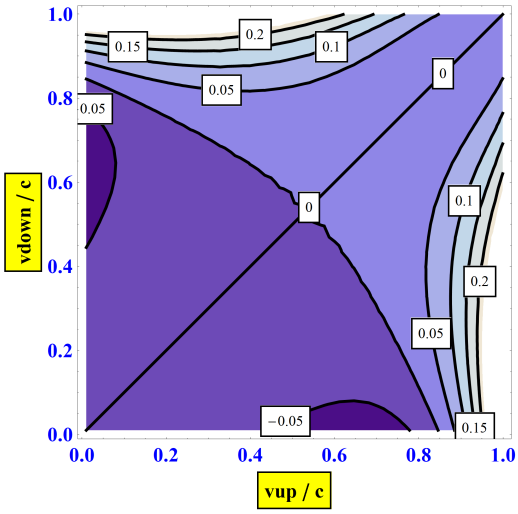

(a) Neutron-neutron quark force, as function of v^n_{up} and v^n_{down}.

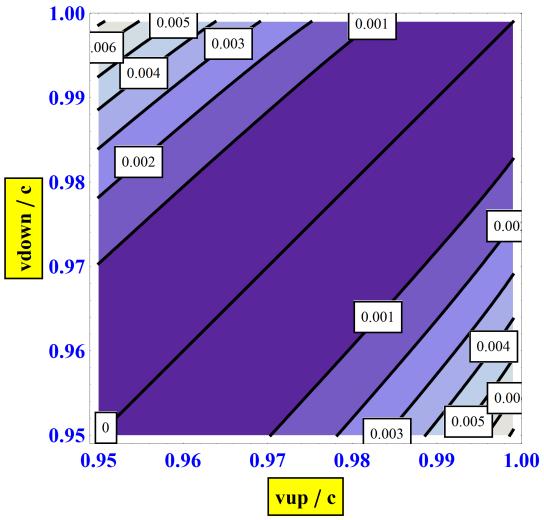

(b) high velocity neutron-neutron quark force.

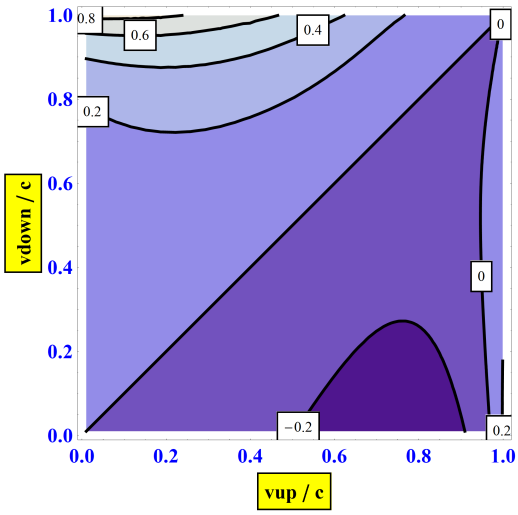

(c) proton-neutron quark force, assuming $v^p_{up} = v^n_{up}$ and $v^p_{down} = v^n_{down}$.

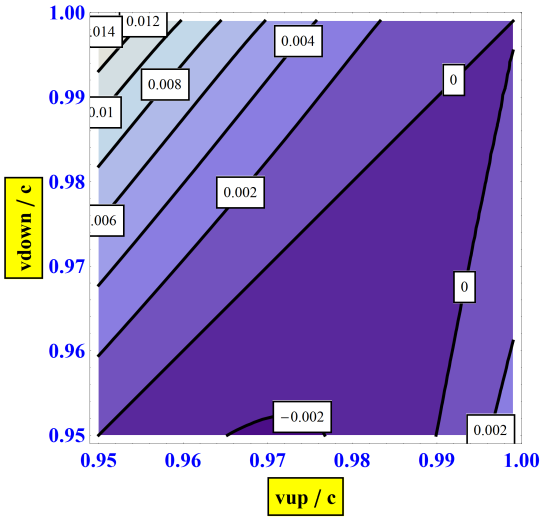

(d) high velocity proton-neutron quark force.

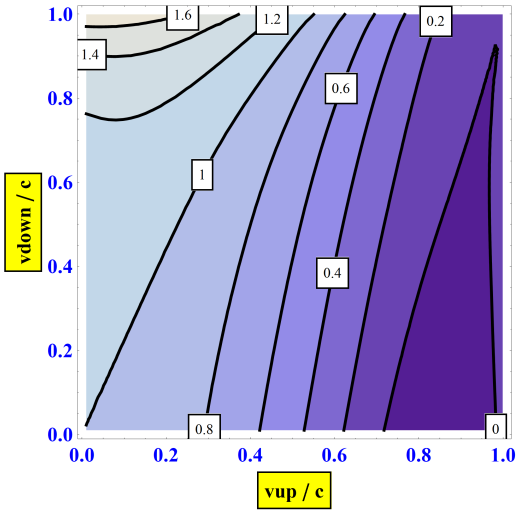

(e) Proton-proton quark force, as function of v^n_{up} and v^n_{down}.

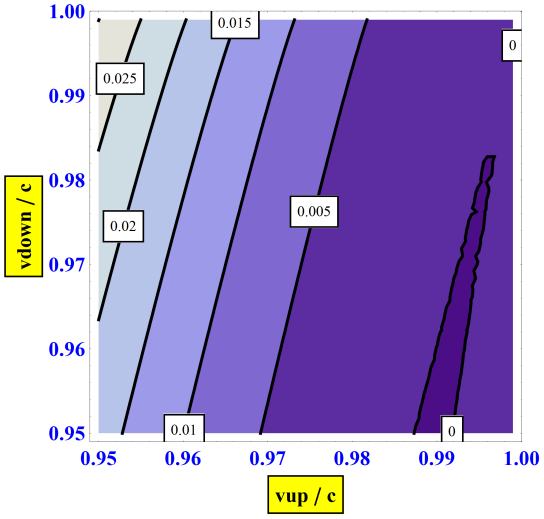

(f) high velocity proton-proton quark force.

Figure 4.3: Electro-dynamical forces in protons and neutrons, due to quark movement.

4.5 Force between proton-neutron and proton-proton

In this paragraph we will study the electro-dynamically induced interaction between 2 protons and a proton-neutron pair, with their different quark (and quark velocity) distributions. As indicated in the previous paragraph a proton can be modeled as consisting of 3 quarks like the neutron, as given in fig. 3.3a and 4.1. When evaluating the electro-dynamical interaction between a proton and a neutron, we find a similar formula like Eq. (4.4):

$$\overrightarrow{F_{p\leftrightarrow n}} = \left(\frac{-q_0^2}{4\pi\epsilon_0 r^2}\right)\left(\frac{1}{9}\right)\left(0,0,\ 8\chi[\delta v_{uu}^{pn}/c] - 10\chi[\delta v_{ud}^{pn}/c] + 2\chi[\delta v_{dd}^{pn}/c]\right) \tag{4.5}$$

For the interaction between two static protons, the following can be found:

$$\overrightarrow{F_{p\leftrightarrow p}} = \left(\frac{-q_0^2}{4\pi\epsilon_0 r^2}\right)\left(\frac{1}{9}\right)\left(0,0,\ 16\chi[\delta v_{uu}^{pp}/c] - 8\chi[\delta v_{ud}^{pp}/c] + \chi[\delta v_{dd}^{pp}/c]\right) \tag{4.6}$$

The results of these calculations are visualized in fig. 4.3. We recognize the static proton-proton force, for $v_{up}^{p} = v_{down}^{p} = 0$, which notably gives a large force for the proton-proton interaction. However, this large static interaction, is reduced towards zero, by the $(1-(v/c)^2)$ term in the Liénard-Wiechert force, as expressed in Eq. (3.6).

4.6 Quark-gravity impact of G

The analysis on the root cause of inertia (chapter 7) and the impact of the gravitational constant G, as will be performed in §7.5, indicates that the **sign of G** is not a consequential parameter, when only gravitational effects are to be taken into account. Therefore it is inconsequential whether we find (only) positive or negative forces when evaluating the total forces, due to the quark interactions, between separated protons or neutrons. Quantum mechanical arguments (as given in §3.4.2) determine that only valid solutions can exist for quark velocity values close to the speed of light.Therefore all 4 quark velocities inside the proton (v_{up}^{p} & v_{down}^{p}) and neutron (v_{up}^{n} & v_{down}^{n}) need to have values close to the speed of light, as visualized in fig 4.3.

Further it is known that the gravitational static mass of protons and neutrons are almost equal [92], and thus $\overrightarrow{F_{p\leftrightarrow p}} \approx \overrightarrow{F_{p\leftrightarrow n}} \approx \overrightarrow{F_{n\leftrightarrow n}}$. The static gravitational forces, as expressed by Eq. (4.4), (4.5) and (4.6), are to be compared with the classical gravitational law: $\vec{F}_g = \frac{m_p m_n G}{r^2}\frac{\vec{r}}{r}$, with $\vec{r} = (0,0,r)$, leading to the quantitiative indication (dropping the minus sign, as G can be negative):

$$\overrightarrow{F_{n\leftrightarrow n}} \approx \vec{F}_g \tag{4.7}$$

$$\left(\frac{q_0^2}{36\pi\epsilon_0 r^2}\right)\left(0,0,4\chi[\delta v_{uu}^{nn}/c] - 8\chi[\delta v_{ud}^{nn}/c] + 4\chi[\delta v_{dd}^{nn}/c]\right) \approx \frac{m_p m_n G}{r^2}(0,0,1)$$

$$\Longrightarrow$$

$$\left(\frac{q_0^2}{36\pi\epsilon_0}\right)\left(4\chi[\delta v_{uu}^{nn}/c] - 8\chi[\delta v_{ud}^{nn}/c] + 4\chi[\delta v_{dd}^{nn}/c]\right) \approx m_p m_n G$$

$$\Longrightarrow$$

$$4\chi[\delta v_{uu}^{nn}/c] - 8\chi[\delta v_{ud}^{nn}/c] + 4\chi[\delta v_{dd}^{nn}/c] \approx m_p m_n G / \frac{q_0^2}{36\pi\epsilon_0} \approx 7\times 10^{-36}$$

And similarly, evaluating $\overrightarrow{F_{p\leftrightarrow p}}$ and $\overrightarrow{F_{n\leftrightarrow n}}$ we find:

$$16\chi[\delta v_{uu}^{pp}/c] - 8\chi[\delta v_{ud}^{pp}/c] + \chi[\delta v_{dd}^{pp}/c] \approx m_p\, m_n\, G/\frac{q_0^2}{36\pi\epsilon_0} \approx 7\times 10^{-36} \tag{4.8}$$
$$8\chi[\delta v_{uu}^{pn}/c] - 10\chi[\delta v_{ud}^{pn}/c] + 2\chi[\delta v_{dd}^{pn}/c] \approx m_p\, m_n\, G/\frac{q_0^2}{36\pi\epsilon_0} \approx 7\times 10^{-36}$$

In conclusions: We need to identify solutions for the quark velocities, as prescribed by Eq. (4.7) and (4.8), visualized in fig. 4.3, while these solutions need to be close to the velocity of light. We have 4 independent quark velocities, while we need to respect 3 (force) equalities. This is a solvable set of equations, as we know from fig. 4.2 that $\chi[v/c] \to 0$ as $v/c \to 1$, in-line with the quantum-mechanical argumentation given before.

As mentioned before: the entire quark-force analysis needs to be redone by quantum mechanical, relativistic means, (with kinetic quark energies as leading output, serving as input for the LW-force calculations). Also quark-movement correlations need to be considered. Thus, these calculations only be considered exploratory.Therefore pursuing accurate solutions for the set of equations mentioned above, serves no practical purpose, as long as a more accurate analysis is lacking. However, the concept that gravity is due to moving, oscillating, quarks inside the nuclei remains valid, despite the crudeness of the models used.

4.7 Gravitational mass upon movement

The concept of oscillating motions of charged particles leading to gravitational mass, means that the *amount* of gravitational mass follows the relativistic Doppler law when the mass is moving macroscopically.

Alternatively, when repeating the 2-quanta thought experiment as mentioned in §3.2, for a *moving* box, we find that the emitted quanta, when deflected to the observer, show a relativistic Doppler effect, as given by Eq. (3.2). Via the Planck law, Eq. (3.3), we find that the energy of the emitted quanta is changed for the moving box. Via the mass-energy equality Eq. (3.1), we therefore find that the quanta, emitted from a moving box, represent a different (gravitational) mass than when emitted from a non-moving box. If we extend this analysis (assuming all mass can be transferred to quantum energy), we find that the *amount* of the moving mass itself is changed, according to the relativistic Doppler law.

$$mass = E/c^2 = h\nu/c^2 = \frac{h\nu_0}{c^2}\,\frac{\sqrt{1-(v_z/c)^2}}{1+(v_z/c)\,Cos[\theta]} \tag{4.9}$$

where ν_0 represents the frequency of the quant as observed when co-moving with the box.

Therefore, the **gravitational mass** amount changes with movement, as given by Eq. (4.9). The **inertial mass** amount increases with velocity as (to be) discussed in §7.3.2, and given by Eq. (7.9).

In short: charge is a motion invariant, but the, charged oscillations *induced*, gravitational mass is not.

4.8 Electron and anti-matter

Sofar, we only discussed the gravitational interaction between protons and neutrons. The gravitational force by an electron is not yet treated in detail, as we do not have a model of the electron, except that of a (near) point charge. This implies, as seen in §3.4, a high (self-vibration?) velocity and thus a small gravitational mass. However, without a proper model for the electron, a further analysis of its gravitational mass is fruitless.

A further thought concerns anti-matter: if we use the analysis of the electron and apply it to the oppositely charged positron, we obtain an opposite force[3].

In conclusion: the gravitational forces of electron and anti-matter need further study.

4.9 Conclusions

We have identified in the previous paragraphs:

- The quantum-mechanically induced charged quark oscillatory movements inside a proton and neutron are the electro-dynamical source of gravity: **quark-gravity**.
- The identified force drops statically as $1/r^2$.
- The speed of gravity equals the speed of electro-dynamical interactions which is the speed of light, as confirmed experimentally in 2017 [1].
- The gravitational vector force follows from the 2 previous bullet points [9], and is given by the Liénard-Wiechert force description, as given by Eq. (3.6), with replacement of $1/(4\pi\epsilon_0)$ by the gravitational constant G and the charges by masses.
- The velocity dependence of the *amount* of gravitational mass follows the relativistic Doppler law.

Finally: the force fields calculations due to moving quarks inside the nuclei, were executed by non-quantum mechanical procedures. It is suggested to perform this analysis with quantum mechanical, relativistic methodology. Further studies are also needed to capture the gravitational effects of electrons and anti-matter.

[3] and eventually an opposite inertial effects (see chapter 7).

5. Optical properties of gravity

5.1 Introduction

In this chapter we will investigate the impact of the concept that gravity is an electro-dynamically induced effect, by studying various typical General Relativity (GR) tests on impact of gravity on light (=electro-dynamic radiation). Both bending of light as well as Shapiro time delay will be discussed. First we will present some historic evaluations of bending of light and then present an assessment based upon electro-dynamically induced gravity. We will confirm this formalism in analyzing the Shapiro time delay. Finally, we will touch upon some theoretical models to further explain the bending of light under gravity.

Figure 5.1: ESA/NASA James Webb image of an Einstein ring around galaxy SMACSJ0028.2-7537.

5.2 Newtonian evaluation of light bending

In this paragraph we want to compute the deflection of light by a central mass, taking a simplified model of deflection of light in a Newtonian sense [53, pages 97–108], as visualized in fig. 5.2. In this model, light is depicted as a particle (with mass m_{light}) moving at the speed of light. We compute the horizontal (x) velocity buildup as the beam of light passes a large mass, with closest approximation of $R0$. Assuming the deflection to be small ($\phi_{hor} \ll 1$), the ray can be approximated (to first order) by a straight line, simplifying the calculation. The horizontal momentum can be expressed as the integration of the horizontal force on the particle and time during the 'flyby'. With the central mass (M_{sun}) located at $(x,y) = (0,0)$, the horizontal gravitational and inertial forces are given as :

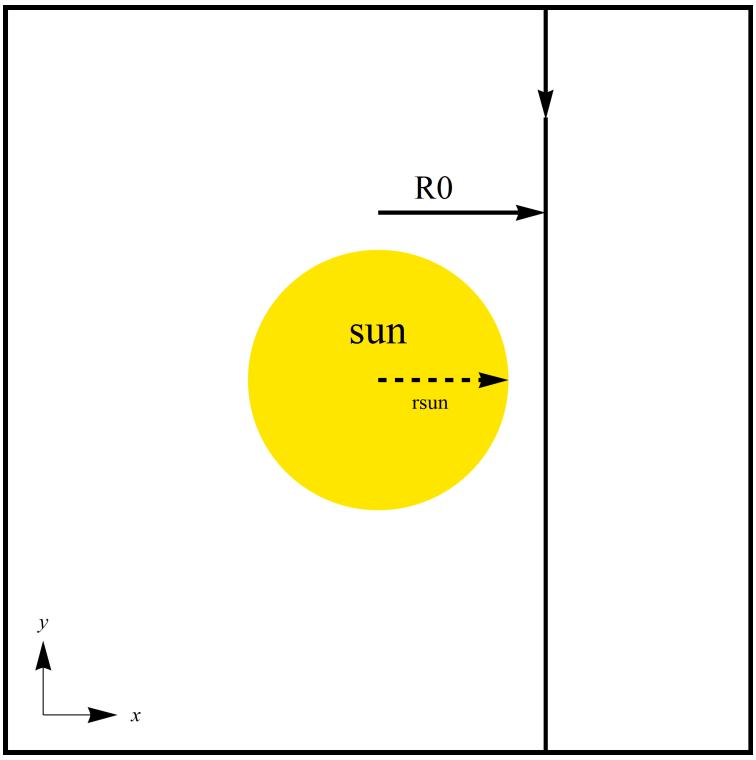

Figure 5.2: Ray of light passing by sun, at distance R0.

$$F^{hor}_{grav}[y] = G M_{sun}\, m_{light}\, R0 / (R0^2 + y^2)^{3/2} \tag{5.1}$$
$$F^{hor}_{grav}[y] = F_{inertial} = m_{light}\, a_{hor}$$

The m_{light} drops out of the equation. Approximating the speed of light to be constant during the fly-by, the total horizontal velocity can be expressed as:

$$v_{hor} = \int_{-\infty}^{\infty} a_{hor}\, dt = \int_{-\infty}^{\infty} a_{hor}\, dy / c \tag{5.2}$$
$$= G M_{sun} / c \int_{-\infty}^{\infty} R0 / (R0^2 + y^2)^{3/2}\, dy = 2 G M_{sun} / c R0$$

Therefore the deflection angle $\phi_{hor} = v_{hor} / v_{ver} = v_{hor} / c$ amounts to :

$$\phi_{hor} = 2 G M_{sun} / c^2 R0 \tag{5.3}$$

This is the Newtonian deflection angle for a beam of light coming close to a heavy object [53, pages 97–108].

5.3 General Relativity evaluation of light bending

In General Relativity [48, 52, 53, 65, 66, 68, 69, 70], bending of light is explained by employing curved space-time, as shown in fig. 5.3. This is described for a static, rotational symmetrical mass (M_{sun}) by the Schwarzschild metric:

$$ds^2 = (1 - \frac{2GM_{sun}}{c^2 r})\, c^2\, dt^2 - (1 - \frac{2GM_{sun}}{c^2 r})^{-1}\, dr^2 - r^2\,(d\theta^2 + Sin^2[\theta]\, d\phi^2) \tag{5.4}$$

where ds^2 represents the line element, and t, r, ϕ, θ are the space and time coordinates of the stationary observer. The evaluation of the deflected light beam then leads to:

$$\phi_{hor} = 4GM_{sun} / c^2 R0 \tag{5.5}$$

Note, that the General Relativity result of Eq. (5.5) amounts to twice the value for the defection angle of the Newton evaluation as given in Eq. (5.3).

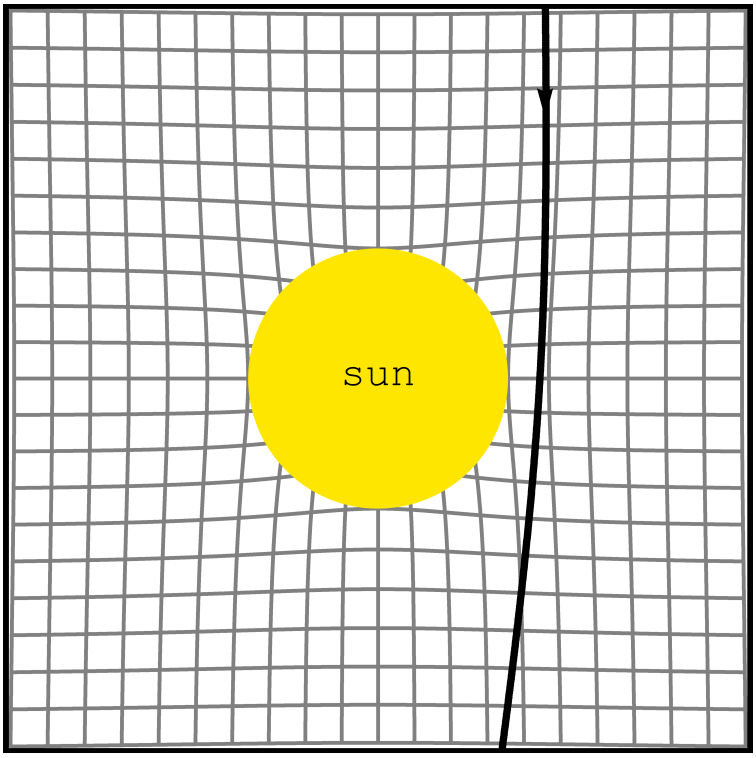

Figure 5.3: General relativity explains light bending by gravitational space-time curvature.

Further it is to be noted that Eq. (5.4) indicates that a ray of light ($ds^2 = 0$), moving radially outward ($d\phi^2 = 0$ and $d\theta^2 = 0$) has a speed (as observed by a stationary observer) of:

$$c_{grav} = \sqrt{\frac{dr^2}{dt^2}} = c\left(1 - \frac{2GM_{sun}}{c^2 r}\right) \tag{5.6}$$

This indicates that the speed of light near a mass (c_{grav}) is lower than further away. In short: gravity reduces the speed of light: it has refractive properties, with refractive index $n = c / c_{grav}, = 1 / (1 - \frac{2GM_{sun}}{c^2 r}) > 1$. This is the starting point for gravitational lensing [44] and Shapiro time delay [38].

5.4 Refraction evaluation of light bending by gravity

In this paragraph we will investigate how the electro-dynamically induced gravity creates deflection of light in Euclidean space. Deflection of light is created at interfaces of material media with different refractive indices, such as an air-glass interface, see in fig. 5.4.

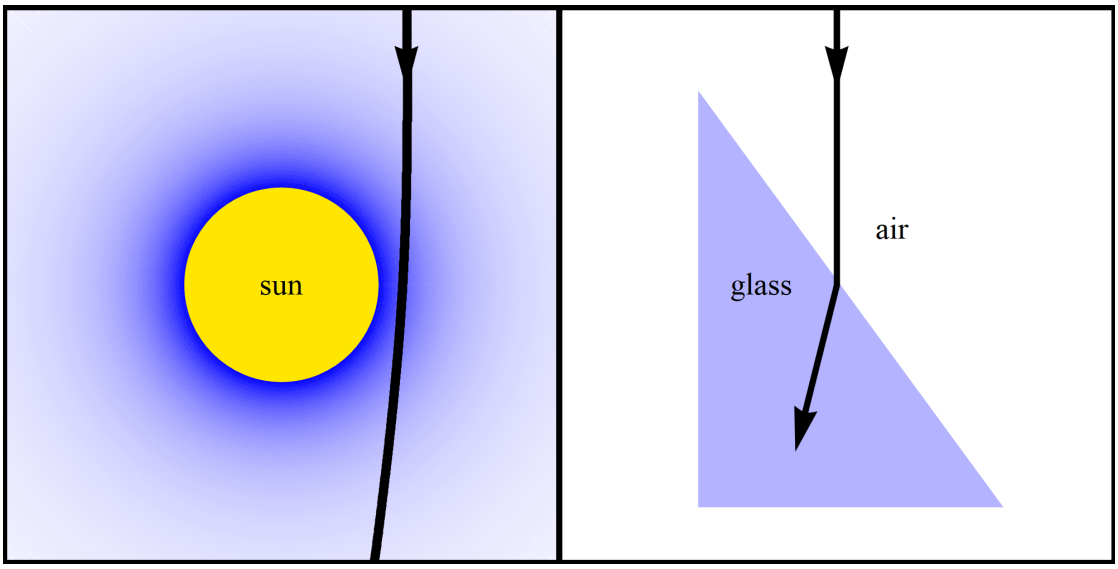

Figure 5.4: Refraction of light due to change of refractive index (represented by the color depth in blue). The discrete change of refractive index for a glass-air interface is shown, as well as the varying refractive index of the varying gravitational field of a large mass, like the sun.

In fact, the definition of the refractive index (n) is the velocity ratio of light between 2 different media. The electrical interactions between light and medium slow down the varying electrical fields that want to pass through the medium, including light. The electrical fields of the moving electrons around the nuclei in the medium act similar as the electrical fields of the moving quarks inside the nuclei that generate gravity. As such, a gravitational field creates speed reduction of light and thus acts as a medium with a refractive index.
A variable refractive index affects the path of light and is studied in a field of physics, known as geometrical optics [49, 61]. It is governed by the eikonal equation:

$$\frac{d}{ds}\left(n[\vec{r}]\,\frac{d\vec{r}}{ds}\right) = \nabla\, n[\vec{r}] \tag{5.7}$$

where: ∇ is the gradient, s indicates the parametric distance along the ray of light and $\vec{r}$ indicates the ray trajectory though Euclidean 3D space.
It must be noted that already in 1920, Eddington [50, page 50], [51, pages 99–100] had pointed out that the ('material medium') eikonal equation Eq. (5.7) properly describes the gravitational light bending, assuming the refractive index of gravity (=speed reduction of light under influence of gravity) is given by Eq. (5.6), see also [14, 15, 16, 35], [48, pages 95–97].

For small deflection angles, a solution to Eq. (5.7) on gravitational light bending, is given in [87]. The horizontal deflection angle is computed by evaluating the bending of the light, due to the gradient of the gravitational field, simplifying the light path to a straight line and then evaluating:

$$\phi_{hor} = \int_{-\infty}^{\infty} \nabla_{hor}\, n[\vec{r}]\, ds = 4\, G\, M_{sun} / c^2\, R0 \tag{5.8}$$

The integration follows identical calculation as used to derive Eq. (5.3), with $G\,M_{sun}$ of the gravitation force replaced by $2\,G\,M_{sun}$ of the gravitational refractive index.

5.5 Shapiro gravitational time delay

Another direct observable of the reduction of the speed of light in a gravitational field, is time delay of light as it passes close to a heavy object, as first described by Shapiro [38].

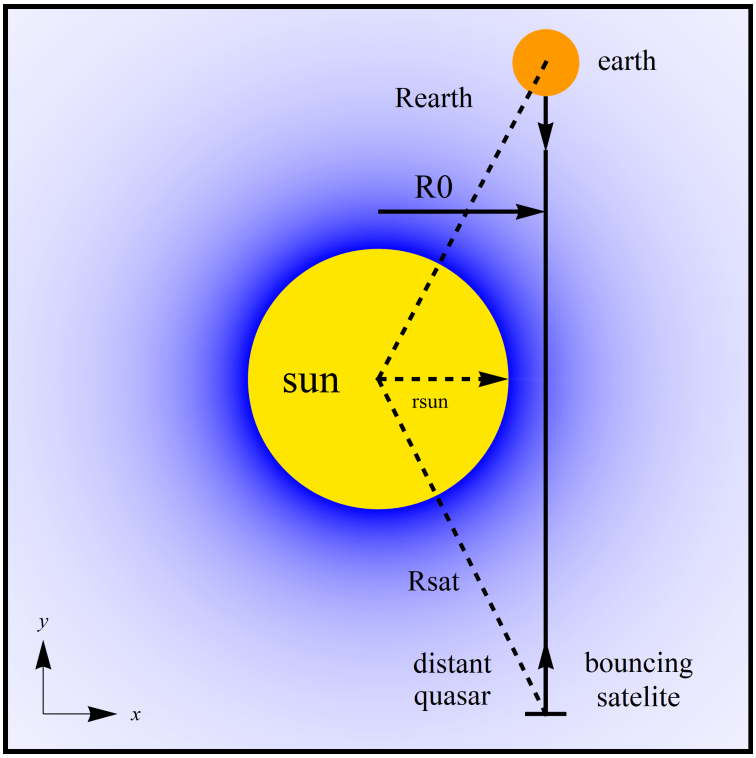

Figure 5.5: Time delay, due to the reduction of speed of light in the gravitation field of sun.

We are studying the time required for an electro-magnetic pulse (light / radar) to travel from earth to a 'bouncing satellite' - and back - which can be an active man-made satellite, or a planet. We use a straight line as approximation for the signal path, which travels through the gravitational field of a central mass (like the sun), at closest proximity of $R0$. The total time for the signal to travel the *double trip* satellite-earth, can be expressed as (using Eq. (5.6) for speed of light and $1/(1-x) \approx 1+x$ for $x \ll 1$):

$$T_{Shapiro} = 2\int_{t1}^{t2} dt = 2\int_{-y_{sat}}^{y_{earth}} \frac{1}{c[y]}\,dy = 2/c\int_{-y_{sat}}^{y_{earth}} \frac{1}{1-\frac{2GM_{sun}}{c^2\sqrt{R0^2+y^2}}}\,dy \tag{5.9}$$

$$= 2\,(y_{earth}+y_{sat})\,/c + \frac{4GM_{sun}}{c^3}\int_{-y_{sat}}^{y_{earth}} \frac{1}{\sqrt{R0^2+y^2}}\,dy$$

$$= 2\,(y_{earth}+y_{sat})\,/c + \frac{4GM_{sun}}{c^3}\,(ArcSinh[y_{earth}/R0] + ArcSinh[y_{sat}/R0)]$$

with $y_{earth} = \sqrt{r_{earth}^2 - R_0^2}$, $y_{sat} = \sqrt{r_{sat}^2 - R_0^2}$. The first term of Eq. (5.9) gives the time duration of a signal traveling from earth to satellite and back, in the absence of a gravitational field. The second term gives the gravitational (refractive) time delay. Assuming $y_{earth}/R0 \gg 1$ and $y_{sat}/R0 \gg 1$ allows the simplification for $x \gg 1$ of $ArcSinh[x] = Ln[x+\sqrt{1+x^2}] \approx Ln[2x]$. Eq. (5.9) can be simplified to (using $Ln[ab] = Ln[a] + Ln[b]$):

$$\delta T_{Shapiro} = \frac{4GM_{sun}}{c^3}\,Ln[4\,\frac{y_{earth}\,y_{sat}}{R0^2}] \tag{5.10}$$

This equals the Shapiro time delay fo a radar bounce experiment [65, 68, 38] as given by General Relativity.

In fact, the Shapiro time delay is a special case of the general time delay created by gravity [48, page 98], [65, page 155], [69, page 233], [70, page 184], [68, page 1055].

5.6 Linearized GR and Newtonian approximation

In this paragraph we compare the various approximations of the General Relativity (GR) metrics with the 'material medium' refractive index analogon (=variation of c). We start with the full Schwarzschild solution (with curved space-time and a finite speed of light), as given in §5.3:

$$ds^2 = (1-\frac{2GM_{sun}}{c^2 r})\,c^2\,dt^2 - (1-\frac{2GM_{sun}}{c^2 r})^{-1}\,dr^2 - r^2\,(d\theta^2 + Sin^2[\theta]\,d\phi^2) \tag{5.11}$$

from which we have found the velocity variation of light passing through a gravitational field (for $ds^2 = 0$, $d\phi^2 = 0$ and $d\theta^2 = 0$) as given by Eq. (5.6):

$$c_{grav}^{GR} = \sqrt{\frac{dr^2}{dt^2}} = c\left(1-\frac{2GM_{sun}}{c^2 r}\right) \tag{5.12}$$

In the linearized General Relativity [68, page 442], [48, 65, 68], [70, §15.5], with a finite light propagation speed in near-Euclidean space, it is found that the Schwarzschild metric can be approximated by:

$$ds^2 = (1-\frac{2GM_{sun}}{c^2 r})\,c^2\,dt^2 - (1+\frac{2GM_{sun}}{c^2 r})\left(dr^2 + r^2\,(d\theta^2 + Sin^2[\theta]\,d\phi^2)\right) \tag{5.13}$$

Then we find for the velocity of light :

$$c_{grav}^{lin} = \sqrt{\frac{dr^2}{dt^2}} = c\sqrt{\frac{1-\frac{2GM_{sun}}{c^2 r}}{1+\frac{2GM_{sun}}{c^2 r}}} \approx c\left(1-\frac{2GM_{sun}}{c^2 r}\right) \tag{5.14}$$

Based on $\sqrt{(1-x)/(1+x)} \approx 1 - x + x^2/2 - ...$, for $0 \le x \ll 1$, we find that the linearized GR velocity of light equals that of the full analytical, Schwarzschild solution Eq (5.11), for small values of $\frac{2GM_{sun}}{c^2 r}$. Thus the gravitational light bending angle is equal to Eq. (5.5).
Sometimes [65, §17.10] this solution is called the 'Newtonian' approximation. However, any Newtwonian theory is characterized by 'immediate action at a distance' which means an infinite interaction speed. The linearized General Relativity approximation is still based on a fiinite speed of light. Therefore, it might be better to speak of the linearized version of General Relativity as 'Maxwellian' approximation.

We now study a Newtonian particle (with finite mass) moving at the speed of light, as done in §5.2. We can formulate the metric, [24, 105] in GR terms of metric tensor elements: $g_{00} = (1-\frac{2GM_{sun}}{c^2 r})\,c^2$ and the other $g_{\mu\nu} = \delta_{\mu\nu}$, with $\delta_{\mu\nu}$ representing the Kronecker delta function. We then find:

$$ds^2 = (1-\frac{2GM_{sun}}{c^2 r})\,c^2\,dt^2 - \left(dr^2 + r^2\,(d\theta^2 + Sin^2[\theta]\,d\phi^2)\right) \tag{5.15}$$

And thus, similar as above, $\sqrt{1-x} \approx 1 - x/2 + x^2/8 - ...$, we find for the Newtonian approximation for the velocity of light:

$$c_{grav}^{Newton} = \sqrt{\frac{dr^2}{dt^2}} = c\sqrt{1-\frac{2GM}{c^2 r}} \approx c\left(1-\frac{GM_{sun}}{c^2 r}\right) \tag{5.16}$$

This leads to only half of the gravitational GR light bending as the driving term is halved.

The pure Newtonian 'particle' evaluation, with infinite propagation speed of light gives pure Euclidean space, as $g_{00} = 1 - \frac{2GM_{sun}}{c^2 r} \to 1$ as $c \to \infty$. This leads to a purely Eucidean metric: $ds^2 = c_{max}^2\,dt^2 + dr^2 + r^2\,(d\theta^2 + Sin^2[\theta]\,d\phi^2)$, which represents (in Newtonian sense) a 'light-particle' with velocity c_{max}, which will give of course zero bending of light as $c_{max} \to \infty$.

5.7 Some qualitative theory on refractive index

The theory on the root cause of the refractive index is given by the Lorentz model [49, 54, 60], which provides a qualitative indication for the trends in refractive indexes. The model is based on an atomic model of matter in which the rotating electrons around the nucleus are influenced by the incoming varying electro-dynamical fields (such as light or radio signals). A resonance frequency then occurs when (in classical mechanical terms) the electron revolves around the nucleus with the same frequency as that of the incoming electro-dynamical field.

In our model for gravity (see chapter 4), we have found the moving quarks in the nucleus to create gravity, and thus refraction. The refractive resonance frequency of gravity is thus the frequency of the quarks (moving at the speed of light) as they move inside the nucleus (with the smallest possible dimensions). Therefore the resulting resonance frequency for gravitational refraction, is much higher than the one resulting from atomic electron orbit interactions. Therefore a frequency dependence of gravitational refraction is not expected, and thus gravitational bending of light and radio signals should be equal.

In summary: we have found that the mechanism creating gravity (=moving electrically charged quarks) is the same mechanism that creates the speed reduction impact on the varying electric field of a light beam. Therefore, gravity must be a direct measure for refraction. However, a quantitative theory, leading up to exact equations for the refractive index, such as Eq. (5.6), is still to be developed[1].

5.8 Conclusion on optical properties of gravity

As gravity is electro-dynamical in essence, due to moving quark charges, it has refractive properties: it reduces the speed of light. Geometrical optics learns that gravity will therefore affect the path of light. Based on the linearized description of General Relativity expression for the refractive index of gravity, a Euclidean space evaluation properly describes the bending of light around a mass as well as Shapiro time delay, in line with the experimental evidence. No frequency dependence of the gravitational refraction is expected.

However, a quantitative theory, leading up to exact equations for the refractive index, such as Eq. (5.6), is still to be developed.

[1] An alternative method to find the refractive index, can be to reverse engineer the linearized GR metric of Eq. (5.13) to the Maxwellian/Liénard-Wiechter equations [70, §15.5], [4] and thus prove Eq. (5.14) and the consequential light bending.

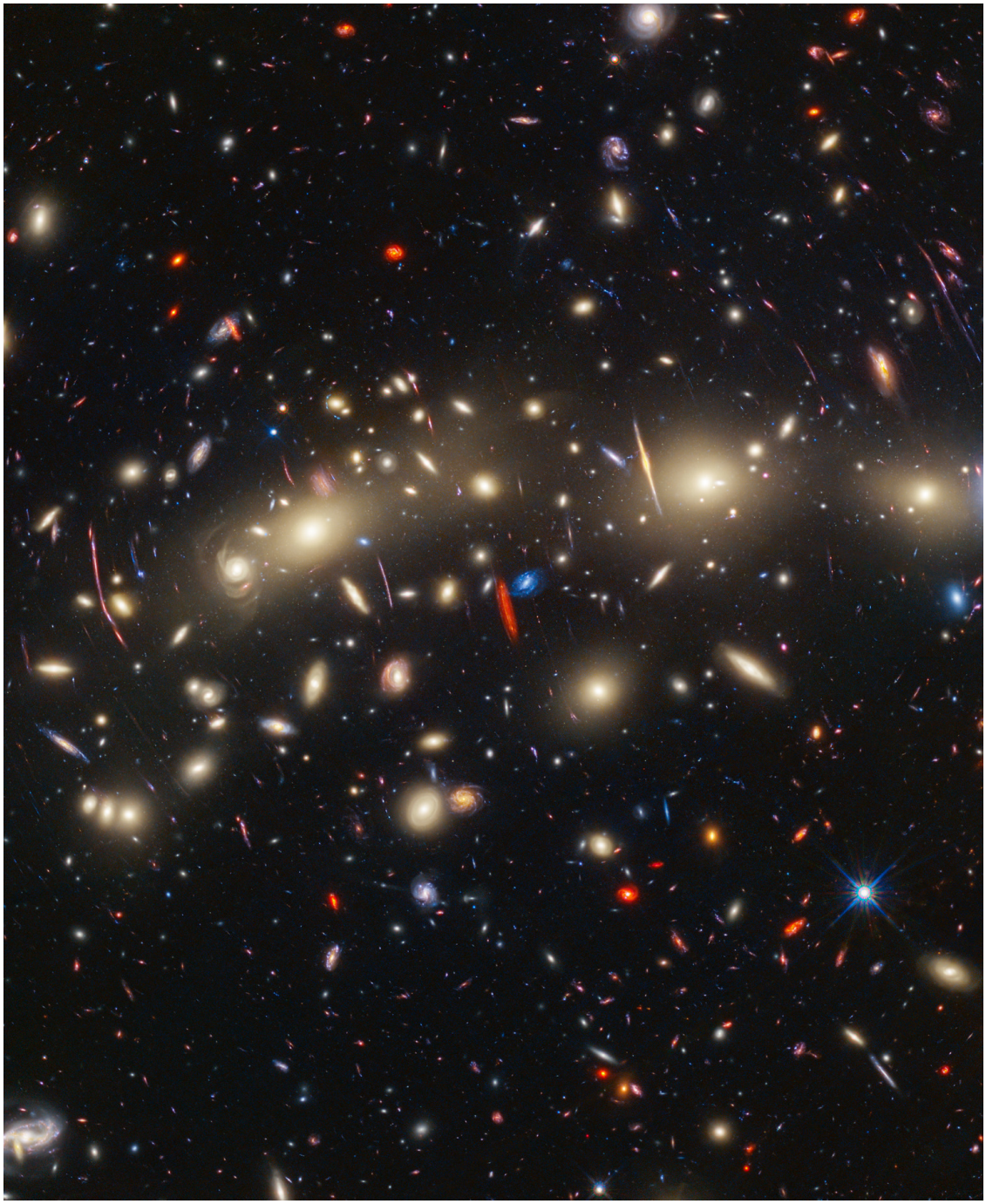

Figure 5.6:
James Webb telescope [90] image of MACS0416,
showing gravitational lensing (image by NASA).

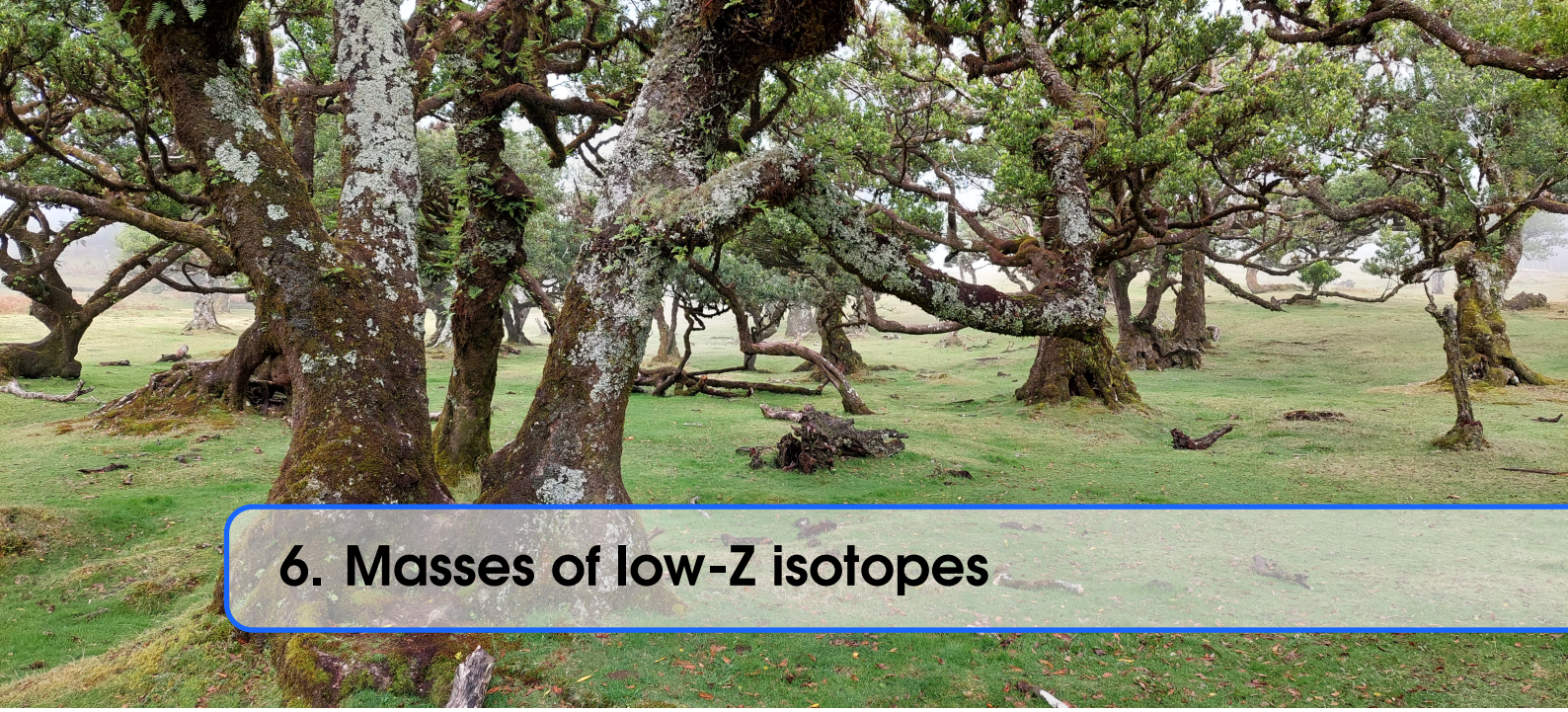

6. Masses of low-Z isotopes

6.1 Introduction

In this chapter, we aim to predict the atomic mass [92] of various low-mass isotopes, based on the model of moving quarks as developed in chapter 4.

Based on the quark model for the proton and neutron, see fig. 3.3a, we extend the analysis of the quark distribution for various light isotopes, like Deuterium, Tritium and Helium-4. We compute the quark configurations and attempt to reach a microscopic explanation for the atomic mass of the nucleus. Of course, the mass is expected to increase linearly with the number of involved particles (=protons and neutrons). However, some fine trends (as the mass of Helium-4) require further attention. The starting assumption is that an extended, 'large-sized' nucleus has a small quantum mechanical lowest energy state, and thus a lower (gravitational) mass. This is based upon the analysis of an infinite deep spherical energy well [57, pages 26, 130], given by: $E = h^2 / (8\, m\, a^2)$, with 'a' : the dimension of the infinite well, $\hbar$ being the Planck constant, and 'm' as mass of the involved particle, see also fig 3.3b. Therefore, if we analyze the geometry of the various nuclei, we expect to find a correlation between the relative atomic mass and the maximum dimension of the nucleus.

A full quantitative analysis of the lowest energy state of a nucleus, containing a multitude of quarks, requires a full relativistic, quantum mechanical analysis. However, this is outside the scope of the current analysis. We limit ourselves to a non-relativistic, classical mechanics analysis and treat the nucleus as a N-particle problem, with force interactions between all quarks in the nucleus. We aim to find the minimum energy (= stable) state of the nucleus, and obtain then the maximum inter-quark distance inside the nucleus, which we aim to correlate with the atomic mass. It is clear that the minimum energy state is not a 'fixed' = 'stable' configuration, such as found in solid state physics (see fig. 2.1), but more the 'most likely' configuration in quantum-mechanical sense.

6.2 Computation of quark distributions

We compute the quark distribution by taking a non-quantum-mechanical, non-relativistic, force approach. As force interaction between the quarks we start from the Cornell potential [76, 83, 86, 29, 97], and add a short term repulsive term, to prevent that the oppositely charged up and down quarks absorb each other. Thus the total potential, between 2 charged quarks at distance r, is described as:

$$V_{q_i-q_j}[r] = q_i\, q_j / r + (r_q / r)^3/3 + glue\ r \tag{6.1}$$

We use a summation of:

1. static electrical Coulomb potential (between charges q_i and q_j [1]),
2. repulsive short range potential (aiming to preserve a minimum distance between quarks), with length parameter r_q,
3. a long range attractive potential (representing the strong nuclear force, keeping all quarks together - even at high starting velocity).

Varying the value of r_q has significant impact on the shape of the total potential, as given in fig. 6.1a.

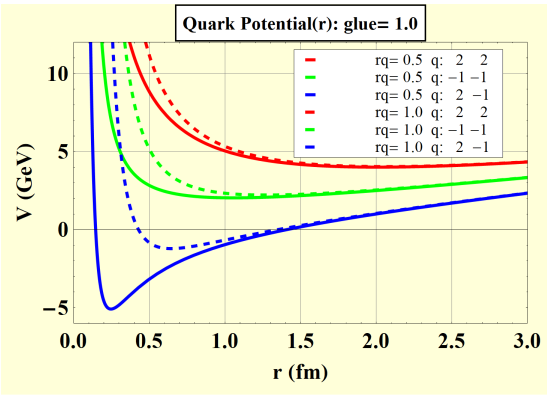

(a) Quark potential.

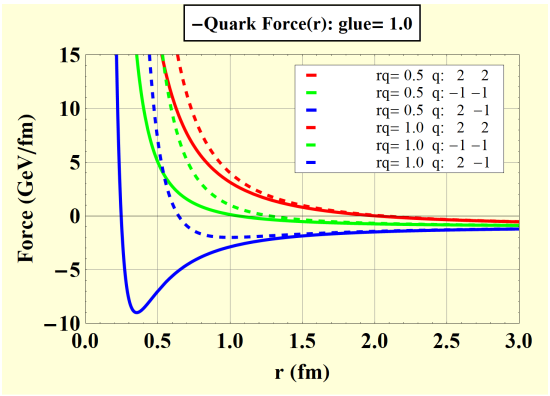

(b) - Quark force: attractive force is negative.

Figure 6.1: Quark potential and force. The (long range) glue function creates stability, whereas the short term part of the potential assures that a minimum quark distance is maintained. Variation of the quark distance parameter r_q leads to a varying balance between Coulomb and binding forces, resulting in significantly different geometries of the nucleus. A larger value of of the 'quark radius' r_q leads to less Coulomb interaction between the quarks and thus a less deep potential (as given by the dashed lines).

To this potential, we have added a friction term, to assure that from varying initial conditions (for quark positions and velocities), the final, stable, quark positions in the nucleus are reached, after integration over time. The total force, per quark pair (i,j), is then given (via $\vec{F} = -\nabla \bullet V$) as, Eq. (6.2):

$$\overrightarrow{F_{q_i-q_j}}[\vec{r}] = q_i\, q_j\, (\vec{r}/r^3) + r_q^3\, (\vec{r}/r^5) - glue(\vec{r}/r) - k\,\vec{v} \tag{6.2}$$

In our N-particle simulations, we started from parameter values as found in literature for the Cornell potential [97], with $glue = 1$ GeV/fm [86, 97]. Further we used varying values of the

[1] In literature this Coulomb factor is multiplied with a baryon QCD pre-factor $(2\,\alpha_s/3)$ [97], with $\alpha_s \approx 1$, The value of α_s varies largely in literature from 0.3 [86, page 7] to 1.0 [97, pages 4, 9]. As such, the involved QCD potentials vary largely in relative effect of the Coulomb force vs the binding nuclear force, leading to variations in final quark distributions in the isotope nucleus.

'quark-radius' r_q, and studied the range from $0.3 < r_q < 2.0$ fm. The friction value (k) is set to $k = 0.005\,a.u.$. As initial conditions we used positions and velocities (for particle i), in a sphere surrounding the origin, in multiple variations of $(x_i, y_i, z_i) = (iCos[i], iCos[2i], iCos[3i],])$. In our simulations, we used q_i for the normalized up and down quark charges: +2 and -1. Based on these parameters, we evaluate Eq. (6.2) for the 3 quark charge combinations, as seen in fig. 6.1b. The resulting numerical integration of the quark positions and velocities were executed by the SW Mathematica [85].

6.3 Simulation results on low-Z nuclei

These simulations were executed for various light isotope nuclei, from a neutron up to Fluor-19. For the 3-quark neutrons and protons, we find the 'semi-stable' final geometry in our simulations to be a linear shape, with the equally charged quarks at the end, see fig. 6.4. The maximum inter-quark distance for a proton is larger than for a neutron, as the 2-up quarks repel stronger than the 2-down quarks. We studied the impact of the 'quark-radius' on the shape of the nucleus, see fig. 6.2a, notably by studying the 'largest inter-quark distance' in the nucleus. We find the linear shape of both proton and neutron to change to a more H_2O molecule shape for higher values of r_q. From fig. 6.1a, it is clear that a larger 'quark-radius' r_q leads to less Coulomb interaction amongst the quarks in a nucleus, and thus the long range binding force (represented by $glue$ in Eq. (6.1) becomes dominant. Therefore the linear shape of the neutron and proton get bended, for increasing r_q. We can identify in fig. 6.2a a specific value of r_q for which the shape of the nucleus changes for both neutron and proton. For a proton this change in shape occurs at a higher value of r_q than for a neutron as the proton has 2 double charged up quarks, whose electrical repellent forces will resist the binding force ($glue$) more.

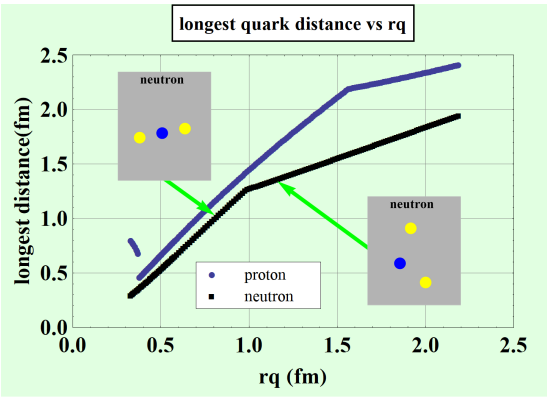

(a) The largest quark distance for protons and neutrons as function of the 'quark-radius' r_q. For the neutron a remarkable change in the slope of the graph occurs around $r_q = 1.0$ fm, as the shape of the neutron changes. For the proton this change occurs at a higher value of $r_q = 1.5$ fm.

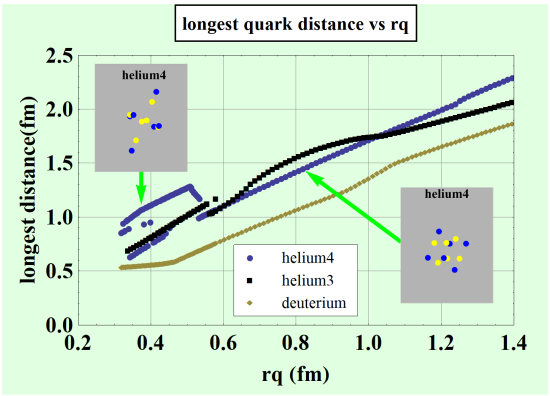

(b) The largest quark distance for deuteriuim and Helium 3 and 4 as function of the 'quark distance' r_q. The Helium-4 distribution changes significantly for $r_q > 0.55$ fm, from an elongated shape to a rounder shape at increasing r_q.

Figure 6.2: Largest quark distance for various low-Z nuclei as function of the 'quark-radius' r_q.

We studied the impact of r_q on some further low-Z nuclei, like Deuterium, Tritium, Helium-3 and Helium-4, as seen in fig. 6.2b. For $r_q = 0.50$ fm, various individual nucleus shapes are given in fig. 6.3.

For r_q = 0.5 fm, the 'stable' quark configurations of more low-Z nuclei are shown in fig. 6.4.

From these quark configurations , we determine the 'largest inter-quark distance', which we then correlate with the Atomic Mass, as shown in table 6.1 (as summary of simulations with varying initial conditions) and visualized in fig. 6.5b. We observe a nice correlation between the 'largest inter-quark distance' and the mass parameter [(M/A-1)*1000)], apart from He3 and Tritium. We find different geometrical structures between He3 and Tritium, as He3 has a centrally +2/3 charged quark, which is not present in Tritium.

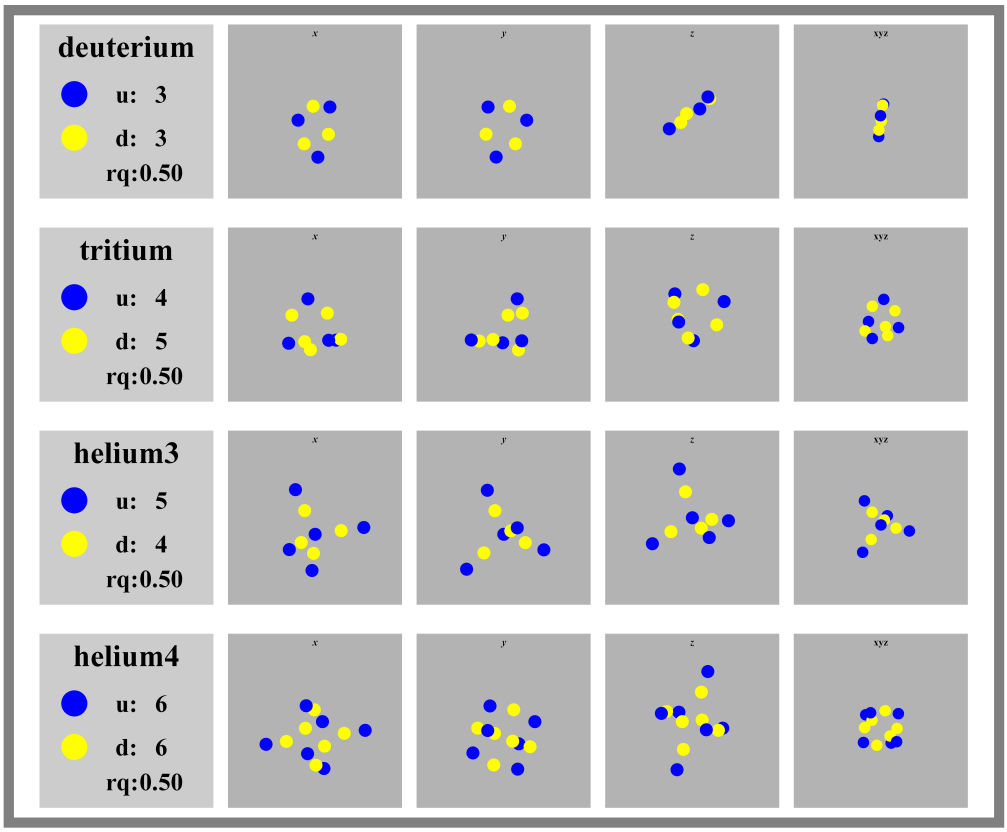

Figure 6.3: The quark distribution of various low-Z elements in 4 different views.

We conclude that the r_q parameter determines the shape of the low-A isotope nuclei, notably up to Lithium-6. For Helium-4, we find various quark configurations for (almost) identical value of r_q , with varying 'largest inter-quark distance'. Therefore, it is crucial to repeat these calculations with a full relativistic, quantum-mechanical model. Then the minimum energy level of a nucleus can be determined and correlated with the atomic mass, in line with chapter 4.

6.4 Conclusions

In this chapter we have looked for a correlation between the quark distributions and the observed atomic mass, using a semi-classical methodology. A correlation between atomic mass and the quark distances has been found, see fig. 6.5b. Notably the atomic mass for helium-4 correlates well with the identified quark distribution.

However, it is clear that these calculations need to be refined, by means of fully relativistic and quantum mechanical analysis. It is then expected that the ground (kinetic) energy state correlates with the mass. This analysis is beyond the scope of this book, and is suggested to the reader.

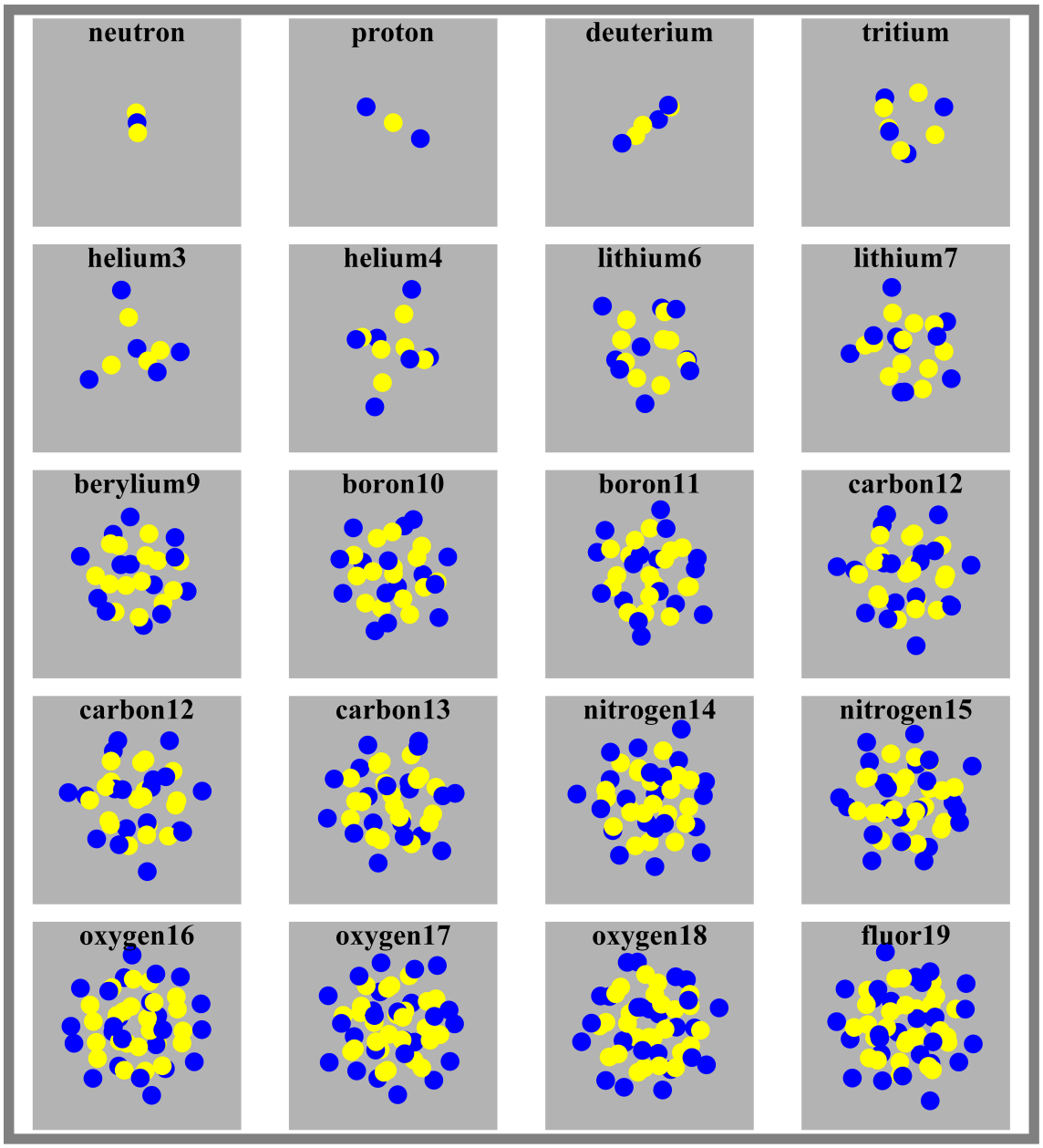

Figure 6.4: Quark distributions inside various light isotopes, based on 'semi-stable-states' arising from the simulations (with parameters: r_q = 0.5 fm, $glue$ = 1.0 GeV/fm). Larger-mass nuclei obtain a spherical shape, with the doubly charged up quark (in blue) positioned at the outside of the nucleus. Low-mass nuclei show various unique shapes: protons and neutrons form a straight line.

Note the extended Helium-4 geometry and the tetrahedron shape of Helium-3, as well as the flat, triangular Deuterium shape, vs the round Tritium shape .

isotope	n	p	Atomic mass	A	(Mass/A-1) *1000	largest distance	2*std	percentage (%)
neutron	0	1	1.008665	1	8.665	0.530	0.000	0.0
proton	1	0	1.007825	1	7.825	0.660	0.002	0.3
deuterium	1	1	2.014102	2	7.051	0.637	0.000	0.0
tritium	1	2	3.016049	3	5.350	0.784	0.000	0.1
helium3	2	1	3.016029	3	5.343	1.011	0.000	0.0
helium4	2	2	4.002603	4	0.651	1.268	0.000	0.0
lithium6	3	3	6.015123	6	2.520	1.185	0.061	5.1
lithium7	3	4	7.016003	7	2.286	1.131	0.000	0.0
berylium9	4	5	9.012183	9	1.354	1.341	0.000	0.0
boron10	5	5	10.012937	10	1.294	1.466	0.000	0.0
boron11	5	6	11.009305	11	0.845	1.407	0.010	0.7
carbon12	6	6	12.000000	12	0.000	1.399	0.020	1.4

Table 6.1: Relative atomic masses (to Carbon-12) of various light isotopes, with A = sum of neutrons (n) and protons (p) [92]. The distance is the largest distance between any quark in a given isotope. We exucted 9 simulations per isotope with varying initial conditions for quark positions and velocities, with $r_q = 0.5\,fm$ and $glue = 1.0\,GeV/fm$. Std represents the standard deviation of the distance for the simulations, and '%' is the percentage of 2*std/(largest distance), as an indicator of the repeatability of the simulation results.

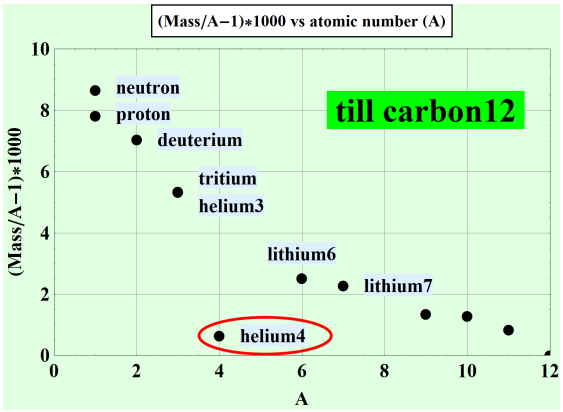

(a) Experimental relative atomic mass (mass/A -1) * 1000 as function of atomic number A [92].
Note the low mass value for Helium-4.

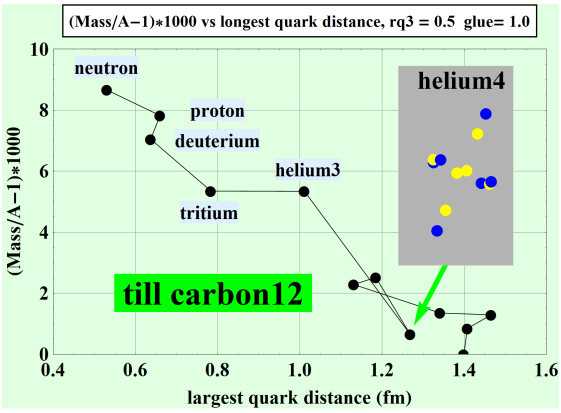

(b) Simulation results of the largest inter-quark distance vs relative atomic mass (mass/A -1)*1000 for various low-A isotopes, for r_q = 0.5 fm and $glue$ = 1.0 GeV/fm. Note the large value of the largest quark distance for Helium-4.

Figure 6.5: Relative atomic mass for various light elements: experimental and simulated results.

7. Inertial force

7.1 Introduction

The origin of inertia has been subject of many debates in physics (see [18, 55] for (historic) reviews)[1]. Starting with Newton's 'absolute space' as reference for acceleration, many physicists were quick to doubt anything that can act (=cause an inertial force) but cannot be acted upon. However, Newton's famous thought experiment on the rotating water bucket [18, 70], see fig. 7.1, clearly showed that only rotation, relative to 'absolute space' results in locally observable facts.

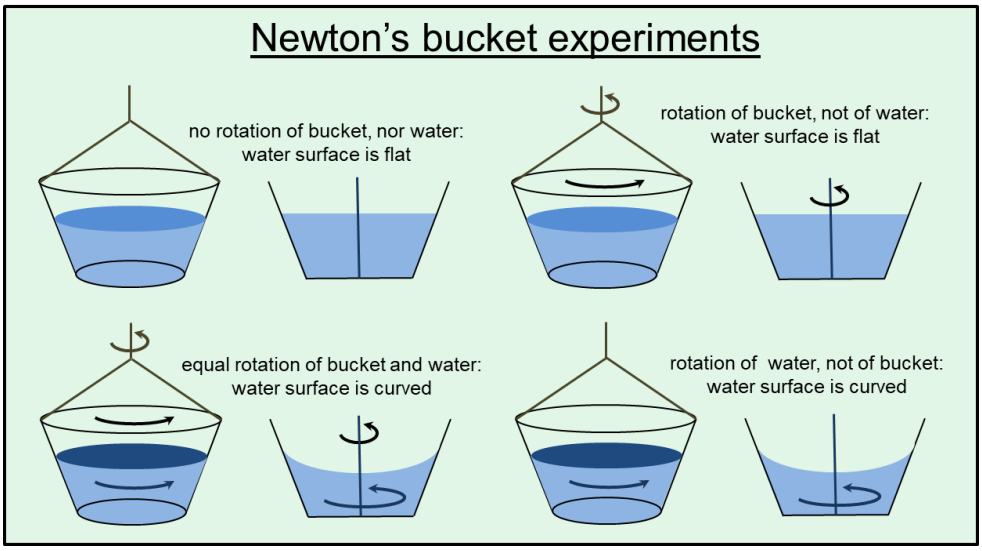

Figure 7.1: Newton's water bucket thought experiment, proving - to Newton - the existence of absolute space, as acting medium. The water shape only changes when the water is rotating relative to absolute space, and is not influenced by the rotation state relative to the bucket.

Mach replaced 'absolute space' by the 'distant stars' as source for inertia, without indicating an interaction mechanism [18, 66, 69, 70]. The instantaneous 'action at a distance' did not fit well into Special Relativity, which is based on a finite speed of interaction. The equivalence principle [66, 69, 70] *postulated* the equality of inertial and gravitational mass. In 1953, Sciama

[1] This chapter is an extended and reworked version of [13].

$\vec{F}_g$	Gravitational interaction force between particle and observer (= 3D vector)
$\vec{E}_g$ $\vec{B}_g$	field vectors to arrive at the interaction force vector
$\vec{r}$	position of gravity field generating particle $\overrightarrow{r_{part}}$ compared to observer $\overrightarrow{r_{obs}}$, in direction particle to observer: $\vec{r} = \overrightarrow{r_{obs}} - \overrightarrow{r_{part}}$. For $\overrightarrow{r_{obs}} = \vec{0}$: observer in center.
$\vec{v}$ $\vec{a}$	velocity $\vec{v} = d\overrightarrow{r_{part}}/dt$ and acceleration $\vec{a} = d\vec{v}/dt$ vectors of particle relative to the observer
r v	vector norm of $\vec{r}$ and $\vec{v}$
c	velocity of the expansion of gravity in vacuum
s	r - ($\vec{r}$ • $\vec{v}$) / c
G	Gravitational constant $\approx 6.67 \times 10^{-11} m^3\, kg^{-1}\, s^{-2}$
m_{obs}	gravitational mass of the static observer, located at the origin $(x, y, z) = (0, 0, 0)$
m_{part}	gravitational mass of the field generating, moving, particle
• *	represent the vector dot product and vector cross product

Table 7.1: Explanation of terms in Eq. (7.1).

[37] proposed an explanation for inertia in a steady-state universe model, based on an analogy between gravity and the electro-magnetic field theory. However, the steady-state universe model is not in accordance with the observation of the Hubble expansion of the universe [69, 70].

In this chapter we will pursue the origin of inertia further, assuming gravity as the interaction mechanism. First we evaluate the origins of inertia in a steady state universe model and will reproduce the results of Sciama in a more explicit form, including mass dilation. Then we will study the Hubble expanding universe. We will start from the linearized General Relativity equations in the weak field, low velocity approximation and later propose a more generalized approach.

7.2 Gravitational Liénard-Wiechert Force

As indicated in §3.6, the tensor equations describing General Relativity [53, page 109] can be simplified to linear differential equations resembling the Maxwell-equations [48, 18, 65], [70, §15.5] when only low mass densities and low velocities are considered. The Maxwell equations describe (in Special Relativity) the electro-dynamical field of a charged particle in 3-dimensions, assuming a finite field propagation velocity. These linear differential equations can be reformulated for gravity as the (retarded) Liénard-Wiechert fields [64, 69], as discussed in §4.9:

$$\begin{aligned} \vec{F}_g &= -\, m_{obs}\,(\vec{E}_g + \vec{v} * \vec{B}_g) \\ \vec{E}_g = (G\, m_{part}/s^3)\,\big(\,(1-(v/c)^2)\,(\vec{r} - r\,\vec{v}/c) + \vec{r} * ((\vec{r} - r\,\vec{v}/c) * \vec{a})/c^2\,\big) \\ \vec{B}_g &= \vec{r} * \vec{E}_g/(r\,c) \end{aligned} \tag{7.1}$$

For details of the orientation of the coordinates in Eq. (7.1), see fig. 3.4b. The observer (mass) is at the center. The formula abbreviations are given in table 7.1. The static attractive Newton law of gravity re-appears, under the conditions $\vec{v} = \vec{0}$ and $\vec{a} = \vec{0}$. Eq. (7.1) is written in an addition form for m_{part}, allowing integration over all masses under consideration.
Inspired by Sciama [37], we will first evaluate the consequences of Eq. (7.1), for a slow moving ($v/c \ll 1$) observer mass (m_{obs}) in a static universe. We assume a constant (low) mass density ρ throughout the universe (cosmological principle). Under these assumptions, the usage of linearized General Relativity is permitted, and we can compute the total gravitational interaction of the universe by integrating Eq. (7.1) over all masses of the entire universe.

$$\overrightarrow{F_g^{tot}} = \int^{all\ mass} d\vec{F}_g \tag{7.2}$$

7.3 Inertia from static universe

7.3.1 Low velocity inertia

In a static, uniform, universe model, for a slow moving observer, the condition $v/c \ll 1$) is fulfilled. Under these conditions Eq. (7.1) can be simplified further, to:

$$\begin{aligned} \vec{F}_g &= -m_{obs}(\vec{E}_g + \vec{v} * \vec{B}_g) = -m_{obs}(\vec{E}_g + (\vec{v}/c) * ((\vec{r}/r) * \vec{E}_g)) \\ &= -m_{obs}\vec{E}_g = -G\,m_{obs}(m_{part}/r^3)(\vec{r} + \vec{r} * (\vec{r} * \vec{a})/c^2) \end{aligned} \tag{7.3}$$

Note that the term involving $\vec{B}_g$ has dropped out of the equations due to $v/c \ll 1$ - see also appendix E. We now start our evaluations of a uniform static universe: a sphere with the slow moving observer in its center. When the observer is moving in the static universe, it appears as if all particles of the universe are **instantaneously** counter moving, see fig. 7.2a. Note that this is not a violation of Special Relativity, as the observer moves in the pre-existing retarded Liénard-Wiechert field.

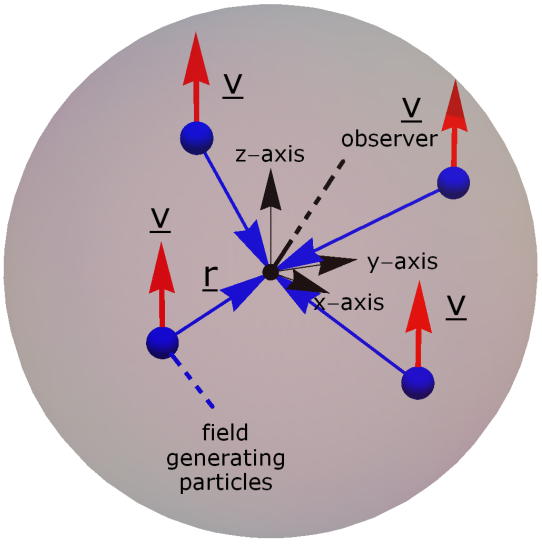

(a) When the observer moves: the universe appears to **instantaneously** counter move.

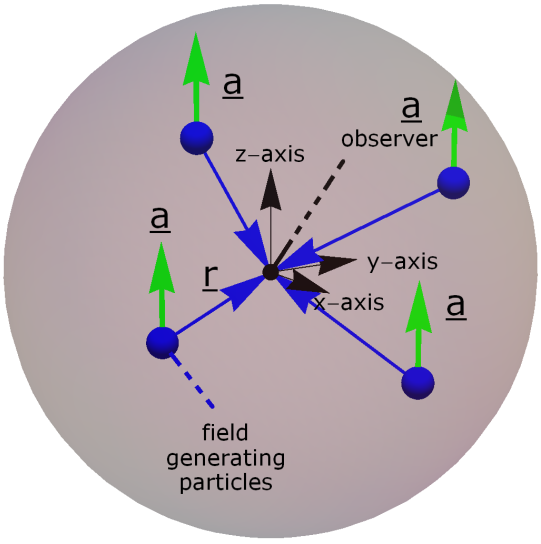

(b) When the observer accelerates: the universe appears to **instantaneously** counter accelerate.

Figure 7.2: Impact of observation of movement status of the static universe, depends on the movement of the observer.

Now we take a full integration of Eq. (7.2) using Eq. (7.3) and $\vec{a} = \vec{0}$, over a sphere in spherical co-ordinates: $(x, y, z) = (r\,Cos[\phi]\,Sin[\theta],\, r\,Sin[\phi]\,Sin[\theta],\, r\,Cos[\theta])$ (see fig. C.1a in appendix C) and replace m_{part} in a uniform universe ($\rho = \rho_0$) by the integration quantity,

$$d\,m_{part}[r] = \rho_0\,Sin[\theta]\,r^2\,d\phi\,d\theta\,dr \tag{7.4}$$

This results in a zero net force, which means that a moving observer experiences no interaction of the entire static universe (for $v/c \ll 1$). This means that any object in slow uniform motion, remains in uniform motion, which is Newtons first law.

Now we compute the interaction of an accelerated, uniform, static universe with the mass of the observer in the center [37], see fig. 7.2b. We execute the integration of Eq. (7.2) using Eq. (7.3) for $v/c \ll 1$ and with $\vec{a} \neq \vec{0}$ [85]:

$$\begin{aligned} \vec{F_g} &= -m_{obs} \int_0^{r_{max}} \int_0^{\pi} \int_0^{2\pi} \rho_0 r^2 \, Sin[\theta] \, \vec{E_g} \, d\phi d\theta dr \\ &= m_{obs} \, \vec{a} \, (8\pi \rho_0 G/3c^2) \int_0^{r_{max}} r \, dr \\ &= m_{obs} \, \vec{a} \, (4\pi \rho_0 G/3) \, r_{max}^2 / c^2 \end{aligned} \tag{7.5}$$

The resulting force of the accelerated universe is proportional to m_{obs} and $\vec{a}$, in the direction of the acceleration, which means that the mass of the observer attempts to join the acceleration of the universe. It resists the acceleration initiated by an external force, which is called inertia!

The upper integration limit r_{max} can be derived from a side step to the Hubble expanding universe. At r_{max}, it is assumed that the masses of universe move away at the maximum allowable velocity c, and consequentially have negligible interaction. Starting from the linear Hubble expansion formula $v = Hr$, the integration limit r_{max} can be found to equal c/H (which we label as r_{Hubble}). Eq. (7.5) reduces to:

$$\vec{F_g} = m_{obs} \, \vec{a} \, (4\pi \rho_0 G/3H^2) \tag{7.6}$$

Identifying Eq. (7.6) as Newtons 2nd law $\vec{F} = m\vec{a}$, (and dropping the 0 in ρ_0) we find that $(4\pi\rho G/3H^2)$ must be close to unity. From WMAP and Planck data [3, 89, 39] we know that the curvature of space is 'flat' to within 0.4%. Cosmological space flatness leads, in the General Relativity Friedman model [65, 70], to the condition: $\Omega_{tot} = 8\pi\rho G/3H^2 = 1$. Therefore we find that $4\pi\rho G/3H^2$ is in the order of unity.

7.3.2 High velocity inertia

For mathematical simplicity we first study the static universe, with one moving, accelerated mass. For the gravitational force impact of the static universe on a moving, accelerated mass we use Eq. (7.1) and (7.2), with a constant mass density ρ in similar was as done in §7.3.1. Using spherical space coordinates, $\vec{x} = (x, y, z) = (r\,Cos[\phi]\,Sin[\theta], r\,Sin[\phi]\,Sin[\theta], r\,Cos[\theta])$, see 2-D image in fig. 7.3. Without loss of generality, we take the velocity $\vec{v} = (0, 0, v_z)$ and acceleration $\vec{a} = (a_x, a_y, a_z)$ as equal for all masses of the universe, as perceived by the observer mass at coordinate $\vec{x} = (0, 0, 0)$.

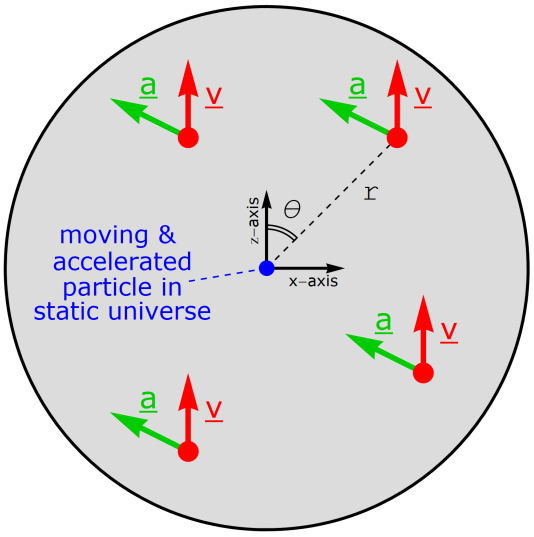

Figure 7.3: accelerated, moving particle (2D), in a static, spherical mass filled, universe.

For a moving, accelerated mass, with $\vec{v} = (0, 0, v_z)$, $\vec{a} = (a_x, a_y, a_z)$, in a static universe, we need to evaluate the total gravitational Liénard-Wiechert force given by (see §7.2):

$$\overrightarrow{F_g^{tot}} = \int^{all\ masses} \vec{F_g^*}\, d\,mass \tag{7.7}$$

where $\vec{F_g^*}$ represents the gravitational force as given by Eq. (7.1), divided by m_{pat}. Also, for later use, we define $\vec{E_g^*} = \vec{E_g}/m_{part}$ and $\vec{B_g^*} = \vec{B_g}/m_{part}$.

The integration over all *moving* masses requires special attention. As discussed in §4.7, we find that the *amount* of the moving mass itself is changed, according to the relativistic Doppler law. Therefore the term $d\,mass$ in Eq (7.7) amounts to:

$$d\,mass = \rho \frac{\sqrt{1-(v_z/c)^2}}{1+(v_z/c)\,Cos[\theta]}\, dx\,dy\,dz \;=\; \rho \frac{\sqrt{1-(v_z/c)^2}}{1+(v_z/c)\,Cos[\theta]}\, r^2\, Sin[\theta]\; d\phi\, d\theta\, dr \tag{7.8}$$

The gravitational force impact of a moving, accelerated mass is given by the Liénard-Wiechert force, Eq (7.1). Therefore the total integration to be evaluated amounts to (see appendix C) [85] :

$$\begin{aligned}\overrightarrow{F_g^{tot}} &= -\,m_{obs} \int_0^{c/H} \int_0^{\pi} \int_0^{2\pi} (\vec{E_g^*} + \vec{v} * \vec{B_g^*})\, \rho \frac{\sqrt{1-(v_z/c)^2}}{1+(v_z/c)\,Cos[\theta]}\, r^2\, Sin[\theta]\; d\phi\, d\theta\, dr \\ &= m_{obs}\, \frac{4\pi\rho\, G}{3\,H^2}\, \left(\frac{a_x}{\sqrt{1-(v_z/c)^2}}, \frac{a_y}{\sqrt{1-(v_z/c)^2}}, \frac{a_z - H\,v_z\,(1-(v_z/c)^2)}{\sqrt{1-(v_z/c)^2}^3}\right)\end{aligned} \tag{7.9}$$

Apart from the factor containing $H\,v_z$, which we will discuss shortly, Eq. (7.9) describes the (gravity induced) force that is needed to accelerate a moving particle. We note that $4\pi\,\rho\,G/(3\,H^2) \approx 1$, as shown in §7.3.1. The inertial force increases compared to a non-moving particle: mass dilation. The mass dilation functions are known from Special Relativity via the gamma function $\gamma[v_z/c] = 1/\sqrt{1-(v_z/c)^2}$, and named 'transverse' and 'longitudinal' mass [53, 30, 69, 70] after multiplication with the (static) **gravitational** mass m_{obs} . The relativistic mechanics force equation is then given by (see also [69, page 82], [70, page 125], [22, 104]) :

$$\overrightarrow{F[v_z, \vec{a}]} = m_{obs}\, (\gamma[v_z/c]^3\, \vec{a}_{\parallel} + \gamma[v_z/c]\, \vec{a_{\perp}}) \;=\; m_{obs}\, d\,(\gamma[v_z/c]\, \vec{v})/d\,t \tag{7.10}$$

where $\vec{a}_{\parallel}$ represents the acceleration in the direction parallel to the velocity vector $\vec{v}$ and $\vec{a_{\perp}}$ indicates the acceleration perpendicular to the velocity. It must be noted that m_{obs} represents the static gravitational mass, which therefore equals the (static - low velocity) inertial mass, as found by Eötvös [63, 69, 70]! This is labeled as the 'weak' equivalence principle. The Mach principle in relativistic form appears, with gravity as acting force. The quantitiy $m_{obs}\gamma[v/c]\,\vec{v}$ is also known as the 'relativistic momentum' [69, §3.2], [70, §6.2].

The energy (E) change of a moving mass is given as $dE = (\overrightarrow{F[v_z, \vec{a}]} \bullet d\vec{x})$ which implies that $dE = (\overrightarrow{F[v_z, \vec{a}]} \bullet d\vec{x}/dt)\,dt = (\overrightarrow{F[v_z, \vec{a}]} \bullet \vec{v})\,dt$. Following integration, it can be shown [64, §9], [66, §17], [69, §3.3], that the energy content of a - gravitational - mass (m) is given by $E = m\,c^2$.

The term proportional to $H\,v_z$ in Eq. (7.9) is a new factor, which is rather small as the value for $1/H \approx 14 \times 10^9$ years (also known as 'age of the universe'). Therefore this term only has impact on extremely large timescales. It is interesting to note that, without external forces, in this static universe model, an initial velocity will increase (as for $v_z/c \ll 1$, we find $a_z = dv_z/dt$ leading to: $dv_z/dt - H\,v_z = 0 \implies v_z(t) = v_0\, e^{H\,t}$. A further line of study could be to verify this property for a Hubble expanding universe. Could this be related to an accelerating expanding universe [94]? A further study of this aspect to the early universe, and thus large values of H, might show a link to the early inflation epoch of the universe [65, 96, 70].

A further notice is that Newton's first law ("An object remains in uniform motion, if no force is employed.") is retrieved from Eq. (7.9), when neglecting the term with $H v_z$. We find that for: $\vec{F}_g = \vec{0} \implies \vec{a} = \vec{0} \implies \vec{v} = \vec{v}_0$.

7.3.3 Critique to the static model

Sofar, we assumed a finite spherical universe with the observer in its center. However, when evaluating the gravitational impact of the universe, assuming the observer is not in its center (see fig. 7.4)[2], it becomes clear that the experienced inertial reaction must be asymmetric. This asymmetry has not been observed in practice in Eötvös [63] type experiments, and would be counter intuitive: its absence would imply (in the static universe model) that the earth has a privileged position in the center of the universe.

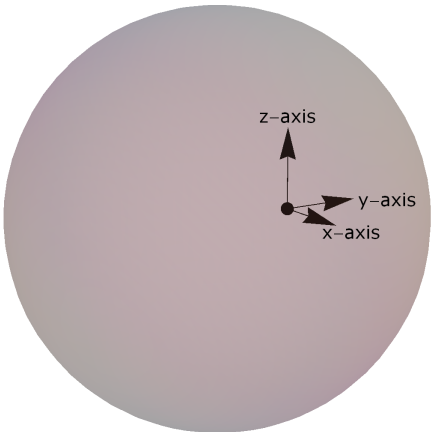

Figure 7.4: When the observer is not in the center of the static universe, asymmetrical inertia results.

A solution to this dilemma can be found by considering the Hubble expansion of the universe. This requires the full generalization of the Liénard-Wiechert equations (7.3) for high velocities, as indicated in §4.9.

7.4 Expanding universe

7.4.1 velocity distribution

Prior to the study of the gravitational impact of the expanding universe on an accelerated mass, we need to establish its mass-velocity distribution for the integration according Eq. (7.2). It was realized by Hubble that objects move away from each other in radial direction [69, 70] (see fig. 7.5). The velocity increases linearly as function of distance, for small values of the resulting velocity compared to c. Our interest is in the interaction between particles at large distances, where the condition $v \ll c$ does not hold. This requires relativistic velocity addition, as given in §3.7 [64, 69]:

$$v_{new}[v_1, v_2] = \frac{v_1 + v_2}{1 + (v_1 \,.\, v_2)/c^2}$$

In order to compute the relativistic Hubble law, we perform a thought experiment with many observers in a row, separated by equal distances (Δr_{Hubble}, with $0 < \Delta \ll 1$), see fig. 7.6.

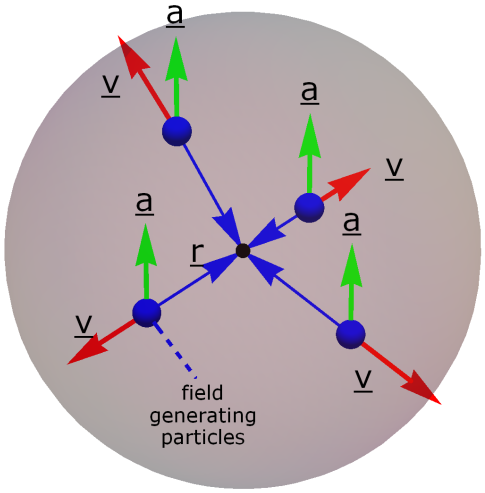

Figure 7.5: Hubble expansion of the universe. Particles move away from the (slowly moving) observer in the center, in radial direction.

[2] or take incomplete integration limits for Eq. (7.5), eg. integrate θ from 0 to $\pi - \delta\theta$.

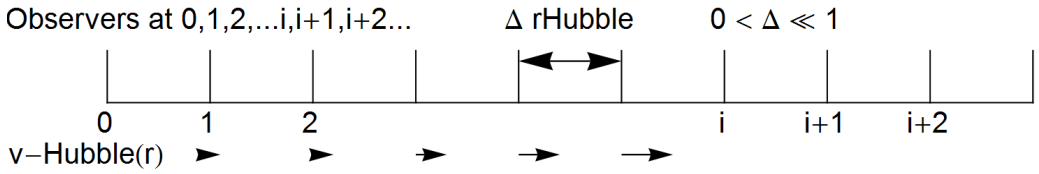

Figure 7.6: Hubble expansion, velocity increase per length increment.

Starting at the origin, we assume each observer (labeled i) to move with a Hubble expansion velocity of $v = H\Delta r_{Hubble} = \Delta c$, with respect to observer $i-1$. To compute the velocity of observer i, compared to the origin, labeled as v_i, we utilize the relativistic velocity addition in a recursive way, and find it to numerically equal $v_i = c\,Tanh[i\,\Delta]$. Thus, the velocity formula for Hubble expansion, as observed by a (static) observer in the center, is:

$$\vec{v}_{Hubble}[\vec{r}] = c\,Tanh[r/r_{Hubble}]\left(\frac{\vec{r}}{r}\right) \tag{7.11}$$

The behavior of this function for $r \ll r_{Hubble}$ corresponds to the original linear Hubble expansion law, see fig. 7.7a.

7.4.2 low velocity inertia

In the Hubble expanding universe, we now evaluate the gravitational impact on an accelerated mass, which co-moves with the masses in its vicinity. This means that the velocity distribution of the masses that it observes from the universe is only radial outwards, as shown in fig. 7.5, with magnitude given by Eq. (7.11). When evaluating the full force integral, Eq. (7.7), we need to consider the Doppler mass contraction, as per Eq. (7.8), which becomes for the radial outward movement ($\theta = 0$):

$$d\,mass = \rho\,\frac{\sqrt{1-(v_{Hubble}/c)^2}}{1+(v_{Hubble}/c)}\,dx\,dy\,dz = \rho\sqrt{\frac{1-(v_{Hubble}/c)}{1+(v_{Hubble}/c)}}\,dx\,dy\,dz \tag{7.12}$$

This is in-line with the relativistic formula for longitudinal frequency Doppler effect [53, page 56]. Combining Eq. (7.11) and (7.12), and expressing in spherical coordinates, assuming a uniform mass density of the universe[3], leads to:

$$d\,mass = \rho\; e^{-r/r_{Hubble}}\; r^2\,Sin[\theta]\;d\phi\,d\theta\,dr \tag{7.13}$$

Now we can calculate the total gravitational force of a (slow moving) accelerated particle in an infinite Hubble expanding universe, see fig. 7.5. We use spherical coordinates for the integration, with infinity as upper limit for the radius. The acceleration is given as $\vec{a} = (a_x, a_y, a_z)$. We define the help variable $x = r\,/\,r_{Hubble}$ to evaluate Eq. (7.7) leading to (more details are given in appendix D):

$$\begin{aligned}\overrightarrow{F_g^{tot}} &= -\,m_{obs}\int_0^{\infty}\int_0^{\pi}\int_0^{2\pi}(\vec{E}_g^* + \vec{v} * \vec{B}_g^*)\,\rho\; e^{-r/r_{Hubble}}\; r^2\,Sin[\theta]\;d\phi\,d\theta\,dr \\ &= m_{obs}\,\frac{4\pi\rho G}{3H^2}\,(a_x, a_y, a_z)\int_0^{\infty} x\,e^{-x}\,(1+e^{-2x})\,dx = m_{obs}\,\vec{a}\,\frac{40\pi\rho G}{27H^2}\end{aligned} \tag{7.14}$$

It is remarkable that an infinitely sized universe gives a finite result on inertia. An analysis of the convergence of Eq. (7.14), shows that the contributions of masses at distances larger than r_{Hubble} are dominant, as shown in fig. 7.7b. This means that the universe is infinitely filled with expanding mass, see fig. 7.8a.

[3] which it has at length scales $> 0.01\,r_{Hubble}$ [31].

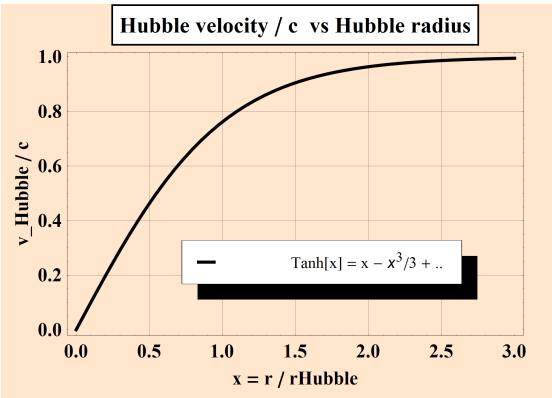

(a) Relativistic Hubble expansion: Tanh function

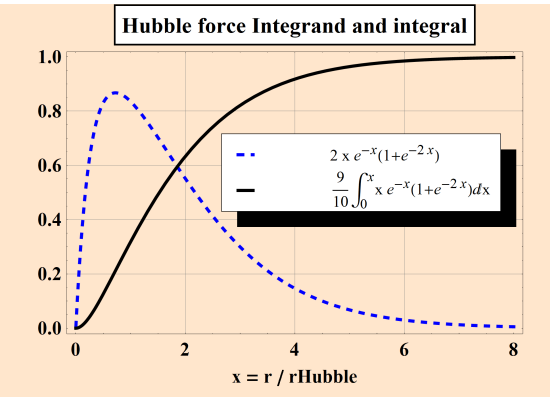

(b) Relative contribution to inertia vs distance: most inertia is generated at distances larger than r_{Hubble}.

Figure 7.7: Hubble expansion impact.

From Eq. (7.14) it is clear that the inertial force is proportional to the gravitational mass of the accelerated observer (m_{obs}) and the acceleration. It gives equality of inertial mass and gravitational mass, as was observed by Eötvös[63] and others [43]. This equality is often labeled as the (weak) equivalence principle [103], see also appendix A. For General Relativity the equivalence principle is a starting postulate (=assumption), where here we find it as result from our theory.

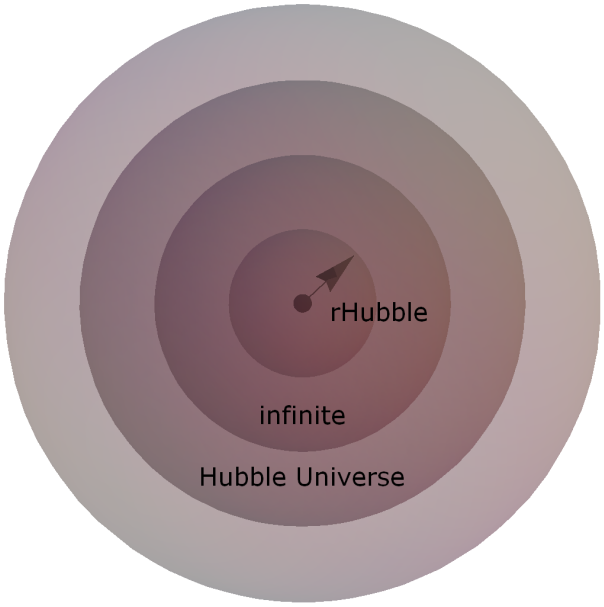

(a) Infinitely mass filled expanding Hubble universe.

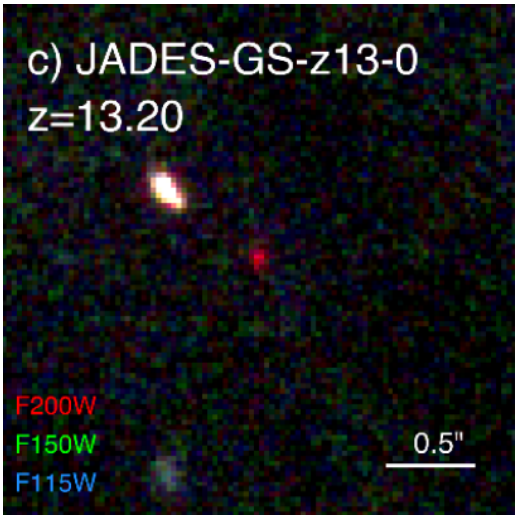

(b) James Webb [90] image of JADES-GS-z13-0: with a z-shift of ≈13.2, being one of the most distant galaxy discovered sofar, at $r/r_{Hubble} \approx 2.6$ according to Eq. (7.26).

Figure 7.8: Some impressions of the infinite expanding universe.

'Small' local deviations from the average mass density ρ [31] have no effect on the overall gravitational force on an accelerated observer. Also moving the observer to another position in the expanding universe does not change the analysis (assuming the observer co-moves, as per Hubble law, with the nearby masses). The asymmetry issue of the finite, static universe does not hold in an infinite, expanding universe. The asymmetry argument will be furher discussed in appendix F.

Note that we have performed these calculations based on Euclidean 3D-space, without intrinsic space curvature. The infinite homogeneity of the universe already implies the model universe without intrinsic curvature, as any local curvature would violate the homogeneity of the universe (= cosmological principle).

7.4.3 High velocity inertia

When evaluating the high velocity gravitational force in the Hubble expanding universe, special attention is needed for the calculation of the velocity of the gravitating masses of the universe as observed by the accelerated, fast moving particle. This velocity is the 3-D relativistic velocity addition [as given in §3.7.2] of the original velocity of the observer particle $\vec{v_{12}} = (0, 0, v_z)$ (with respect to the average of nearby masses ($r < 0.01\, r_{Hubble}$) of the expanding universe) and the Hubble velocity of the masses of the universe $\vec{v_{23}} = c\,(\vec{r}\,/\,r)\,Tanhr[\,r\,/\,r_{Hubble}\,]$. An impression of the resulting velocity distribution of the universe, as perceived by the moving (accelerated) particle, located at position $(x, y, z) = (0,0,0)$, is given in fig. 7.9.

From this velocity distribution we can compute the mass Doppler impact as given by Eq. (7.8), which now needs to be generalized as [69, page 109] (with m_0) the static gravitational mass):

$$mass[\,\vec{v}, \vec{r}\,] = m_0 \frac{\sqrt{1-(v/c)^2}}{1-(\vec{v}.\vec{r})\,/\,(r\,c)} \tag{7.15}$$

An example of the resulting gravitational mass Doppler effect ($\frac{mass[\,\vec{v},\vec{r}\,]}{m_0}$) is given in fig. 7.10.

Now we have all components to evaluate the total gravitational force as expressed in the first line of Eq. (7.9). For an infinitely sized ($r \to \infty$), homogeneous ($\rho = \rho_0$) universe the (inertial) gravitational force can be reformulated to:

$$\overrightarrow{F_g^{tot}} = -\,m_{obs}\,\rho_0 \int_0^{\infty}\int_0^{\pi}\int_0^{2\pi} (\vec{E_g^*} + \vec{v} * \vec{B_g^*}) \frac{\sqrt{1-(v/c)^2}}{1-(\vec{v}.\vec{r})\,/\,(r\,c)}\, r^2\, Sin[\theta]\, d\phi\, d\theta\, dr \tag{7.16}$$

An analytical evaluation of Eq. (7.16) is a task yet to be resolved. When analyzing the integrand only, we find:

1. **Force at constant velocity** : is found in the direction of the movement, leading to additional acceleration, as discussed at the end of §7.3.2
2. **Extra force under acceleration** : An acceleration in z- (or x-) direction results in a force (on top of the constant velocity force), purely in the direction of acceleration.

In short: Solving Eq. (7.16) is key to completion of the 'inertia-by-gravity' study.

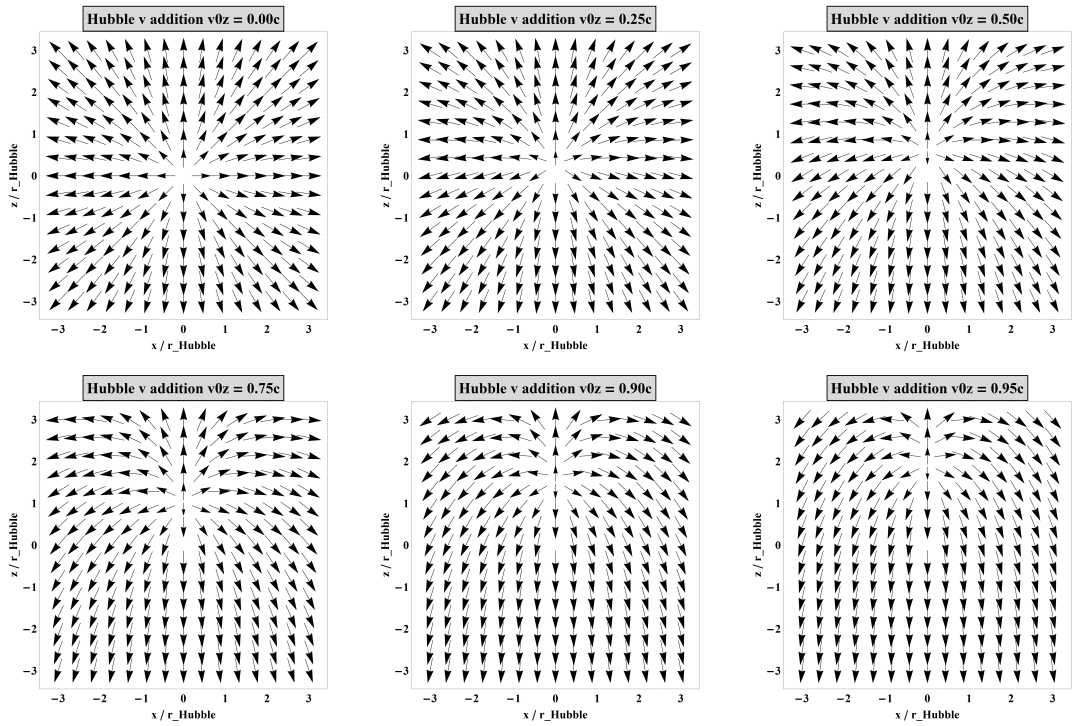

Figure 7.9: Velocity of the masses in the Hubble expanding universe as experienced by an (upwards) moving particle with velocity v_z, located at $(x, y, z) = (0,0,0)$, for various particle velocities, represented in 2D. The x- and z-axis (with $y = 0$) are scaled to $r_{Hubble} = c/H$. The top-left image (for $v_z/c = 0$) is a two-dimensional representation of fig. 7.7a. The bottom left graph (for $v_z/c = 0.75$) gives a zero velocity impression (by the fast moving observer particle) for a mass located at $(x, z)/r_{Hubble} \approx (0, 1)$, as there the (receeding) Hubble velocity equals the (approaching) velocity of the observer particle, see fig. 7.7a.

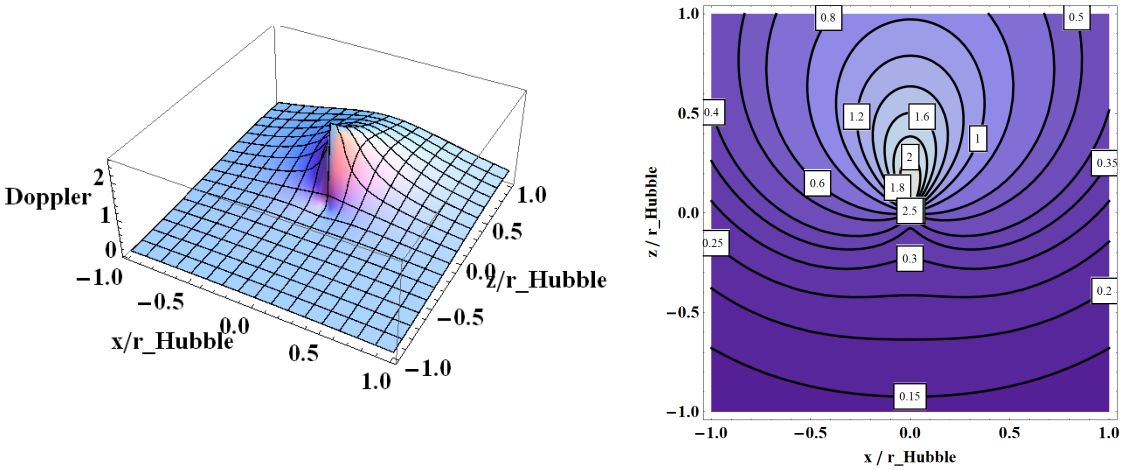

Figure 7.10: Mass Doppler effect, for $v_z = 0.75\,c$ in a Hubble expanding universe. We recognize the increase near $(x,z)/r_{Hubble} = (0,0)$ for positvie z-values (=approaching gravitating masses), and the decrease for negative z-values, as the gravitating masses receed from the observer particle. At $(x,z)/r_{Hubble} \approx (0,1)$, we find from the bottom left graph of fig. 7.9, that $\vec{v_{tot}}/c = \vec{0}$ and thus, from Eq. (7.15), that the mass Doppler effect is absent (= equals unity). Further we find an (exponential) decrease for large distances from the observer particle.

7.5 Gravitational impact of G

We have identified inertia as a gravitational force, proportional to G (see Eq. (7.9)). For an orbiting object around a central mass (M) we find, for non-relativistic velocities, Newton's law. From Eq. (7.1) and Eq. (7.2) - with position of the central mass $\overrightarrow{r_{part}}$ and acceleration[4] defintions from table 7.1 - we find the summation of the gravitational force of the central mass and the inertial force of the - Hubble expanding - universe (see Eq. (7.14) :

$$\overrightarrow{F_g^{tot}} = \frac{m_{obs}\, M\, G}{r^2}\left(\frac{\overrightarrow{r_{part}}}{r}\right) + \frac{40\,\pi\,\rho\, m_{obs}\, G}{27\, H^2}\overrightarrow{a_{part}} = \vec{0} \tag{7.17}$$

More generally, when only gravitational effects are present, Eq. (7.1) learns that these effects are proportional to G. Therefore G drops out of the equation. The actual value (or **sign!**) of G is not an orbit influencing factor! This implies that it is inconsequential for astronomical phenomena, such as star or planet formation whether we call gravity attractive or repulsive. The net effect of 2 gravitating particles (initially at rest, as part of the expanding universe) remains the same: reduction of their distance over time. As such gravity will always be experienced as attractive!

We studied the origins of gravity in chapter 4 and identified the electro-dynamical forces of moving quarks as root cause. This leads to the value of G, as expressed by Eqs. (4.7) and (4.8), requiring quark velocities, inside protons and neutrons, near the speed of light. This is expected from quantum mechanical considerations as given in chapter §3.4.2. Thus our inertia assessment ('due to gravity'), leading to freedom of sign of G, allows consistency of the the quark-gravity model.

7.6 Planetary motion - Mach

Another computation is the slow motion orbit[5] ($v/c \ll 1$) of the observer around a large central mass comparable to a planetary motion, where $m_{obs}/M \ll 1$. Assuming movement in only (x,y) plane (z=0), we find from Eq. (7.17) (dropping m_{obs}):

$$\begin{aligned}(40\,\pi\,\rho\, G/27H^2)\, a_x + G\,M\,Cos[\phi]/r_m^2 &= 0\\ (40\,\pi\,\rho\, G/27H^2)\, a_y + G\,M\,Sin[\phi]/r_m^2 &= 0\end{aligned} \tag{7.18}$$

with: r_m as distance from observer to the central mass and $\vec{a} = (a_x, a_y, 0)$. Equations (7.18) allow a circular orbit (as well as an elliptical orbit), as $x[t] = r_m\, Cos[\omega\, t]$, $y[t] = r_m\, Sin[\omega\, t]$, resulting in the Kepler law:

$$\omega^2\, r_m^3 = 27\, M\, H^2/(40\,\pi\,\rho) \tag{7.19}$$

Equation (7.19) is an explicit form of Mach's principle: planetary movements are determined by the mass distribution of the universe, with gravity as interaction.

The realization that inertia is the result of the gravitational impact of all masses in the infinite expanding universe, ends the debate on 'absolute space' (as introduced by Newton, following his famous rotating water bucket thought experiment [18, 70], see fig. 7.1 - criticized by Mach). 'Absolute space' in itself does not exist. Everything needs to be evaluated relative to everything else, but... our (only available) universe provides an absolute inertial reference frame[6], through the gravitational interaction with all masses of the infinite expanding universe.

[4] The central mass has the same acceleration as the average of other masses of the universe (which create inertia).

[5] A more extended treatment of orbits will be given in chapter 8.

[6] In appendix A, we revisit the equivalence principle.

7.7 Evolution of the universe

We have shown the expanding universe to be infinitely large. This means that it will always be infinitely large, but also that it has always been infinitely large. In this paragraph we evaluate the time evolution of a small part of the universe. Sofar we have assumed a constant value for the

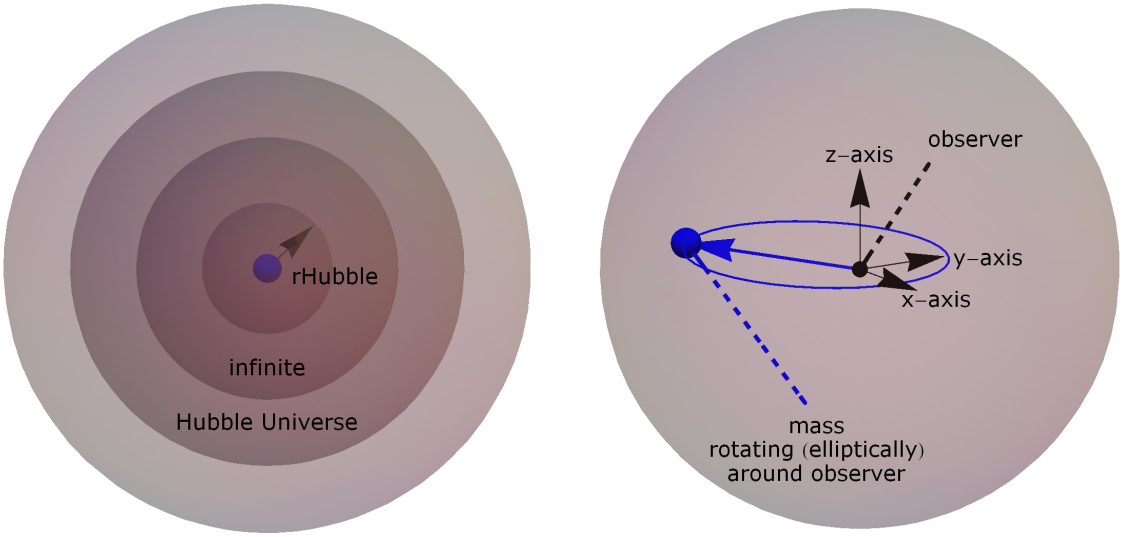

(a) A small part in the infinitely mass filled expanding Hubble universe.

(b) Elliptical orbit around central mass.

Figure 7.11: Hubble expansion of small sphere & elliptical planet orbit.

Hubble expansion factor H. However, when studying a small expanding sphere of $r \ll r_{Hubble}$ with fixed mass M, we realize that the condition of unity in Eq.(7.6) (static universe model) and (7.14) (Hubble expanding universe model) implies a change in mass density ρ, even for constant H. We now study the time evolution of the radius *r[t]* in which the mass M is contained, with assumed homogeneous mass density ρ. We will assume G to be a universal constant (indicating that the gravitational force between two objects is a constant) and assume (see Eq. (7.14)) $40\pi\rho\,G/27\,H^2 = 1$ to be valid over time, leading to constancy of the $\vec{F} = m\,\vec{a}$ formula. We rewrite H as:

$$H[t] = (dr/dt)/r \quad \Longrightarrow \quad (dr/dt)/r = \sqrt{40\pi\rho\,G/27} \tag{7.20}$$

and identify the mass M of the sphere under study as constant, in flat space-time ($M = 4/3\pi\,\rho\,r^3$). With this, we re-arrange Eq. (7.20) (and use for simplification[7] $\sqrt{40/27} \approx \sqrt{4/3}$) to arrive at:

$$(dr/dt)/r = \sqrt{MG/r^3} \quad \Longrightarrow \quad dr/dt - \sqrt{MG/r} = 0 \tag{7.21}$$

This equals the Einstein-deSitter equation for the flat - mass filled - universe [70, page 401], [69, §9.4], [65, §15.5] which can be solved as:

$$r[t] = r_0\,(1 + \sqrt{3\pi G\rho_0}\;t)^{2/3} \tag{7.22}$$

where r_0 and ρ_0 indicate the initial size and initial mass density of the small part of the infinite universe. Eq. (7.22) can be further simplified re-using $4\pi\rho\,G/3\,H^2 = 1$ and introducing H_0 as initial Hubble expansion coefficient, to arrive at:

$$r[t] = r_0\,(1 + 3/2\,H_0\,t)^{2/3} \quad \Longrightarrow \quad dr/dt \approx H_0\,r_0 - \frac{1}{2}\,H_0^2\,r_0\,t \tag{7.23}$$

[7] It must be noted that if we replace the factor 4/3 in $4\pi\rho\,G/3\,H^2 = 1$ by any other number (such as 8/3, to arrive at the Friedmann 'critical mass density' condition [65, 69, 70]), the result of Eq. (7.23) remains identical.

For small timescales compared to the initial Hubble time scale ($H_0\, t \ll 1$), the linear Hubble expansion law ($v = H\, r_0$) is regained, by series expansion. Re-inserting Eq. (7.23) in Eq. (7.20) to find the evolution of the Hubble constant over time, we find:

$$H[t] = \frac{2\, H_0}{2 + 3\, H_0\, t} \tag{7.24}$$

Thus the Hubble expansion coefficient will decrease over time.

7.8 Redshift

It was shown that the model of choice for the universe at large is an expanding model of homogeneous mass density and infinite size, without intrinsic space curvature (as deduced from WMAP and Planck data [3, 89, 39]). The infinite homogeneity implies that no net gravitational force exists when moving from one place to another. Therefore observed red shifts from far away galaxies are not due to gravitational effects, but originate purely from velocity-Doppler effects, due to Hubble expansion. For a pure motion away from the observer, the red shift z is given in §3.2 by [69, 70]:

$$z = \sqrt{1 + v/c}\,/\,\sqrt{1 - v/c} - 1 \tag{7.25}$$

With the relativistic Hubble velocity Eq. (7.11), the redshift formula simplifies to:

$$z[r] = e^{r/r_{Hubble}} - 1 \tag{7.26}$$

Therefore, it can be expected that with the ever increasing quality of observation techniques, we will find stars with ever increasing red-shifts $z[r]$. Examples from infra-red studies by the James Webb telescope are given in fig. 7.8b and 7.12.

The Cosmic Microwave Background (CMB) radiation is considered to have a z-shift of ≈ 1100 [71], which leads through Eq. (7.26), to a photon observable universe with a radius of $r_{photon}^{universe} \approx 7\, r_{Hubble}$. Note: the photon radius of the universe is a result of the Big Bang theory, where photons could not penetrate the early plasma (for the first 380.000 years [59, page 149], [71]). However, gravitational forces can penetrate a plasma, therefore no length restrictions exist for the maximum radius of the universe (for gravitational forces, leading to inertia), see also fig. 7.7b.

7.9 Conclusions

In this chapter, it is demonstrated that inertia is the result of the gravitational interaction of all masses of the, infinitely sized, expanding universe. Therefore, the so-called inertial and gravitational masses are equal. The Mach principle was thus made explicit. The value and sign of the gravitational constant G are of no consequence on astronomical scale.

We were able to show the well known inertial mass dilation formula - in Eq. (7.9) - for a static universe model (which is one way [53, page 63], [69, pages 82–83] to prove $E = m\, c^2$). For a Hubble expanding universe, this is still to be shown, by solving Eq. (7.16).

We found that the magnitude of quark velocities for quark-gravity (as discussed in chapter 4) is in the order of the speed of light as was expected from quantum-mechanical reasons, as given in §3.4.2.

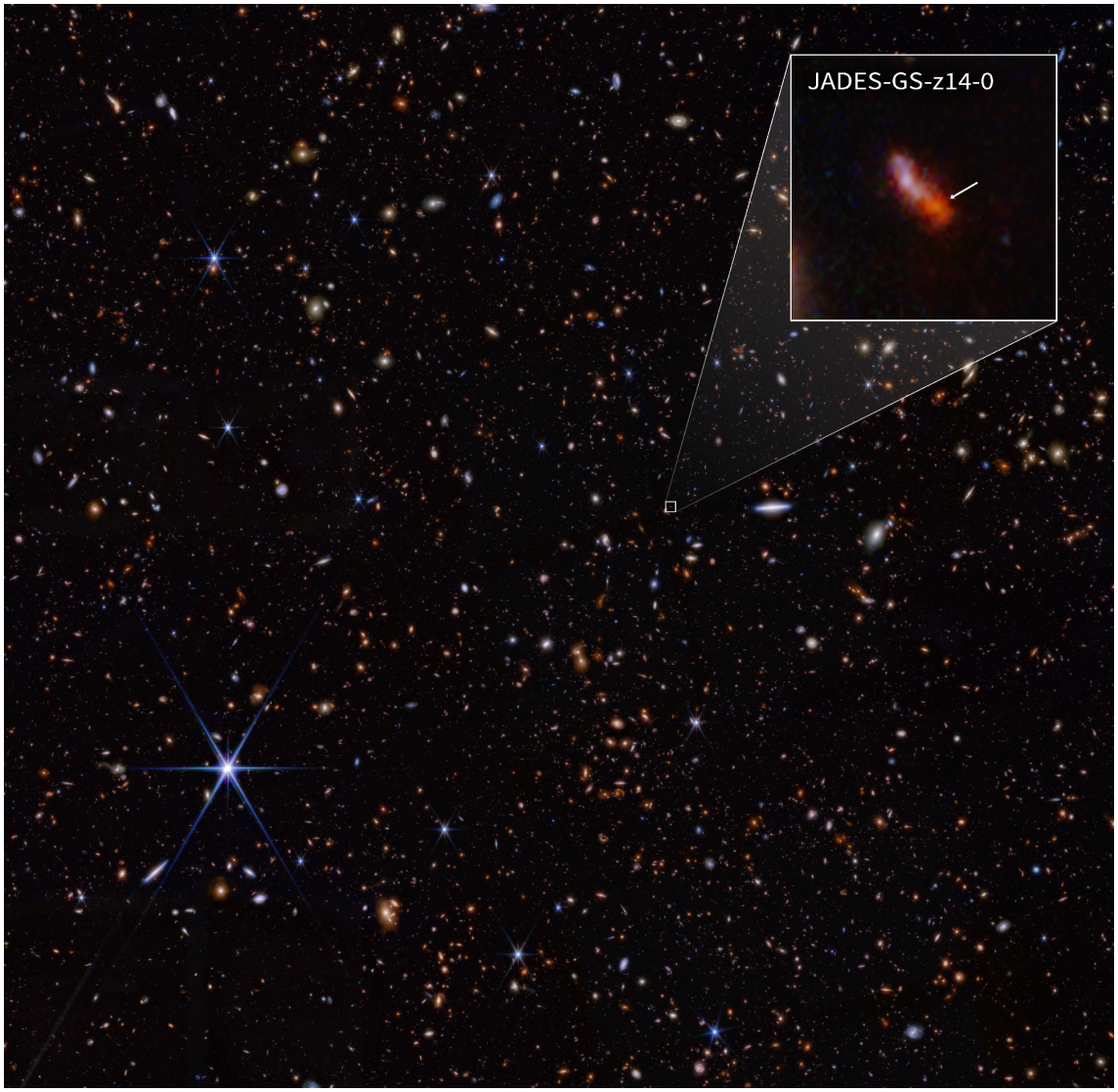

Figure 7.12:
NASA James Webb telescope [90] deep field image,
containing the z-shift $\approx$ 14.3 galaxy JADES-GS-z14-0,
at a distance r from earth, with $r/r_{Hubble} \approx 2.7$ according to Eq. (7.26) .

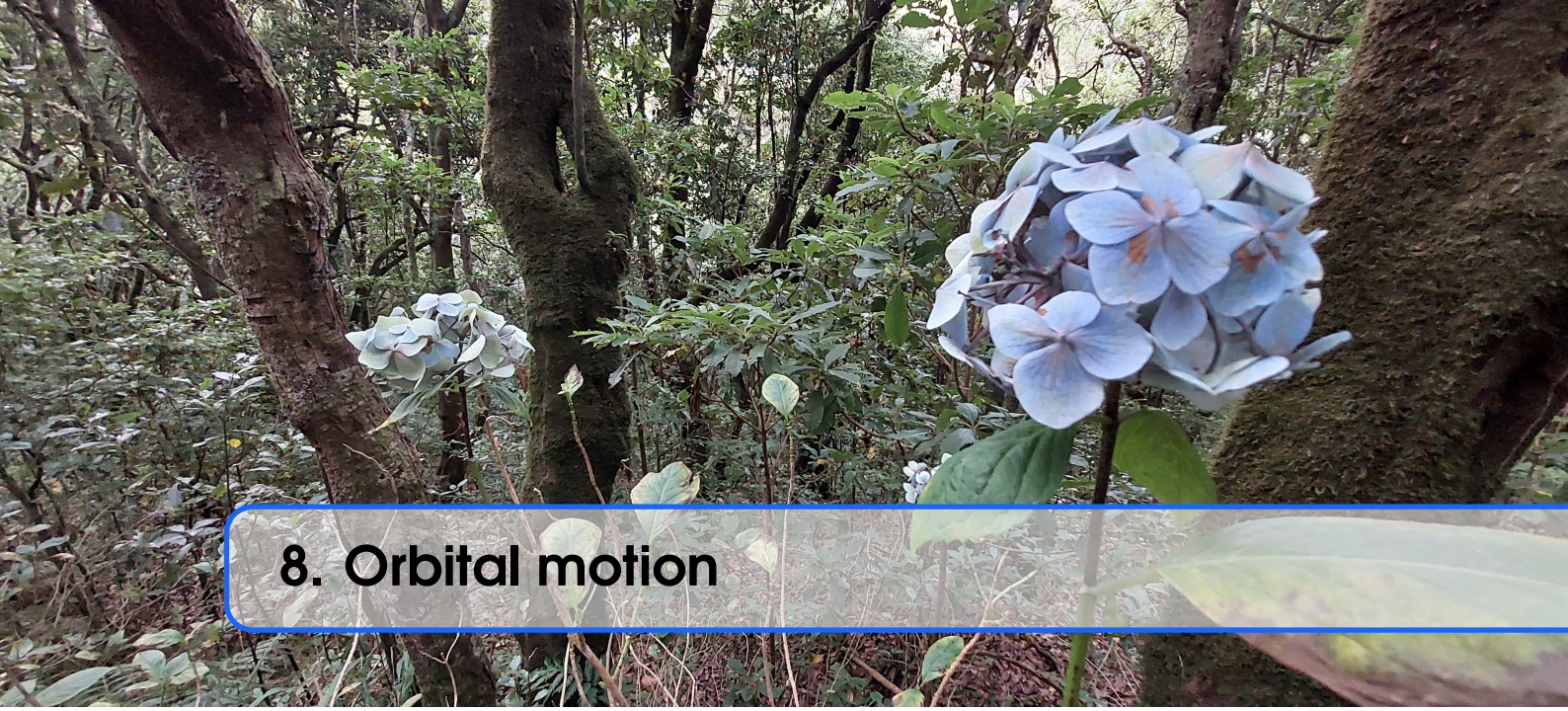

8. Orbital motion

8.1 Introduction

Orbital motion is an important topic for it describes the motion of the planets and at larger scale the galaxies and their interactions. As an example the orbits of stars around the massive black hole in the center of our galaxy (Sagittarius A) have been studied extensively, as seen in fig. 8.1.

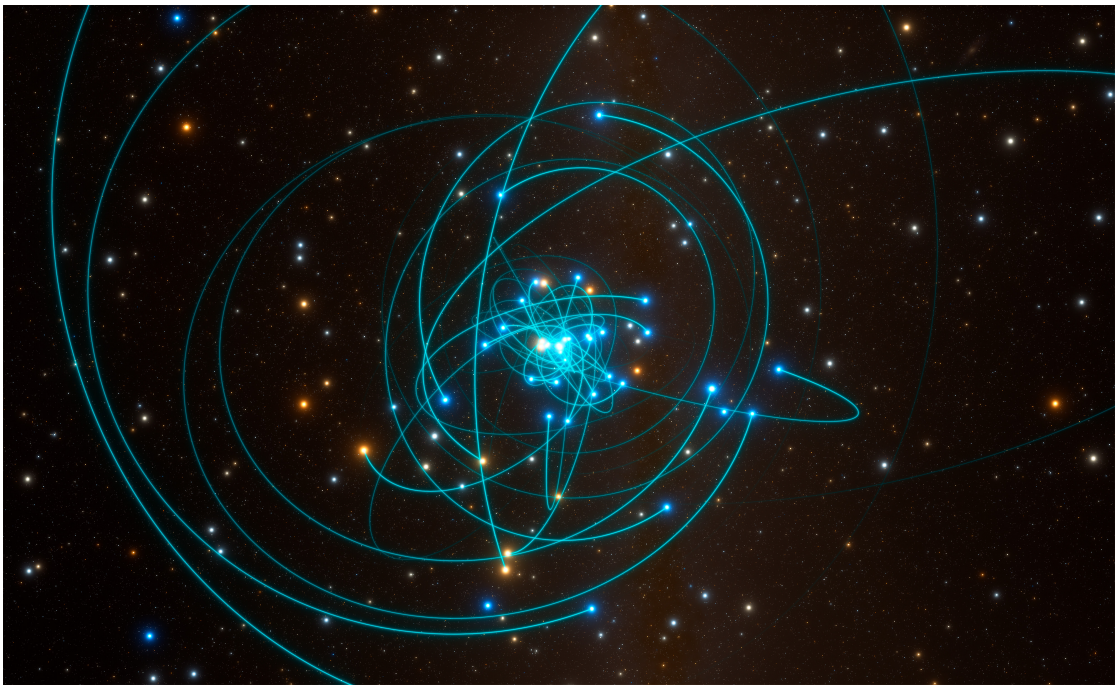

Figure 8.1: ESO/L. Calçada/spaceengine.org [78]:
Observed orbits of stars around Sagittarius A, in the center of our galaxy.

Therefore, we will study orbital motion here, starting with one observer with mass (m_{obs}) orbiting a large central mass (M_0). When an observer mass is only influenced by gravitational forces, it is clear that the vector summation of all gravitational forces is zero. The summation over all gravitational forces ($\vec{F}_g$) due to all masses of the universe and the central mass can be expressed - as also done in Eq. (7.2) - by means of:

$$\overrightarrow{F_g^{tot}} = \int^{all\ mass} d\vec{F}_g = \int^{central\ mass} d\vec{F}_g + \int^{rest\ of\ universe} d\vec{F}_g = \vec{0} \tag{8.1}$$

where $\vec{F}_g$ is expressed as the Liénard-Wiechert force, as given by Eq. (7.1) and Eq.(7.7), where the Doppler function as expressed by Eq. (7.15), is taken into account for the central gravitating mass.

The (net zero) total gravitational force is proportional to $m_{obs}\,G$ and thus these factors fall out of the equations. This proves (once again) the (weak) equivalance principle ('a mass moves independently of its magntitude[1], through a fixed gravitational field' and 'inertial mass is due to gravitational mass'). As already found in §7.5 the sign and magnitude of the gravitational constant G are not orbit determining factors.

As seen in §7.3.2 the gravitational force as perceived by the observer (=orbiting mass) amounts to:

$$\int^{central\ mass} d\vec{F}_g = -G\,m_{obs}\,M_0\,\frac{\sqrt{1-(v/c)^2}}{1-(\vec{r}.\vec{v})/(r\,c)}\left(\vec{E}_g^{*} + \vec{v} * \vec{B}_g^{*}\right) \tag{8.2}$$

The (inertial) impact of the $'rest-of-universe'$ term in Eq. (8.1) has been discussed in chapter 7. The outcome coincides with the Special Relativity prediction of 'transverse' and 'longitudinal' mass impact. We use for the moving particle as velocity $\vec{v} = (v_x, v_y, v_z)$ and acceleration $\vec{a} = (a_x, a_y, a_z)$, with acceleration split into $\vec{a}_{\parallel}$ and $\vec{a}_{\perp}$ (parallel and perpendicular to velocity). Therefore, the inertial forces on a mass, in free motion, is given by Eq. (7.10) [69, page 82], [70, page 125], [22, 104]:

$$\int^{rest\ of\ universe} d\vec{F}_g = m_{obs}\,(\gamma[v/c]^3\,\vec{a}_{\parallel} + \gamma[v/c]\,\vec{a_{\perp}}) = m_{obs}\,d\,(\gamma[v/c]\,\vec{v})\,/\,d\,t \tag{8.3}$$

with $\gamma[v/c] = 1/\sqrt{1-(v/c)^2}$.

In this chapter we study orbit theory. We start in a historical order: from a Newtonian analysis via a General Relativity summary to a quark-gravity analysis of gravitational orbits. This allows to see commonality and differences in approach and results.

[1] More precisely: the moving mass should be sufficiently small compared to the mass that generates the 'fixed' gravitational field. Any falling object on earth (like a Newtonian apple [68, §1.1]) complies to this constraint.

8.2 Newtonian gravity orbit: 1 moving body problem

The evaluation of the orbit of an observer with mass (m_{obs}) around a central mass (M_0) in Newtonian physics is well studied [70, pages 241–242], [4, 75], based on cylindrical coordinates $\vec{r[t]} = (x, y, z) = (r\,Cos[\phi], r\,Sin[\phi], z)$. The Newtonian equations of motion are known as: $m_{obs}\,\vec{a} + G\,M_0\,m_{obs}\,\vec{r}\,/\,r^3 = \vec{0}$ - see also Eq. (7.17)) . Here we assumed that $M_0 \gg m_{obs}$ and thus that the central large mass does not move. The Newtonian force equations can be rewritten in cylindrical coordinates, using the cylindrical coordinates equations for acceleration: $a_r = \ddot{r} - r\dot{\phi}^2$ and $a_\phi = r\ddot{\phi} + 2\dot{r}\dot{\phi}$, with $\dot{\phi} = d\phi/dt, \ddot{\phi} = d^2\phi/dt^2, \dot{r} = dr/dt$ and $\ddot{r} = d^2r/dt^2$. Knowing that we start from an orbit with initially $z = 0$ & $v_z = 0$, we find, expressed in cylindrical coordinates (F_r, F_ϕ, F_z):

$$\begin{aligned} F_r^{tot} &= G\,M_0\,m_{obs}\,\frac{1}{r^2} + m_{obs}\,(\ddot{r} - r\dot{\phi}^2) = 0 \\ F_\phi^{tot} &= m_{obs}\,(r\ddot{\phi} + 2\dot{r}\dot{\phi}) = 0 \\ F_z^{tot} &= m_{obs}\,\ddot{z} = 0 \end{aligned} \tag{8.4}$$

Notably the F_ϕ^{tot} equation in Eq. (8.4) allows an important simplification [4, 75],[82, pages 68–70]. When multiplied by the radius r we arrive at $r^2\ddot{\phi} + 2r\dot{r}\dot{\phi} = d\,(r^2\dot{\phi})\,/\,d\,t = 0$ and thus: $r^2\dot{\phi} = h$, with h being a new orbital constant. This allows a change of variables in the first equation of Eq. (8.4) from time (t) to angular position (ϕ), using $\dot{\phi} = h/r^2$ and $\dot{r} = \frac{dr}{d\phi}\frac{d\phi}{dt} = \frac{dr}{d\phi}\,(h/r^2)$. Then the F_r^{tot} equation in Eq. (8.4) becomes (dropping the mass of the orbiting object m_{obs}:

$$\frac{G\,M_0}{r^2} + \ddot{r} - \frac{h^2}{r^3} = 0 \tag{8.5}$$

We switch to a new orbit variable $u(\phi(t)) = 1/r(t)$, which leads to [75]: $\dot{r} = -u^{-2}\,\dot{u} = -u^{-2}\dot{\phi}u' = -h\,u'$ and $\ddot{r} = -h^2u^2u"$, where the ' and " indicate (single and double) differentiation to ϕ. Then Eq. (8.5) transforms to:

$$G\,M_0\,u^2 - h^2u^2u" - h^2\,u^3 = 0 \implies u" + u = G\,M_0\,/\,h^2 \implies u = \frac{G\,M_0}{h^2}\,(1 + e\,Cos[\phi - \phi_0]) \tag{8.6}$$

where (ellipticity) e and ϕ_0 are constants of integration. Switching back to $r = 1/u$, we arrive at the elliptical orbit (Kepler's law) with the period of revolution (T_{per}) given in line with Eq. (7.19):

$$r[\phi] = \frac{h^2\,/\,(G\,M_0)}{1 + e\,Cos[\phi - \phi_0]} \qquad T_{per}^2 = \frac{4\pi^2}{G\,M_0}\,r_{max}^3 \tag{8.7}$$

with r_{max} is the maximum of the $r[\phi]$, being the semi-major axis of the elliptical orbit (labeled as a), $a = r_{max} = G\,M_0/(1 - e^2)h^2$. We find the velocity and acceleration for the orbit angle $\phi[t]$ and $d\phi/dt = \dot{\phi} = h/r^2$:

$$\begin{aligned} \overrightarrow{x[\phi]} &= r[\phi]\,(Cos[\phi], Sin[\phi]) \\ \overrightarrow{v[\phi]} &= d\vec{x}/dt = d\vec{x}/d\phi\,\dot{\phi} = d\vec{x}/d\phi \;\; h/r^2 \\ \overrightarrow{a[\phi]} &= d\vec{v}/dt = d\vec{v}/d\phi\,\dot{\phi} = d\vec{v}/d\phi \;\; h/r^2 \end{aligned}$$

with $\overrightarrow{a[\phi]}$ of course also given by the Newtonian orbit equation (7.17).

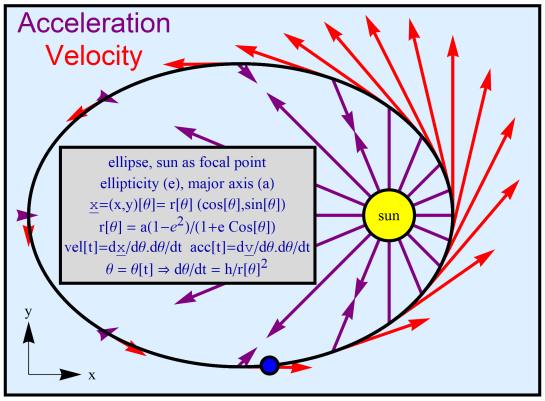

Figure 8.2: Elliptical orbit around central mass, in Newtonian gravity.

The resulting orbit, velocities and accelerations are given (for an example of ellipticity) in fig. 8.2.

8.3 Newtonian gravity orbit: 2-body problem

In the previous paragraph we calculated the orbit of a low-mass particle around a heavy (non-moving) mass, as depicted by the condition ($m_{obs} \ll M_0$). Here we will study the orbits of 2 particles under Newtonian gravity, when their masses (m_1 & m_2) are of equal order. It is then convenient [79, 102, 109] to define the 'Center of Mass' (COM) of the 2 particles and we know each mass is subject to Newtonian gravity in opposite direction. Then we find:

$$\begin{aligned} \overrightarrow{x_{COM}} &= (m_1\,\vec{x}_1 + m_2\,\vec{x}_2)\,/\,(m_1+m_2) \\ m_1\,\vec{a}_1 &= -\,m_2\,\vec{a}_2 = \frac{G\,m_1\,m_2}{|\vec{x}_1-\vec{x}_2|^3}\,(\vec{x}_1-\vec{x}_2) \\ &\Longrightarrow \\ (m_1+m_2)\,d^2\overrightarrow{x_{COM}}/\,dt^2 &= m_1\,\vec{a}_1 + m_2\,\vec{a}_2 = \vec{0} \end{aligned} \tag{8.8}$$

Thus the center of mass movement is independent of the gravitational forces between the 2 masses. We can thus set $\overrightarrow{x_{COM}} = \vec{0}$ as center of the reference system. We now define the vector $\vec{R} = \overrightarrow{x_{COM}} - x_1$, and thus we have $x_2 = \overrightarrow{x_{COM}} - (m_1/m_2)\,x_1$. When we take $R = |\vec{R}|$, we find the distance between the 2 masses $(m_1+m_2)/m_2)\,R$. Then we can express the Newtonian gravity law as:

$$m_1\,d^2\vec{R}/\,dt^2 + \frac{G\,m_1\,m_2}{(\frac{m_1+m_2}{m2})^2\,R^2}\left(\frac{\vec{R}}{R}\right) = \vec{0} \;\Longrightarrow\; d^2\vec{R}/\,dt^2 + \frac{G\,m_2^3}{(m_1+m_2)^2\,R^2}\left(\frac{\vec{R}}{R}\right) = \vec{0} \tag{8.9}$$

This is exactly the same gravitational orbit equation as occurred in the 1-body equations, as discussed in the previous paragraph §8.2, with elliptical solutions. Assuming a non-rotational reference system for the Center of Mass, we find that the 2-body Newtonian problem gives 2 synchronous counter-moving elliptical orbits, as depicted in the fig. 8.3.

The subtle impact of 1-body vs. 2-body orbits on gravitational wave generation, will be discussed in chapter 9.

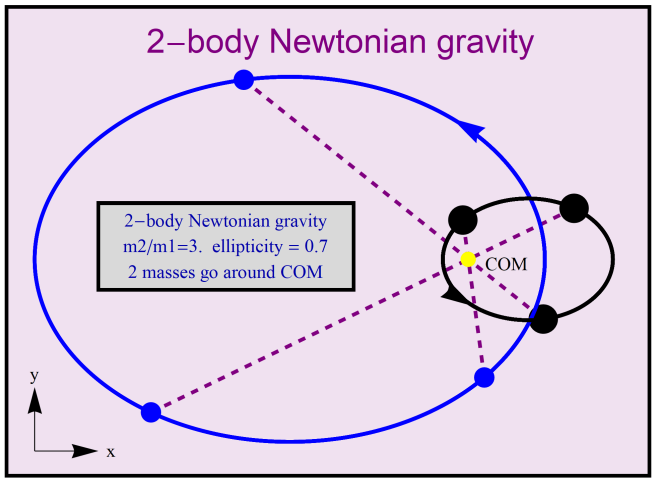

Figure 8.3: 2-body elliptical orbits around center of mass, in Newtonian gravity.

8.4 General Relativity orbit

Orbits in General Relativity have also been extensively studied [52, §39 & §40], [65, pages 230–233], [66, pages 147–150], [68, pages 1110–1116], [69, pages 218–225], [70, pages 241–245], [4] resulting in the well known perihelion shift of planets. The Newtonian equation of motion, as given by Eq. (8.6), receives a relativistic addition, to yield:

$$u'' + u - 3\frac{GM_0}{c^2}u^2 = GM_0/h^2 \qquad \Longrightarrow \qquad \Delta\phi = \frac{6\pi GM_0}{a(1-e^2)c^2} \tag{8.10}$$

where $\Delta\phi$ represents the advance of the perihelion angle of the elliptical planetary orbit per orbit, as shown[2] in fig. 8.4. Interestingly, the perihelion shift also occurs for small values of ellipticity (e). Even a (near) circular orbit has a perihelion shift, which is only possible when an angular force is present.

It is important to remark that the General Relativity orbit assessment has as one of its intermediate results the relation: $r^2\dot{\phi} = h$, which is similar to the Newtonian angular momentum conservation.

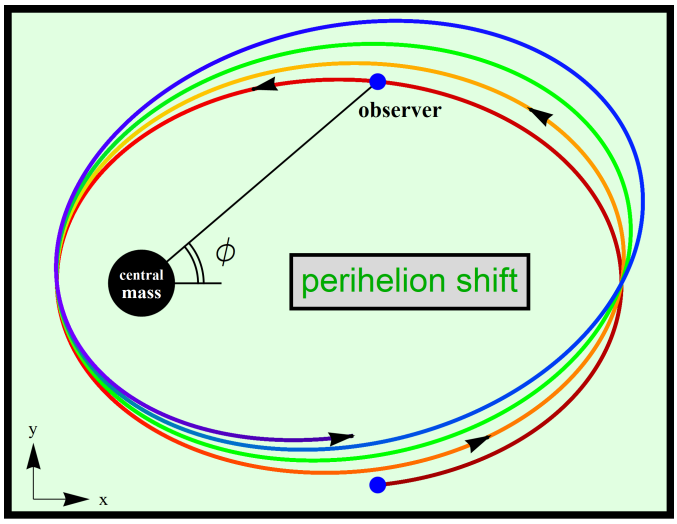

Figure 8.4: Exaggerated perihelion shift of an elliptic orbit, in General Relativity. Color shift - red to blue - shows progress of the orbit.

[2] with exaggerated parameters for ellipticity (e) and perihelion shift intensity $\left(\frac{GM_0}{ch}\right)^2$, also used in fig. 8.5.

8.5 Quark-Gravity: equations of motion

Starting from Eq. (8.1), we first study a mass (M_0) in a motion around an observer. The position is given by $\overrightarrow{r_{part}[t]} = (x[t], y[t], 0)$, $\overrightarrow{v_{part}[t]} = (v_x[t],\ v_y[t], 0)$, $\overrightarrow{a_{part}[t]} = (a_x[t], a_y[t], 0)$, indicating an initial flat orbit. This leads to a Liénard-Wiechert force (in gravitational form Eq. (7.1) - see also table 7.1) without a z-component. Thus a flat orbit is a solution and we continue our analysis in cylindrical co-ordinates $\vec{r}[t] = (r, \phi, 0)$, by using the general equations and its time derivatives. The gravitational force is evaluated by executing the vector calculations of Eq. (8.2), in Cartesian co-ordinates and then switching to cylindrical co-ordinates. The force components (radial: F_r and angular F_ϕ) are found (after an assisted calculation [85]) to be:

$$F_r = \left(\frac{G M_0 m_{obs}}{r^2}\right)\sqrt{1-\frac{\dot{r}^2+\dot{\phi}^2 r^2}{c^2}}\ldots \tag{8.11}$$

$$\ldots\frac{c(c-\dot{r})(c+\dot{r})^2-\dot{\phi}^2(c+\dot{r})(2c+\dot{r})r^2+\dot{\phi}(\ddot{r}\dot{\phi}-\ddot{\phi}(c+\dot{r}))r^3}{(c+\dot{r})^4} \tag{8.12}$$

$$F_\phi = \left(\frac{G M_0 m_{obs}}{r^2}\right)\sqrt{1-\frac{\dot{r}^2+\dot{\phi}^2 r^2}{c^2}}\ldots \frac{\dot{\phi}r(c+\dot{r})^2+(\ddot{\phi}(c+\dot{r})-\ddot{r}\dot{\phi})r^2}{(c+\dot{r})^3}$$

This is the driving gravitational force for a mass in orbit. This force is balanced by the inertial forces, as expressed in Eq. (8.3). We now need to evaluate the components of $\vec{a}_\parallel$ and $\vec{a}_\perp$:

$$\vec{a}_\parallel = \frac{(\vec{a}\bullet\vec{v})}{\|\vec{v}\|^2}\ \vec{v} \qquad\qquad \vec{a}_\perp = \vec{a}-\vec{a}_\parallel \tag{8.13}$$

with $\|\vec{v}\|$ representing the vector norm of the velocity (=total velocity, which is never zero in orbital motion): $\|\vec{v}\| = \sqrt{v_x^2+v_y^2+v_z^2} = \sqrt{\dot{r}^2+r^2\dot{\phi}^2}$, knowing $v_z = 0$.

Now we need to derive the force equation Eq. (8.3), using Eq. (8.13).

$$\int^{rest\ of\ universe} d\vec{F}_g = m_{obs}\,(\gamma[v]^3\,\vec{a}_\parallel + \gamma[v]\,\vec{a_\perp}) \tag{8.14}$$

$$= m_{obs}\,(\gamma[v]^3\,\frac{(\vec{a}\bullet\vec{v})}{\|\vec{v}\|^2}\ \vec{v} + \gamma[v]\,(\vec{a}-\vec{a}_\parallel))$$

As the orbit can best be described in cylindrical coordinates, but the vector dot product $(\vec{a}\bullet\vec{v})$ and vector subtraction $(\vec{a}-\vec{a}_\parallel)$ are best defined in Cartesian coordinates, we start this evaluation from the position in Cartesian coordinates $\vec{x}[t] = r[t]\,(Cos[\phi[t]], Sin[\phi[t]], 0)$. We find the velocity $\vec{v}[t] = d\vec{x}/dt = \dot{r}\,(Cos[\phi], Sin[\phi], 0) + \dot{\phi}\,r\,(-Sin[\phi], Cos[\phi], 0)$ and acceleration $\vec{a}[t] = d\vec{v}/dt = (\ddot{r}-r\dot{\phi}^2)\,(Cos[\phi], Sin[\phi], 0) + (r\ddot{\phi}+2\dot{r}\dot{\phi})\,(-Sin[\phi], Cos[\phi], 0)$. After insertion in Eq. (8.14) and expressing in cylindrical coordinates (by taking the vector dot-product with the base vectors: $\vec{e}_r = (Cos[\phi], Sin[\phi], 0)$, $\vec{e}_\phi = (-Sin[\phi], Cos[\phi], 0)$, $\vec{e}_z = (0, 0, 1)$), we find for the radial and angular coordinates of $\vec{a}_\parallel\,(r, \phi, \dot{r}, \dot{\phi}, \ddot{r}, \ddot{\phi})$ and $\vec{a_\perp}\,(r, \phi, \dot{r}, \dot{\phi}, \ddot{r}, \ddot{\phi})$:

$$a_{\parallel\,r} = \frac{\dot{r}(\ddot{r}\dot{r}+\dot{\phi}r(\dot{\phi}\dot{r}+\ddot{\phi}r))}{\dot{r}^2+\dot{\phi}^2r^2} \qquad a_{\parallel\,\phi} = \frac{\dot{\phi}r(\ddot{r}\dot{r}+\dot{\phi}r(\dot{\phi}\dot{r}+\ddot{\phi}r))}{\dot{r}^2+\dot{\phi}^2r^2} \tag{8.15}$$

$$a_{\perp\,r} = -\frac{\dot{\phi}r(2\dot{\phi}\dot{r}^2-\ddot{r}\dot{\phi}r+\ddot{\phi}\dot{r}r+\dot{\phi}^3r^2)}{\dot{r}^2+\dot{\phi}^2r^2} \qquad a_{\perp\,\phi} = \dot{r}(\dot{\phi}+\frac{\dot{\phi}\dot{r}^2-\ddot{r}\dot{\phi}r+\ddot{\phi}\dot{r}r}{\dot{r}^2+\dot{\phi}^2r^2})$$

Combining Eq's. (8.1), (8.11), (8.14) and (8.15), we arrive at the 2 equations of motion to describe the position over time of a mass (M_0) as seen by an observer (m_{obs}) located at the origin. They are given in cylindrical coordinates (r , ϕ with $z = 0$) as:

$$
\begin{aligned}
F_r^{tot} = 0 \;=\; & \frac{G M_0 m_{obs}}{r^2} \sqrt{1 - \frac{\dot{r}^2 + \dot{\phi}^2 r^2}{c^2}} \ldots \\
\ldots & \frac{c(c-\dot{r})(c+\dot{r})^2 - \dot{\phi}^2 (c+\dot{r})(2c+\dot{r}) r^2 + \dot{\phi}(\ddot{r}\dot{\phi} - \ddot{\phi}(c+\dot{r}))r^3}{(c+\dot{r})^4} + \ldots \\
\ldots + m_{obs} & \frac{\dot{r}(\ddot{r}\dot{r} + \dot{\phi} r(\dot{\phi}\dot{r} + \ddot{\phi} r))}{(\dot{r}^2 + \dot{\phi}^2 r^2) \sqrt{1 - \frac{\dot{r}^2 + \dot{\phi}^2 r^2}{c^2}}^3} - m_{obs} \frac{\dot{\phi} r (2\dot{\phi}\dot{r}^2 - \ddot{r}\dot{\phi} r + \ddot{\phi}\dot{r} r + \dot{\phi}^3 r^2)}{(\dot{r}^2 + \dot{\phi}^2 r^2) \sqrt{1 - \frac{\dot{r}^2 + \dot{\phi}^2 r^2}{c^2}}}
\end{aligned}
\tag{8.16}
$$

$$
\begin{aligned}
F_\phi^{tot} = 0 \;=\; & \frac{G M_0 m_{obs}}{r^2} \sqrt{1 - \frac{\dot{r}^2 + \dot{\phi}^2 r^2}{c^2}} \ldots \\
\ldots & \frac{\dot{\phi} r (c+\dot{r})^2 + (\ddot{\phi}(c+\dot{r}) - \ddot{r}\dot{\phi}) r^2}{(c+\dot{r})^3} + \ldots \\
\ldots + m_{obs} & \frac{\dot{\phi} r (\ddot{r}\dot{r} + \dot{\phi} r (\dot{\phi}\dot{r} + \ddot{\phi} r))}{(\dot{r}^2 + \dot{\phi}^2 r^2) \sqrt{1 - \frac{\dot{r}^2 + \dot{\phi}^2 r^2}{c^2}}^3} + m_{obs} \dot{r} \left(\dot{\phi} + \frac{\dot{\phi}\dot{r}^2 - \ddot{r}\dot{\phi} r + \ddot{\phi}\dot{r} r}{(\dot{r}^2 + \dot{\phi}^2 r^2) \sqrt{1 - \frac{\dot{r}^2 + \dot{\phi}^2 r^2}{c^2}}} \right)
\end{aligned}
$$

As all forces in Eq. (8.16) are proportional to the observer mass (m_{obs}). Therefore m_{obs} drops out of the general equation of motion, thus proving the 'weak equivalence principle'. This can already be concluded from Eq. (8.2) and (8.3). Also the gravitational constant G can be dropped/replaced, as explained in §7.5. All forces in the equation of motion Eq. 8.16 are gravitational in nature, and thus proportional to G.

Attempting to find a general analytical solution for Eq. (8.16) is beyond expectation. In the following paragraphs, we start with various case studies:

1. §8.5.1 : **Newtonian limit**: impact of $c \to \infty$.
2. §8.5.2 : **Angular momentum**: using 'instantaneous positions' vs 'retarded positions' to arrive at $r^2 \dot{\phi} = h$.
3. §8.5.3 : **Perihelion shift**: study the (near) elliptical orbit, re-using $r^2 \dot{\phi} = h$. Compare this solution to the General Relativity solution.

8.5.1 Newtonian limit

Now we study the impact of the general equation of motion in quark-gravity Eq. (8.16), from the condition $c \to \infty$. We expect to regain the Newtonian equations, as given by Eq. (8.4). The angular force $F_{\phi\, tot}$ in Eq. (8.16) simplifies, when using $\dot{r} \ll c$ and $r\dot{\phi} \ll c$ to:

$$
\begin{aligned}
F_{\phi}^{tot} = 0 = & \qquad (8.17)\\
& \frac{G M_0 m_{obs}}{r^2}\sqrt{1-0}\,\frac{\dot{\phi}c^2 + (\ddot{\phi}\dot{r}c - \dot{r}\dot{\phi})r^2}{c^3} + \\
& + m_{obs}\frac{\dot{\phi}r(\ddot{r}\dot{r} + \dot{\phi}r(\dot{\phi}\dot{r} + \ddot{\phi}r))}{(\dot{r}^2 + \dot{\phi}^2 r^2)\sqrt{1-0}^3} + m_{obs}\dot{r}\,(\,\dot{\phi} + \frac{\dot{\phi}\dot{r}^2 - \ddot{r}\dot{\phi}r + \ddot{\phi}\dot{r}r}{(\dot{r}^2 + \dot{\phi}^2 r^2)\sqrt{1-0}}\,)\\
F_{\phi}^{tot} = 0 = & \frac{G M_0 m_{obs}}{r^2}0 + \\
& + \frac{m_{obs}}{\dot{r}^2 + \dot{\phi}^2 r^2}\,(\dot{\phi}r(\ddot{r}\dot{r} + \dot{\phi}r(\dot{\phi}\dot{r} + \ddot{\phi}r)) + \dot{r}\,(\,\dot{\phi}(\dot{r}^2 + \dot{\phi}^2 r^2) + \dot{\phi}\dot{r}^2 - \ddot{r}\dot{\phi}r + \ddot{\phi}\dot{r}r\,))\\
= & \frac{m_{obs}}{\dot{r}^2 + \dot{\phi}^2 r^2}\,(\dot{\phi}r(\dot{\phi}r(\dot{\phi}\dot{r} + \ddot{\phi}r)) + \dot{r}\,(\,\dot{\phi}(\dot{r}^2 + \dot{\phi}^2 r^2) + \dot{\phi}\dot{r}^2 + \ddot{\phi}\dot{r}r\,))\\
= & \, m_{obs}\dot{r}\dot{\phi} + \frac{m_{obs}}{\dot{r}^2 + \dot{\phi}^2 r^2}\,(\dot{\phi}^3\dot{r}r^2 + \dot{\phi}^2\ddot{\phi}r^3 + \dot{\phi}\dot{r}^3 + \ddot{\phi}\dot{r}^2 r)\\
= & \, m_{obs}\dot{r}\dot{\phi} + \frac{m_{obs}}{\dot{r}^2 + \dot{\phi}^2 r^2}\,(\dot{\phi}^2 r^2\,(\dot{r}\dot{\phi} + \ddot{\phi}r) + \dot{r}^2\,(\dot{r}\dot{\phi} + \ddot{\phi}r))\\
= & \, m_{obs}\dot{r}\dot{\phi} + \frac{m_{obs}\,(\dot{r}\dot{\phi} + \ddot{\phi}r)}{\dot{r}^2 + \dot{\phi}^2 r^2}\,(\dot{\phi}^2 r^2 + \dot{r}^2)\\
= & \, m_{obs}\,(\,\ddot{\phi}r + 2\dot{r}\dot{\phi}) = 0
\end{aligned}
$$

which equals the Newtonian equation in the angular direction, as given in Eq. (8.4).

For the force component in radial direction $F_{r\, tot}$ we use a similar approach:

$$
\begin{aligned}
F_{r}^{tot} = 0 \qquad & (8.18)\\
= & \frac{G M_0 m_{obs}}{r^2}\sqrt{1-0}\,\frac{c^4 - 2\dot{\phi}^2 c^2 r^2 + \dot{\phi}(\ddot{r}\dot{\phi} - \ddot{\phi}c)r^3}{c^4} + \ldots\\
\ldots + & \, m_{obs}\frac{\dot{r}(\ddot{r}\dot{r} + \dot{\phi}r(\dot{\phi}\dot{r} + \ddot{\phi}r))}{(\dot{r}^2 + \dot{\phi}^2 r^2)\sqrt{1-0}^3} - m_{obs}\frac{\dot{\phi}r(2\dot{\phi}\dot{r}^2 - \ddot{r}\dot{\phi}r + \ddot{\phi}\dot{r}r + \dot{\phi}^3 r^2)}{(\dot{r}^2 + \dot{\phi}^2 r^2)\sqrt{1-0}}\,)\\
F_{r}^{tot} = 0 = & \frac{G M_0 m_{obs}}{r^2} + \ldots\\
\ldots + & \frac{m_{obs}}{(\dot{r}^2 + \dot{\phi}^2 r^2)}\,\dot{r}(\ddot{r}\dot{r} + \dot{\phi}r(\dot{\phi}\dot{r} + \ddot{\phi}r)) - \frac{m_{obs}}{(\dot{r}^2 + \dot{\phi}^2 r^2)}\,\dot{\phi}r(2\dot{\phi}\dot{r}^2 - \ddot{r}\dot{\phi}r + \ddot{\phi}\dot{r}r + \dot{\phi}^3 r^2)\,)\\
= & \frac{G M_0 m_{obs}}{r^2} + \frac{m_{obs}}{(\dot{r}^2 + \dot{\phi}^2 r^2)}\,(\,\dot{r}(\ddot{r}\dot{r} + \dot{\phi}r(\dot{\phi}\dot{r} + \ddot{\phi}r)) - \dot{\phi}r(2\dot{\phi}\dot{r}^2 - \ddot{r}\dot{\phi}r + \ddot{\phi}\dot{r}r + \dot{\phi}^3 r^2)\,))\\
= & \frac{G M_0 m_{obs}}{r^2} + \frac{m_{obs}}{(\dot{r}^2 + \dot{\phi}^2 r^2)}\,(\ddot{r}\dot{r}^2 + \dot{\phi}^2\dot{r}^2 r + \ddot{\phi}\dot{\phi}\dot{r}r^2 - 2\dot{\phi}^2\dot{r}^2 r + \dot{\phi}^2\ddot{r}r^2 - \ddot{\phi}\dot{\phi}\dot{r}r^2 - \dot{\phi}^4 r^3)\\
= & \frac{G M_0 m_{obs}}{r^2} + \frac{m_{obs}}{(\dot{r}^2 + \dot{\phi}^2 r^2)}\,(\dot{r}^2\,(\ddot{r} - \dot{\phi}^2 r) + \dot{\phi}^2 r^2\,(\ddot{r} - \dot{\phi}^2 r)\,)\\
= & \, m_{obs}\,(\frac{G M_0}{r^2} + \ddot{r} - \dot{\phi}^2 r) = 0
\end{aligned}
$$

We recognize in Eq. (8.17) and (8.18) the Newtonian equations of motions, as given by Eq. (8.4) and studied further in §8.2.

The condition $c \to \infty$ allows a quicker simplification of the force equation (8.3). We can use $\gamma = \gamma^3 = 1$ and find via Eq. (8.13) and Eq. (8.3):

$$\int^{rest\ of\ universe} d\vec{F}_g = m_{obs}\ (\gamma[0]^3\,\vec{a}_{\parallel} + \gamma[0]\,\vec{a_{\perp}}) \\ = m_{obs}\ (\vec{a}_{\parallel} + \vec{a_{\perp}}) = m_{obs}\,\vec{a} \tag{8.19}$$

8.5.2 Angular momentum

In both Newtonian gravity and General Relativity the conservation of angular momentum is found, as expressed by $r^2\dot{\phi} = h$. In §3.5.1 we found for a constant moving charge that the electro-dynamical force field points towards the 'instantaneous position' of the moving charge[3]. This means that the vector cross product $\overrightarrow{r_{inst}} * \vec{F}_g = \vec{0}$. As $\vec{F}_g = m\,\vec{a} = m\,d\,\vec{v}/d\,t$, we find $\overrightarrow{r_{inst}} * \vec{v} = \vec{h}$. For the vector cross product with the position, only the angular part of the velocity vector is relevant, which can be expressed as: $v_\phi = \dot{\phi}\,r$, and we thus find: $r^2\dot{\phi} = h$.

In summary: we found that the result known from Newtonian gravity and General relativity ($r^2\dot{\phi} = h$) is also valid in quark-gravity. This result will be used in further orbit calculations, as it gives the opportunity to eliminate $\dot{\phi}$ & $\ddot{\phi}$ from the radial force equation Eq. (8.16).

8.5.3 Perihelion shift

We now study the radial force equation of Eq. (8.16), which we separate in a gravitational term for the central mass ($\overrightarrow{F_r^{central}}$) and the inertial effects for the 'rest-of-the-universe' ($\overrightarrow{F_r^{inertia}}$). We assume $(c \pm \dot{r}) \approx c$. Then we sort for orders of $1/c$. We further use: $\sqrt{1-x} \approx 1 - x/2$ and $1/\sqrt{1-x} \approx 1 + x/2$ for $x \ll 1$. Dropping terms containing $1/c^3$ and $1/c^4$, we arrive at:

$$F_r^{central} = \frac{G\,M_0\,m_{obs}}{r^2}\sqrt{1-\frac{\dot{r}^2+\dot{\phi}^2 r^2}{c^2}}\ldots \\ \ldots\frac{c(c-\dot{r})(c+\dot{r})^2 - \dot{\phi}^2(c+\dot{r})(2c+\dot{r})r^2 + \dot{\phi}(\ddot{r}\dot{\phi} - \ddot{\phi}(c+\dot{r}))r^3}{(c+\dot{r})^4} \\ \approx \frac{G\,M_0\,m_{obs}}{r^2}\sqrt{1-\frac{\dot{r}^2+\dot{\phi}^2 r^2}{c^2}}\left(\frac{c^4 - 2\dot{\phi}^2\,r^2\,c^2 + \dot{\phi}(\ddot{r}\dot{\phi} - \ddot{\phi}c)r^3}{c^4}\right) \\ \approx \frac{G\,M_0\,m_{obs}}{r^2}\left(1-\frac{\dot{r}^2+\dot{\phi}^2 r^2}{2\,c^2}\right)\left(1 - \frac{2\dot{\phi}^2\,r^2}{c^2} - \cancel{\frac{\dot{\phi}\ddot{\phi}r^3}{c^3}} + \cancel{\frac{\dot{\phi}^2\,r^3\dot{r}}{c^4}}\right) \\ \approx \frac{G\,M_0\,m_{obs}}{r^2}\left(1 - \frac{\dot{r}^2}{2\,c^2} - \frac{5\dot{\phi}^2\,r^2}{2\,c^2}\right) \tag{8.20}$$

Anticipating the orbit to be a small deviation from Newtonian/Kepler ellipses, with low ellipticity, we assume the radial velocity to be small compared to the angular velocity[4]. We can then neglect the term $\frac{\dot{r}^2}{2\,c^2}$ to arrive at:

$$F_r^{central} = \frac{G\,M_0}{r^2}\left(1 - \frac{5\dot{\phi}^2\,r^2}{2\,c^2}\right) \tag{8.21}$$

For the inertial effects, from Eq. (8.18), we realize that we are notably studying orbit effects with elliptical shapes. For low ellipticities, we have $\frac{(\vec{a}.\vec{v})}{\|\vec{v}\|^2} \approx 0$ and thus from Eq. (8.14), we find

[3] The acceleration term in the Liénard-Wiechert force, Eq. (7.1), has negligible impact for a single gravitating mass, as this term contains the factor $1/c^2$.

[4] Comparing $\dot{r}$ to $r\dot{\phi}$ we use Eq. (8.7) to find: $\dot{r}\,/\,r\dot{\phi} = dr/dt/(rd\phi/dt) = dr/(rd\phi) = eSin[\phi]/(1 + eCos[\phi])$ with e being the orbit ellipticity.. Thus small ellipticities lead to $\left(\dot{r}\,/\,(r\,\dot{\phi})\right)^2 \ll 1$.

that the parallel acceleration terms can be neglected. Therefore the perpendicular (to velocity) acceleration term amounts to $\vec{a}_\perp = (\ddot{r} - r\dot{\phi}^2)\,\vec{e}_r$. Then the total acceleration force term can then be approximated, again using $\dot{r} \ll r\dot{\phi}$ and $\dot{\phi} = h/r^2$:

$$\overrightarrow{F_\perp^{inertia}} = \overrightarrow{F_r^{inertia}} = m_{obs}\,\gamma[v/c]\,\vec{a}_\perp = m_{obs}\,\frac{\vec{a}_\perp}{\sqrt{1-\frac{\dot{r}^2+r^2\dot{\phi}^2}{c^2}}} \approx m_{obs}\,\frac{\ddot{r}-r\dot{\phi}^2}{1-\frac{r^2\dot{\phi}^2}{2c^2}}\,\vec{e}_r \tag{8.22}$$

The radial forces as expressed in Eq. (8.21) and (8.22) are added to yield the total equation of motion in radial direction, dropping m_{obs} and terms containing $1/c^4$:

$$\frac{GM_0}{r^2}\left(1-\frac{5r^2\dot{\phi}^2}{2c^2}\right)+\frac{\ddot{r}-r\dot{\phi}^2}{1-\frac{r^2\dot{\phi}^2}{2c^2}}=0 \quad\Longrightarrow\quad \frac{GM_0}{r^2}\left(1-\frac{6r^2\dot{\phi}^2}{2c^2}\right)+\ddot{r}-r\dot{\phi}^2=0 \tag{8.23}$$
$$\Longrightarrow\quad \frac{GM_0}{r^2}\left(1-\frac{3h^2}{r^2c^2}\right)+\ddot{r}-h^2/r^3=0$$

Now we proceed with the Newtonian orbit theory substitution $u = 1/r[\phi]$, as done in §8.2, with $\ddot{r} = -h^2u^2u"$, where " indicates double differentiation to ϕ. We arrive at:

$$GM_0\,u^2\left(1-\frac{3h^2u^2}{c^2}\right)-h^2u^2u"-h^2u^3=0 \quad\Longrightarrow\quad u"+u=\frac{GM_0}{h^2}-\frac{3GM_0\,u^2}{c^2} \tag{8.24}$$
$$\Longrightarrow\quad u"+u+3\frac{GM_0}{c^2}u^2=\frac{GM_0}{h^2}$$

This is to be compared with the General Relativity result as given by Eq. (8.10), where we find an identical formula, except with a negative sign for the relativistic correction term. We now study the impact on the actual orbit. First we rewrite Eq. (8.24) into a dimensionless form, by dividing through a (inverse length) parameter u_m, which can be chosen freely. We choose: $u_m = 1/r_m =$, with $r_m = GM_0/c^2$ is half of the Schwarzschild radius, as given in §3.6 [65, 69, 70] and thus $u_m = c^2/GM_0$. This leads to:

$$\frac{u"}{u_m}+\frac{u}{u_m}+\frac{3GM_0}{u_m\,c^2}u^2=\left(\frac{u"}{u_m}\right)+\left(\frac{u}{u_m}\right)+\frac{3u_mGM_0}{c^2}\left(\frac{u}{u_m}\right)^2=\frac{GM_0}{u_m\,h^2}=\frac{G^2M_0^2}{c^2h^2} \tag{8.25}$$
$$\Longrightarrow\quad \left(\frac{u"}{u_m}\right)+\left(\frac{u}{u_m}\right)+3\left(\frac{u}{u_m}\right)^2=\left(\frac{GM_0}{ch}\right)^2$$

Defining the new parameter $w[\phi] = u/u_m$ we find:

$$w"+w+3w^2=\left(\frac{GM_0}{ch}\right)^2 \qquad w[\phi]=u/u_m=r_m/r[\phi]\ll 1 \tag{8.26}$$

The condition $w \ll 1$ is valid for normal planetary orbits around stars with masses of order of that of the sun. Now we use perturbation techniques [65, pages 230–233] ($w[\phi] = w_0 + \Delta w$), with $\Delta w \ll w_0$) starting from the Newtonian equation (as given by Eq. (8.6) and (8.7) :

$$w_0"+w_0=\left(\frac{GM_0}{ch}\right)^2 \qquad\Longrightarrow\qquad w_0[\phi]=\left(\frac{GM_0}{ch}\right)^2(1+eCos[\phi]) \tag{8.27}$$

To allow a comparison to the General Relativity orbit equation, Eq. (8.10)] we replace, in Eq. (8.26), the factor +3 by integer n, which can be positive or negative.

Then we find to first approximation:

$$w_0'' + \Delta w'' + w_0 + \Delta w + n(w_0 + \Delta w)^2 = \left(\frac{G M_0}{c\,h}\right)^2 \quad \Longrightarrow \tag{8.28}$$

$$w_0'' + w_0 + \Delta w'' + \Delta w + n\,w_0^2 + \cancel{2n\,w_0\,\Delta w + n\,\Delta w^2} = \left(\frac{G M_0}{c\,h}\right)^2 \quad \Longrightarrow$$

$$\Delta w'' + \Delta w + n\,w_0^2 = 0 \quad \Longrightarrow$$

$$\Delta w'' + \Delta w = -n\left(\frac{G M}{c\,h}\right)^4 (1 + e\,Cos[\phi])^2$$

A particular solution for Δw is found (inspired by the General Relativity orbit analysis, [65, page 231], [66, page 149], [70, §11.9]) to be:

$$\Delta w = -n\left(\frac{G M_0}{c\,h}\right)^4 \left[\, 1 + e^2\left(\tfrac{1}{2} - \tfrac{1}{6}\,Cos[2\phi]\right) + e\phi\,Sin[\phi] \,\right] \tag{8.29}$$

Going from the variable $w = u/r_m$ back to variable $u = 1/r$, and limiting only to the ϕ cumulative element in Eq. (8.29) (= the term with $\phi\,Sin[\phi]$), we find:

$$u = w\,u_m = \left(\frac{c^2}{G M_0}\right)\left[\left(\frac{G M_0}{c\,h}\right)^2 (1 + e\,Cos[\phi]) - n\left(\frac{G M_0}{c\,h}\right)^4 e\phi\,Sin[\phi]\,\right] \tag{8.30}$$

$$= \left(\frac{G M_0}{h^2}\right)\left[\,1 + e\,Cos[\phi] - n\left(\frac{G M_0}{c\,h}\right)^2 e\phi\,Sin[\phi]\,\right]$$

The solution for $r[\phi] = 1/u$ (which gives the perihelion shift per orbit $\Delta\phi$) is approximated, using [65, §10.1] $Cos[\phi(1-\delta)] \approx Cos[\phi] + \delta\phi\,Sin[\phi]$ for $\delta \ll 1$, and re-using, from §8.2 that the semi-major axis of the elliptical orbit (labeled as a) is given as $a = G M_0/(1-e^2)h^2$. We then find:

$$r[\phi] = \frac{h^2/G M_0}{1 + e\,Cos[\phi(1 + n(\frac{G M_0}{c\,h})^2)]} \quad \Longrightarrow \quad \Delta\phi = -n\,\frac{2\pi\,G M_0}{a(1-e^2)\,c^2} \tag{8.31}$$

As can be expected, the relativistic correction term to the Newtonian original - see Eq. (8.7) - is of order $1/c^2$ and thus very small.

The radial function $r[\phi]$ needs to be inserted into the position function: $\overrightarrow{r_{part}[\phi]} = r[\phi]\,(Cos[\phi], Sin[\phi], 0)$, which gives the position of the central mass (M_0), as seen by the observer. The observer sees the central mass AND the universe move in near elliptical orbits.

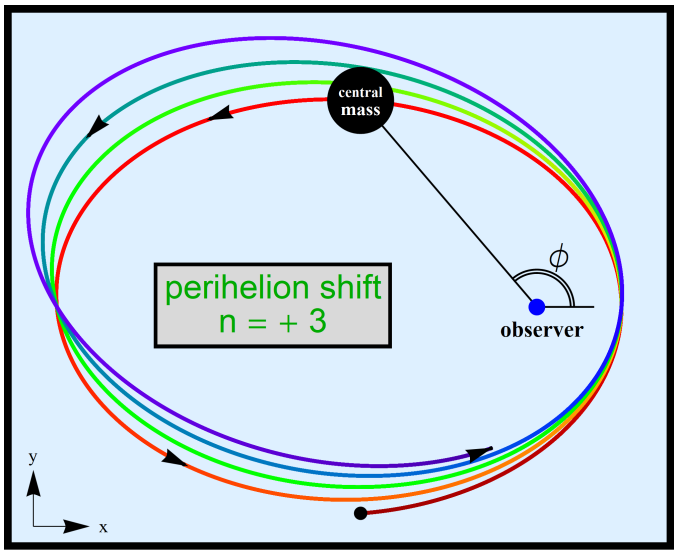

Figure 8.5: Perihelion shift of an -extreme - elliptic orbit, in quark-gravity. Color shift - red to blue - shows progress of the orbit. The (exaggerated) perihelion shift is equally large but opposite from General Raltivity - see fig 8.4.

Now we take a step back and make some observations, which are puzzling at the moment:

property	General Relativity	quark-gravity
center of evaluation	center mass M_0	observer mass m_{obs}
direction of $\vec{r}$	from M_0 to m_{obs}	from m_{obs} to M_0
pre-factor n in orbit equation	- 3 Eq. (8.10)	+ 3 Eq. (8.24)

Table 8.1: Orbit theory comparison General Relativity vs quark-gravity

1. **vector field theory should show a small perihelion shift of correct sign**: In [68, page 179], [101, §7.2], it is shown for an example of a vector theory for gravity, that this theory fails as it shows a perihelion shift that is only +1/6 value of the GR (=actual) value. Here we find the *opposite* value of GR .

2. **Linearized GR should show proper perihelion shift**: General Relativity can be linearized (for low velocities and 'small' gravitational fields) [23], [48, pages 91–109], [65, pages 490–492], [70, pages 335–341] (see §3.6) to reveal equations that are similar to the Maxwell-equations. Lense-Thirring [40] derived these equations to analyze 'frame-dragging' of an object orbiting a central mass, in a polar orbit. However, these equations can also be used to analyze equatorial orbits (as was done for planetary orbits in the previous paragraphs). Under these assumptions, the first successful perihelion shift analysis was done by Einstein [53, pages 163–164] (even before the Schwarzschild solution was known). It can be expected that the Lense-Thirring equations can also be used to come up with identical results. However, limited literature references are known to the author (apart from [4, Eq. 48]) that give the proper perihelion shift equations, see also appendix E. In fact such an analysis should result in identical results as an analysis starting from the Liènard-Wiechert equations (as given in §8.5.3), as both mathematical representations of the electro-dynamical fields and linearized GR are interchangeable.

8.6 Conclusions and recommendations

We have derived the orbit equations in quark-gravity. We reproduced the orbit equations in Newtonian limit ($c \to \infty$).

However we could not reproduce the perihelion shift equations. We found identical equations, with opposite sign of the critical relativistic corrections, hinting at a reduction of the gravitational force in quark-gravity, where an increase is expected in General Relativity. This discrepancy gives rise to further investigations, in future updates of the book, where help from readers is very much appreciated.

Figure 8.6: Perihelion shift requires further attention.

9. Gravitational waves

9.1 Introduction

Gravitational waves have been considered [5], once it was realized that gravity could have a finite velocity, as opposed to the Newtonian concept of 'immediate' impact. Inspired by the Maxwellian equations for electrodynamics, Heaviside [19] proposed gravitational waves, as early as 1893, followed by Poincaré in 1905. After the definition of General relativity, Einstein studied gravitational waves in 1918 [11], corrected by Eddington [10]. The energy loss from gravitational waves was first found theoretically, followed by experiment [8]. The direct discovery of gravitational waves by LIGO [1] occured in 2017.

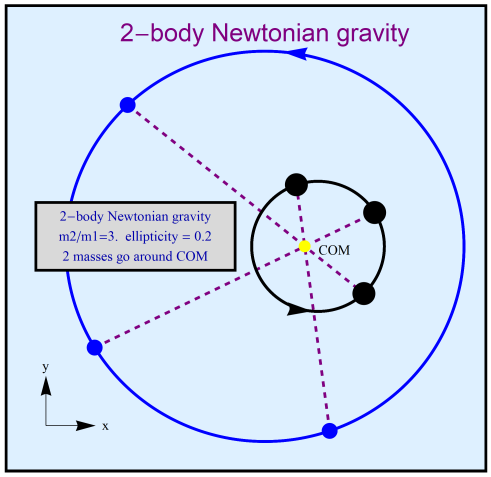

Figure 9.1: Newtonian orbits with low ellipticity of 2 masses moving around a common Center of Mass.

Gravitational waves have already been studied in literature , under linearized GR, using either tensor formalism [64, §71 & §110], [10, 11, 25, 68] or mathematics of potentials [problem 11.24][58], [solution to 11.24] [100], [20]. The results are *identical* for elctro-magnetic and gravitational formulations for wave generation, under identical physical situations. However, the physical boundary conditions for electromagnetic and gravitational waves are significantly different as will be discussed in this chapter.

It is clear that the propagation speed of gravitational waves equals that of light, as found experimentally [1] and theoretically in chapter 4.

In the electrical case, we can separate positive charges (ions - fixed in a metallic lattice) and negative charges ('free' electrons) and move these independently, which leads to di-pole radiation. For the gravitational case, we cannot move the masses independently, as a change in position or velocity of one mass has impact on the other. Both masses move around a common 'Center of

mass' (COM), see fig. 9.1. This results in gravitational quadrupole radiation. We will compute the consequential gravitational Poynting (power) vector and obtain the total emitted energy per time unit.

9.2 Gravitational Poynting vector - radiated power

In this paragraph, we will study a comparison between electro-magnetic and gravitational waves, based on the Liénard-Wiechtert (LW) field description of Eq. (7.1) in combination with the (gravitational) Poynting vector ($\vec{P_g} = 1/\mu_g\, \vec{E}_g * \vec{B}_g$, see: §3.5.6). We realize that μ_g is the gravitational copy of the electro-dynamical vacuum magnetic permeability μ_0. Using the analogy $\epsilon_0 \rightarrow 1/(4\pi G)$ and knowing that the speed of gravity equals the speed of light ($c^2 = 1/\epsilon_0\mu_0 = c_g^2 = 1/\epsilon_g\mu_g$), we find $1/\mu_g = c^2/(4\pi G)$. Further we re-use from Eq. ((7.1) $\vec{B}_g = \vec{r} * \vec{E}_g/(r\,c)$. We will also use the vector rule (see appendix G) $\vec{x} * (\vec{v} * \vec{a}) = (\vec{x} \bullet \vec{a})\,\vec{v} - (\vec{x} \bullet \vec{v})\,\vec{a}$. Then we calculate the total radiated gravitational power P_{grav}^{tot} as done in §3.17, leading to:

$$
\begin{aligned}
P_{grav}^{tot} &= \frac{c^2}{4\pi G} \oiint \left(\vec{E}_g * \left(\frac{\vec{r}}{r\,c} * \vec{E}_g \right) \right) \bullet \left(\frac{\vec{r}}{r} \right) dA \qquad (9.1)\\
&= \frac{c}{4\pi G\, r^2} \oiint (\vec{E}_g \bullet \vec{E}_g)(\vec{r} \bullet \vec{r}) - (\vec{r} \bullet \vec{E}_g)(\vec{E}_g \bullet \vec{r})\, dA \\
&= \frac{c}{4\pi G} \oiint (\vec{E}_g \bullet \vec{E}_g) - (\vec{r} \bullet \vec{E}_g)^2/r^2\, dA
\end{aligned}
$$

It was shown in §3.5.6 [69, page 146], [64, page 176] that only the accelerated part of the LW force of Eq. (7.1) contributes to the generation of radiation, when observed from large distances. Therefore in upcoming evaluations of the total gravitational radiated energy we use Eq. (9.1), with the evaluation of $\vec{E}_g$ limited to the accelerated part.

9.3 One mass oscillation

Electro-magnetic waves are created by displacements of single charges, leading to Larmor radiation as shown in §3.5.6. Essential in the derivation of the Larmor radiation is that a neutral particle can be 'split' into 2 charges of opposite sign (electrons and ions), with only ONE moving charge and the other remaining stationary. The charged particles can move *independently* from each other. This is comparable to the 1-body problem as given in §8.2.

Here, we will study the resulting power emitted by gravitational waves, emerging from a 1-body orbit. We assume the masses to move in the low velocity regime ($v/c \ll 1$). This leads to simpler formulas of the E_g-field:

$$
\vec{E}_g = (G\,m_{part}/r^3)\,(\vec{r} * ((\vec{r} - \cancel{\vec{r}\vec{v}/c}) * \vec{a})/c^2) \quad \Longrightarrow \quad \vec{E}_g = \frac{G\,m_{part}}{c^2\,r^3}\,\vec{r} * ((\vec{r} * \vec{a}) \qquad (9.2)
$$

We note that the E_g-field is perpendicular to the position vector and thus $(\vec{r} \bullet \vec{E}_g) = 0$. Now we use the vector identity (see appendix G) : $\vec{x} * (\vec{v} * \vec{a}) = (\vec{x} \bullet \vec{a})\,\vec{v} - (\vec{x} \bullet \vec{v})\,\vec{a}$, and thus $\vec{r} * (\vec{r} * \vec{a}) = (\vec{r} \bullet \vec{a})\,\vec{r} - (\vec{r} \bullet \vec{r})\,\vec{a} = (\vec{r} \bullet \vec{a})\,\vec{r} - r^2\,\vec{a}$. Using these results in Eq. (9.1), we find:

$$
P_{grav}^{tot} = \frac{c}{4\pi G} \oiint (\vec{E}_g \bullet \vec{E}_g)\, dA \quad \& \quad \vec{E}_g = \frac{G\,m_{part}}{c^2\,r^3} \left((\vec{r} \bullet \vec{a})\,\vec{r} - r^2\,\vec{a} \right) \qquad (9.3)
$$

This instantaneous energy loss per time per opening angle needs to be integrated over all opening angles, in similar fashion as done for the flux calculations in §3.5.2. For simplicity, we use a circular orbit equation for a particle moving around a non-moving central massive

object, located at position $\vec{r}_0 = r_0\,(Cos[\phi]\,Sin[\theta]\,,\,Sin[\phi]\,Sin[\theta]\,,\,Cos[\theta]) = r_0\,\overrightarrow{e_0^{\phi\theta}}$ (as given in §8.2). The position of the moving particle, related to the central object is then given as: $\overrightarrow{r_{part}^{\omega t}}[t] = r_{part}\,(Cos[\omega_{part}\,t]\,,\,Sin[\omega_{part}\,t]\,,\,0) = r_{part}\,\overrightarrow{e_{part}^{\omega t}}$ leading to the acceleration $\vec{a}[t] = -\omega_{part}^2\,\overrightarrow{r_{part}^{\omega t}}$, and thus $a^2 = (\vec{a}\bullet\vec{a}) = \omega_{part}^4\,r_{part}^2$. For the total position of the orbiting mass we use the assumption that the observation distance is much larger than the orbit radius $(r_{part} \ll r_0)$, and thus $\vec{r} = \vec{r}_0 + \overrightarrow{r_{part}^{\omega t}}[t] \approx \vec{r}_0$. We find for the total gravitational field:

$$\vec{E}_g = \frac{G\,m_{part}}{c^2\,r_0^3}\left(r_0^2\,\omega_{part}^2\,\overrightarrow{r_{part}^{\omega t}} - \omega_{part}^2\,(\vec{r}_0\bullet\overrightarrow{r_{part}^{\omega t}})\,\vec{r}_0\right) \tag{9.4}$$

$$= \frac{G\,m_{part}}{c^2\,r_0^3}\,(r_0^2\,r_{part}\,\omega_{part}^2)\left(\overrightarrow{e_{part}^{\omega t}} - (\overrightarrow{e_0^{\phi\theta}}\bullet\overrightarrow{e_{part}^{\omega t}})\,\overrightarrow{e_0^{\phi\theta}}\right)$$

$$= \frac{G\,m_{part}\,r_{part}\,\omega_{part}^2}{c^2\,r_0}\left(\overrightarrow{e_{part}^{\omega t}} - (\overrightarrow{e_0^{\phi\theta}}\bullet\overrightarrow{e_{part}^{\omega t}})\,\overrightarrow{e_0^{\phi\theta}}\right)$$

Now we calculate the dot-products that are used in Eq. (9.3), using $(\overrightarrow{e_{part}^{\omega t}}\bullet\overrightarrow{e_{part}^{\omega t}}) = (\overrightarrow{e_0^{\phi\theta}}\bullet\overrightarrow{e_0^{\phi\theta}}) = 1$:

$$(\vec{E}_g\bullet\vec{E}_g) = \tag{9.5}$$

$$= \left(\frac{G\,m_{part}\,r_{part}\,\omega_{part}^2}{c^2\,r_0}\right)^2\left((\overrightarrow{e_{part}^{\omega t}}\bullet\overrightarrow{e_{part}^{\omega t}}) - 2\,(\overrightarrow{e_0^{\phi\theta}}\bullet\overrightarrow{e_{part}^{\omega t}})^2 + (\overrightarrow{e_0^{\phi\theta}}\bullet\overrightarrow{e_{part}^{\omega t}})^2\,(\overrightarrow{e_0^{\phi\theta}}\bullet\overrightarrow{e_0^{\phi\theta}})\right)$$

$$= \left(\frac{G\,m_{part}\,r_{part}\,\omega_{part}^2}{c^2\,r_0}\right)^2\left(1 - (\overrightarrow{e_0^{\phi\theta}}\bullet\overrightarrow{e_{part}^{\omega t}})^2\right)$$

Now we can detail the total radiated gravitational energy integration, integrating $\vec{P}_g$ over a (large radius) spherical surface (with $dA = r_0^2\,Sin[\theta]\,d\phi d\theta$, via Eq. (9.3), to find [85]:

$$P_{grav}^{tot} = \frac{c}{4\pi\,G}\oiint(\vec{E}_g\bullet\vec{E}_g)\,dA \tag{9.6}$$

$$= \left(\frac{G\,m_{part}\,r_{part}\,\omega_{part}^2}{c^2\,r_0}\right)^2\frac{c}{4\pi\,G}\oiint\left(1 - (\overrightarrow{e_0^{\phi\theta}}\bullet\overrightarrow{e_{part}^{\omega t}})^2\right)dA$$

$$= \frac{G\,m_{part}^2\,r_{part}^2\,\omega_{part}^4}{4\pi\,c^3\,r_0^2}\left(\oiint dA - \oiint(\overrightarrow{e_0^{\phi\theta}}\bullet\overrightarrow{e_{part}^{\omega t}})^2\,dA\right)$$

$$= \frac{G\,m_{part}^2\,r_{part}^2\,\omega_{part}^4}{4\pi\,c^3\,r_0^2}\,r_0^2\,(4\pi - 4\pi/3) = \frac{2\,G\,m_{part}^2\,r_{part}^2\,\omega_{part}^4}{3\,c^3}$$

This result is known [58, 69] as Larmor radiation of one oscillatory source, generating dipole radiation.

9.4 Gravitational waves: binary

9.4.1 First order estimation

When 2 gravitating masses (m_1 and m_2) are moving (far from other masses), they interact as a 2-body problem as discussed in §8.3 and visualized in figs 8.3 and 9.1. They co-move around their Center of Mass (COM) [1] and thus: $m_1 \overrightarrow{r_1^{orbit}} + m_2 \overrightarrow{r_2^{orbit}} = \vec{0}$. Thus we also have: $m_1 \vec{v}_1 + m_2 \vec{v}_2 = \vec{0}$ and $m_1 \vec{a}_1 + m_2 \vec{a}_2 = \vec{0}$. Therefore, although the underlying physical interactions are identical, as expressed by the Liénard-Wiechert forces in Eq. (7.1), the independent movement of electrical charges can give rise to electro-magnetical dipole fields, whereas the always coupled gravitational fields of 2 masses, do not allow a dipole field. This can be seen when we calculate the radiation LW E_g-field due to 2 orbiting masses, re-using Eq. (9.2), which expresses the first order estimation of the full LW field, by omitting the term containing $r\dot{\vec{v}}/c$ and assuming that the distance to the observer is much larger than the orbit radius ($\|\overrightarrow{r_{COM}}\| \gg \|\overrightarrow{r_1^{orbit}}\|$), and thus we use $\vec{r} = \overrightarrow{r_{COM}}$ for both masses. We add the $\vec{E}_g$-field from the 2 masses, using $\vec{a}_2 = -(m_1/m_2)\,\vec{a}_1$.

$$\begin{aligned}\overrightarrow{E_g^{tot}} &= \overrightarrow{E_g^1} + \overrightarrow{E_g^2} = \left(\frac{G}{r^3\,c^2}\right)\Big(\,m_1\,(\vec{r}*(\vec{r}*\vec{a}_1)) \;+\; m_2\,(\vec{r}*(\vec{r}*\vec{a}_2))\,\Big) \\ &= \left(\frac{G}{r^3\,c^2}\right)\Big(\,m_1\,(\vec{r}*(\vec{r}*\vec{a}_1) \;-\; m_2\,(\vec{r}*(\vec{r}*\frac{m_1}{m_2}\,\vec{a}_1)\,\Big) \;=\; \vec{0}\end{aligned} \tag{9.7}$$

When $\overrightarrow{E_g^{tot}} = \vec{0}$, also the Poynting vector is zero and thus the emitted radiation energy is zero. We therefore have to remove some of the approximations we have made in deducing Eq. (9.7) to identify whether a binary object (= 2 masses in orbit around each other) emits gravitational wave energy.

9.4.2 Second order estimation

We now calculate the total radiated power emitted by 2 orbiting masses as shown in fig. 9.1. We calculate the Poynting vector for circular orbits (ellipticity: $e = 0$), using the LW fields of Eq. (7.1). As mentioned earlier, the electromagnetic and gravitational[2] radiation energy can be calculated via tensor or potential equations, as done in [10, 11, 58, 64]. Here we will use the gravitational LW fields and Eq. (9.1) to compute the total radiated gravitational power.

As found in §9.4.1, we need to evaluate the (radiating) LW $\overrightarrow{E_g^{tot}}$-field to higher order, than done previously. So we re-use the (circular) orbit description as done in §9.3, with:

$$\begin{aligned}\overrightarrow{e_r^{\omega t}} &= (Cos[\omega_{part}\,t],\,Sin[\omega_{part}\,t],\,0) \text{ and } \overrightarrow{e_\phi^{\omega t}} = (-Sin[\omega_{part}\,t],\,Cos[\omega_{part}\,t],\,0) \\ \overrightarrow{r_i^{\omega t}} &= r_i^{part}\,(Cos[\omega_{part}\,t],\,Sin[\omega_{part}\,t],\,0) = \quad r_i^{part}\,\overrightarrow{e_r^{\omega t}} \\ \overrightarrow{v_i^{\omega t}} &= d\,\overrightarrow{r_i^{\omega t}}/dt = \omega_{part}\,r_i^{part}\,(-Sin[\omega_{part}\,t],\,Cos[\omega_{part}\,t],\,0) = \quad \omega_{part}\,r_i^{part}\,\overrightarrow{e_\phi^{\omega t}} \\ \overrightarrow{a_i^{\omega t}} &= d\,\overrightarrow{v_i^{\omega t}}/dt = -\omega_{part}^2\,r_i^{part}\,(Cos[\omega_{part}\,t],\,Sin[\omega_{part}\,t],\,0) = -\omega_{part}^2\,r_i^{part}\,\overrightarrow{e_r^{\omega t}}\end{aligned} \tag{9.8}$$

with $i = 1, 2$ related to the masses m_1 and m_2. Therefore the total position vector, as seen by the observer (in the origin), of the 2 masses that are co-moving around their common Center of Mass (COM), is then given as:

$$\begin{aligned}\overrightarrow{r_1^{tot}} &= \overrightarrow{r_{COM}} + \overrightarrow{r_1^{\omega t}} \\ \overrightarrow{r_2^{tot}} &= \overrightarrow{r_{COM}} + \overrightarrow{r_2^{\omega t}} = \overrightarrow{r_{COM}} - (m_1/m_2)\,\overrightarrow{r_1^{\omega t}}\end{aligned} \tag{9.9}$$

[1] with $\overrightarrow{r_{COM}} = r_{COM}\,(Cos[\phi]\,Sin[\theta],\,Sin[\phi]\,Sin[\theta],\,Cos[\theta]) = r_{COM}\,\overrightarrow{e_{COM}}$ defining the position of the binary system in spherical coordinates, as observed from the origin.

[2] in linearized General Relativity formulation

We also do not use the approximation in the 's' term of the LW field, Eq. (7.1), but use the full $s = r - (\vec{r} \bullet \vec{v})/c$. Under the assumptions $v/c = \omega_{part}\, r_i^{part}/c \ll 1$ and $r_i^{part} \ll r_{COM}$, we can develop the LW force term 's' to first order of v/c as:

$$s = r - (\vec{r} \bullet \vec{v})/c \approx r_{COM} - (\overrightarrow{r_{COM}} \bullet \vec{v})/c = r_{COM}\,(1 - (\overrightarrow{e_{COM}} \bullet \vec{v})/c) \tag{9.10}$$
$$\frac{1}{s^3} = \frac{1}{r_{COM}^3\,(1 - (\overrightarrow{e_{COM}} \bullet \vec{v})/c)^3} \approx \frac{1}{r_{COM}^3}\,(1 + 3\,(\overrightarrow{e_{COM}} \bullet \vec{v})/c)$$

Where we have used the approximation, for $x \ll 1$, $1/(1-x)^3 \approx 1 + 3x$. Now we can develop the radiative part of the LW formula to first order of v/c, from the orignal Eq. (7.1):

$$\vec{E}_g = \frac{G\,m_{part}}{(r - (\vec{r} \bullet \vec{v})/c)^3}\,(\vec{r} * ((\vec{r} - r\,\vec{v}/c) * \vec{a})/c^2) \tag{9.11}$$
$$\approx \frac{G\,m_{part}}{r_{COM}^3}\left(1 + 3\,(\overrightarrow{e_{COM}} \bullet \vec{v})/c\right)\left(\vec{r} * (\vec{r} * \vec{a})/c^2 - \vec{r} * (\frac{r_{COM}}{c}\,\vec{v} * \vec{a})/c^2\right)$$
$$\approx \frac{G\,m_{part}}{r_{COM}^3}\left(\overbrace{1}^{A} + \overbrace{3\,(\overrightarrow{e_{COM}} \bullet \vec{v})/c}^{B}\right)\left(\vec{r} * (\vec{r} * \vec{a})/c^2\right) - \overbrace{\frac{G\,m_{part}}{r_{COM}^2}\,\vec{r} * (\vec{v} * \vec{a})/c^3}^{C}$$

where we dropped the term containing $(v/c)^2$. We can now separate $\vec{E}_g$ in a part (labeled: A) that is identical to the first order estimation as treated in §9.3, yielding a zero emission result, and two new parts (B & C) that contain terms proportional to v/c. We now study the impact of these terms on the $\overrightarrow{E_g^{tot}}$ for the 2 (co-orbiting) mass binary. We use the fact that both masses are bound to a common Center of Mass and thus [3]: $m_1\,\vec{v}_1 + m_2\,\vec{v}_2 = \vec{0}$ and $m_1\,\vec{a}_1 + m_2\,\vec{a}_2 = \vec{0}$. We tackle the 3 terms of Eq. (9.11) separately, starting with the A term:

$$\overbrace{\overrightarrow{E_g^{tot}}}^{A} = \overbrace{\overrightarrow{E_g^{m1}}}^{A} + \overbrace{\overrightarrow{E_g^{m2}}}^{A} = \frac{G\,m_1}{r_{COM}^3}\left(\vec{r} * (\vec{r} * \vec{a}_1)/c^2\right) + \frac{G\,m_2}{r_{COM}^3}\left(\vec{r} * (\vec{r} * \vec{a}_2)/c^2\right) \tag{9.12}$$
$$= \frac{G\,m_1}{r_{COM}^3}\left(\vec{r} * (\vec{r} * \vec{a}_1)/c^2\right) + \frac{G\,m_2}{r_{COM}^3}\left(\vec{r} * (\vec{r} * \frac{m_1}{m_2} - \vec{a}_1)/c^2\right) = \vec{0}$$

The result of Eq (9.12) is (of course) identical to Eq (9.7). We now proceed to the (relativistic) corrections as expressed by terms B & C of Eq. (9.11), which both contain v/c terms. [4]

$$\overbrace{\overrightarrow{E_g^{tot}}}^{B} = \overbrace{\overrightarrow{E_g^{m1}}}^{B} + \overbrace{\overrightarrow{E_g^{m2}}}^{B} \tag{9.13}$$
$$= \frac{3\,G\,m_1}{c^3\,r_{COM}^3}\,(\overrightarrow{e_{COM}} \bullet \vec{v}_1)\,\left(\vec{r} * (\vec{r} * \vec{a}_1)\right) + \frac{3\,G\,m_2}{c^3\,r_{COM}^3}\,(\overrightarrow{e_{COM}} \bullet \vec{v}_2)\,\left(\vec{r} * (\vec{r} * \vec{a}_2)\right)$$
$$= \frac{3\,G\,m_1}{c^3\,r_{COM}^3}\,(\overrightarrow{e_{COM}} \bullet \vec{v}_1)\,\left(\vec{r} * (\vec{r} * \vec{a}_1)\right) + \frac{3\,G\,m_2}{c^3\,r_{COM}^3}\,(\overrightarrow{e_{COM}} \bullet \left(\frac{-m_1}{m_2}\right)\vec{v}_1)\,\left(\vec{r} * (\vec{r} * \left(\frac{-m_1}{m_2}\right)\vec{a}_1)\right)$$
$$= \frac{3\,G\,m_1}{c^3\,r_{COM}}\,(1 + \frac{m_1}{m_2})\,(\overrightarrow{e_{COM}} \bullet \vec{v}_1)\,\left(\overrightarrow{e_{COM}} * (\overrightarrow{e_{COM}} * \vec{a}_1)\right)$$

[3] We do not use the relativistic mass dilation in this approximation, as this would lead to factors of order $(v/c)^2$ in the $\overrightarrow{E_g^{tot}}$-field, where we now only develop $\overrightarrow{E_g^{tot}}$ up to linear factors of v/c.

[4] This immediately leads to the conclusion that the Poynting vector and thus the total radiated gravitational wave energy of Eq. (9.1) will be a factor $(v/c)^2$ smaller for a 2-mass system than for the 1-mass system, as the Poynting vector is proportional to $(\vec{E}_g \bullet \vec{E}_g) - (\vec{r} \bullet \vec{E}_g)^2/r^2$.

Now we fill in the orbit parameters $\overrightarrow{v_1^{\omega t}}$ and $\overrightarrow{a_1^{\omega t}}$, as given in Eq. (9.8), using the short-hands: $\omega = \omega_{part}$ and $r_\omega = r_1^{part}$:

$$\overbrace{\overrightarrow{E_g^{tot}}}^{B} = \frac{-3\,G\,m_1\,r_\omega^2\,\omega^3}{c^3\,r_{COM}}\,(1+\frac{m_1}{m_2})\,(\overrightarrow{e_{COM}}\bullet\overrightarrow{e_\phi^{\omega t}})\,\left(\overrightarrow{e_{COM}}*(\overrightarrow{e_{COM}}*\overrightarrow{e_r^{\omega t}})\right) \tag{9.14}$$

Similarly, we find for the C term of Eq. (9.11):

$$\overbrace{\overrightarrow{E_g^{tot}}}^{C} = \overbrace{\overrightarrow{E_g^{m1}}}^{C} + \overbrace{\overrightarrow{E_g^{m2}}}^{C} = -\frac{G\,m_1}{r_{COM}^2}\,\vec{r}*(\vec{v}_1*\vec{a}_1)/c^3 - \frac{G\,m_2}{r_{COM}^2}\,\vec{r}*(\vec{v}_2*\vec{a}_2)/c^3 \tag{9.15}$$

$$= -\frac{G\,m_1}{c^3\,r_{COM}}\,\overrightarrow{e_{COM}}*(\vec{v}_1*\vec{a}_1) - \frac{G\,m_2}{c^3\,r_{COM}}\,\overrightarrow{e_{COM}}*\left(\left(\frac{-m_1}{m_2}\right)\vec{v}_1*\left(\frac{-m_1}{m_2}\right)\vec{a}_1\right)$$

$$= -\frac{G\,m_1}{c^3\,r_{COM}}\,(1+\frac{m_1}{m_2})\,\left(\overrightarrow{e_{COM}}*(\vec{v}_1*\vec{a}_1)\right)$$

$$= \frac{G\,m_1\,r_\omega^2\,\omega^3}{c^3\,r_{COM}}\,(1+\frac{m_1}{m_2})\,\left(\overrightarrow{e_{COM}}*(\overrightarrow{e_\phi^{\omega t}}*\overrightarrow{e_r^{\omega t}})\right)$$

$$= \frac{-G\,m_1\,r_\omega^2\,\omega^3}{c^3\,r_{COM}}\,(1+\frac{m_1}{m_2})\,\left(\overrightarrow{e_{COM}}*\vec{e}_z\right)$$

where we have used $\overrightarrow{e_\phi^{\omega t}}*\overrightarrow{e_r^{\omega t}} = (0,0,-1) = -\vec{e}_z$. Now we can add Eqs. (9.12), (9.14) and (9.15):

$$\overrightarrow{E_g^{tot}} = \frac{-G\,m_1\,r_\omega^2\,\omega^3}{c^3\,r_{COM}}\,(1+\frac{m_1}{m_2})\left(3\,(\overrightarrow{e_{COM}}\bullet\overrightarrow{e_\phi^{\omega t}})\,\left(\overrightarrow{e_{COM}}*(\overrightarrow{e_{COM}}*\overrightarrow{e_r^{\omega t}})\right)+(\overrightarrow{e_{COM}}*\vec{e}_z)\right) \tag{9.16}$$

For computing the total radiated gravitational (wave) power, as given by Eq. (9.1) we need to evaluate the dot product $(\vec{r}\bullet\vec{E}_g)$, where $\vec{r}\approx\overrightarrow{r_{COM}} = r_{COM}\,\overrightarrow{e_{COM}}$. Thus we realize that the vector direction of $\overrightarrow{E_g^{tot}}$ is given by the two cross-products, with $\overrightarrow{e_{COM}}$ as direction determining vector and thus the electric field is perpendicular to the position vector and therefore: $(\vec{r}\bullet\vec{E}_g) = 0$. We can thus omit this term from the Poynting vector integration.

We now define the help parameter $\overrightarrow{E_g^{tot*}} = \overrightarrow{E_g^{tot}}/\left(\frac{G\,m_1\,r_\omega^2\,\omega^3}{c^3\,r_{COM}}\,(1+\frac{m_1}{m_2})\right)$. We can now compute the Poynting vector and the total power radiated as gravitational wave energy, in similar way as in §9.3 as given in Eq. (9.1):

$$P_g^{tot}[t] = \frac{c}{4\pi\,G}\oiint(\vec{E}_g\bullet\vec{E}_g) - \cancel{(\vec{r}\bullet\vec{E}_g)^2/r_{COM}^2}\,dA \tag{9.17}$$

$$= \frac{G\,m_1^2\,r_\omega^4\,\omega^6}{4\pi\,c^5}\,(1+\frac{m_1}{m_2})^2\oiint(\overrightarrow{E_g^{tot*}}\bullet\overrightarrow{E_g^{tot*}})\,dA = \frac{76\,G\,m_1^2\,r_\omega^4\,\omega^6}{15\,c^5}\,(1+\frac{m_1}{m_2})^2$$

as the last surface integration evaluates to [85] $304\pi/15$. Apart from a numerical factor ≈ 2, these results co-incide with the results from linearized General Relativity [64, page 379], [65, page 516], [69, page 252], [70, page 334].

From these equations the orbital decay (=reduction of orbital radius) has been studied extensively [65, §18.8], [25]. From this analysis binary collapse was predicted, as was actually recently observed by LIGO [1].

9.5 Conclusions

In conclusion, we identified the gravitational energy emitted by masses in orbit. We found that a 1-mass oscillation generates dipole radiation. However, as gravitating masses in orbit influence each other, when they orbit around a common Center of Mass, the 1-mass oscillation is not realistic. When evaluating the emitted radiation from a binary system, we find relations as found in linearized General Relativity. We find these results using the 'normal' Liénard-Wiechert force equations, as used as basis for all our evaluations.

We do not find any intrinsic (='given by physics laws') difference when treating electro-dynamics and gravity for the generation of waves. We only need to realize that in electro-dynamics, we can move the radiation generating charges independently, whereas with gravitating masses the movements are always interlinked. As a result, gravitational radiation is described by equations which look like quadrupole radiation as known in electro-dynamics.

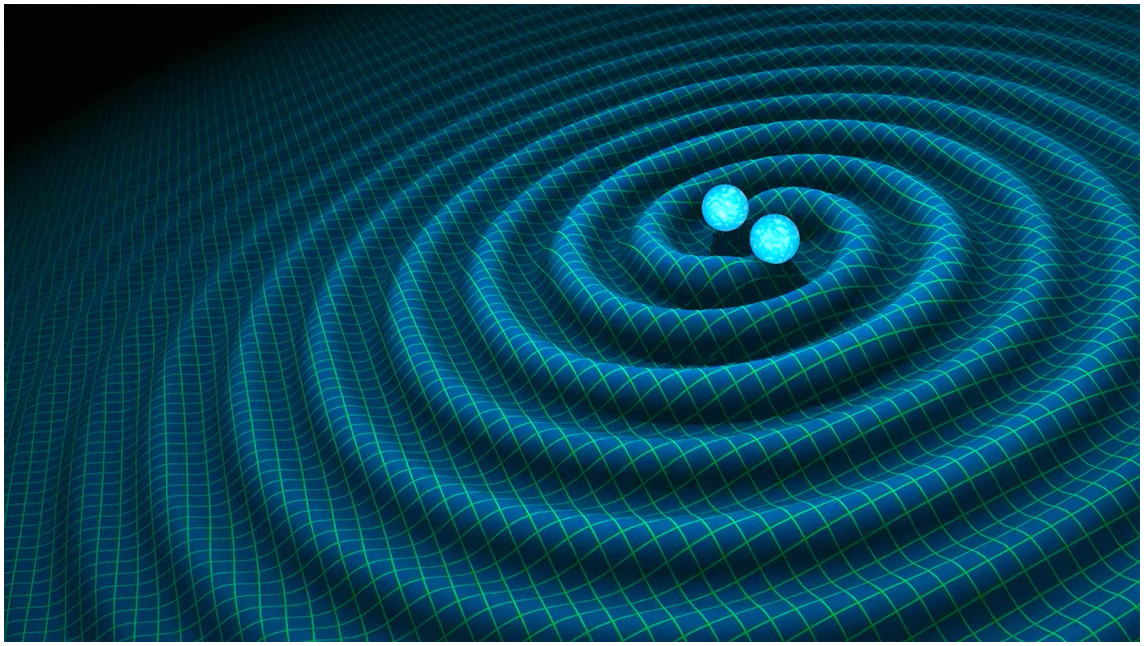

Figure 9.2:
R. Hurt/Caltech-JPL visualization of gravitational waves,
by a binary star combination about to collide,
due to loss of gravitational energy.

Figure 9.3:
NASA James Webb image: Arp 142, two interacting galaxies.

10. Forces in physics: a summary

In this book, we have attempted to identify gravity and inertia as induced properties. Based upon experimental facts and known theories, we have aimed to establish that gravity is an induced electro-dynamical effect due to charged quark (quantum mechanical initiated) movements. This leads directly to equality of speed of gravity and light, as well as some qualitatively understanding of gravitational bending of light and time delay. Furthermore, inertia is proven to be the gravitational induced effect of all masses of the universe (Mach principle). Mass dilation effects (leading up to $E = m c^2$) can then be attributed to gravitational effects of moving masses.

In fig. 10.1 the inter linkages between the various experiments, theories and predictions are summarized, with orbit theory (perihelion shift) yielding unsatisfactory results.

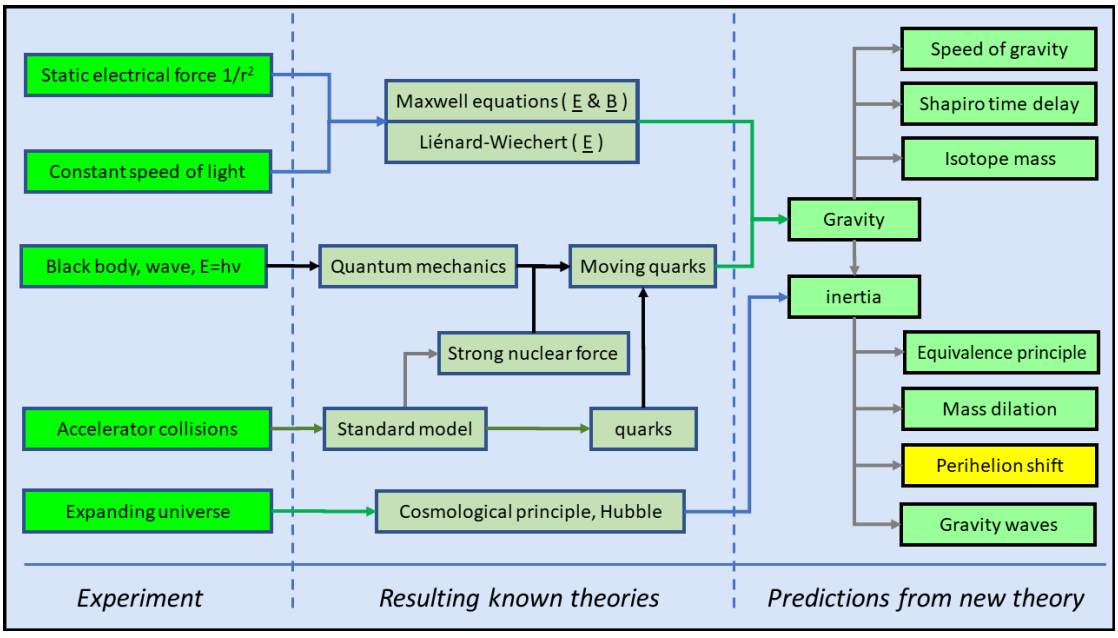

Figure 10.1: The inter linkage of experiments, known theories and the new theory.

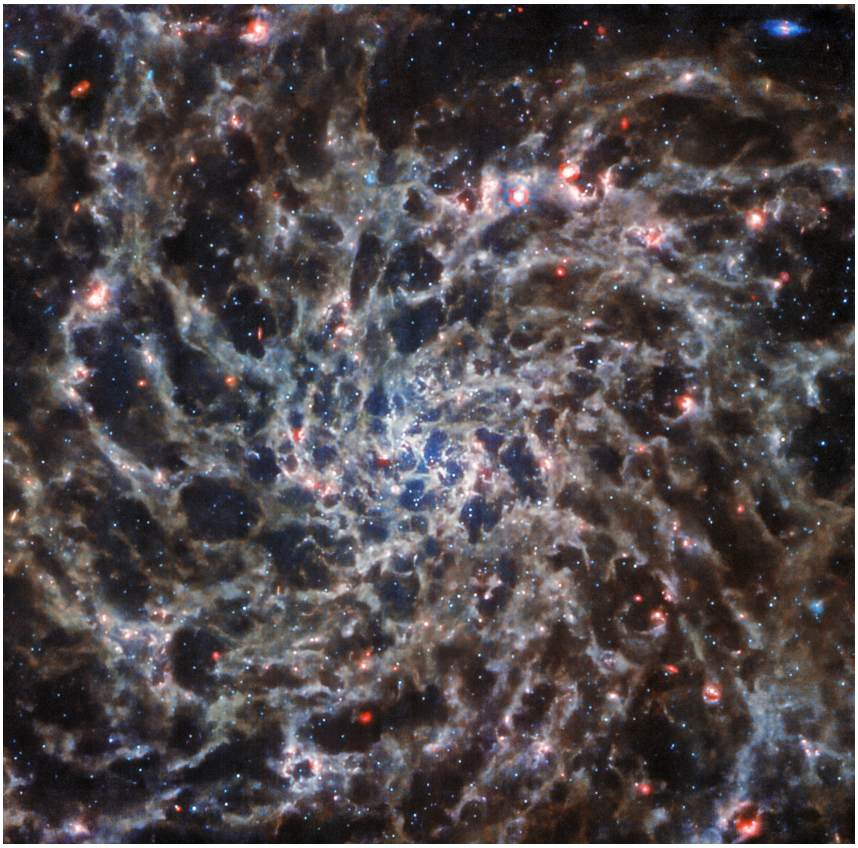

Figure 10.2:
NASA James Webb image of spiral galaxy IC 5332:
a balancing act of gravity and inertia.

The summary in words only:

1. **Electrical forces spread evenly over 3D-space and 1D-time: Liénard-Wiechert force.**

2. **Physics at the smallest space scales: quantum mechanically moving charged quarks lead to gravity.**

3. **Boundary conditions at the largest space scales: expanding, mass filled, universe leads to inertia.**

From the fundamental forces in nature (strong & weak nuclear force, electro-dynamical force, gravity and inertia) only 2 remain: strong nuclear and electro-dynamical force.

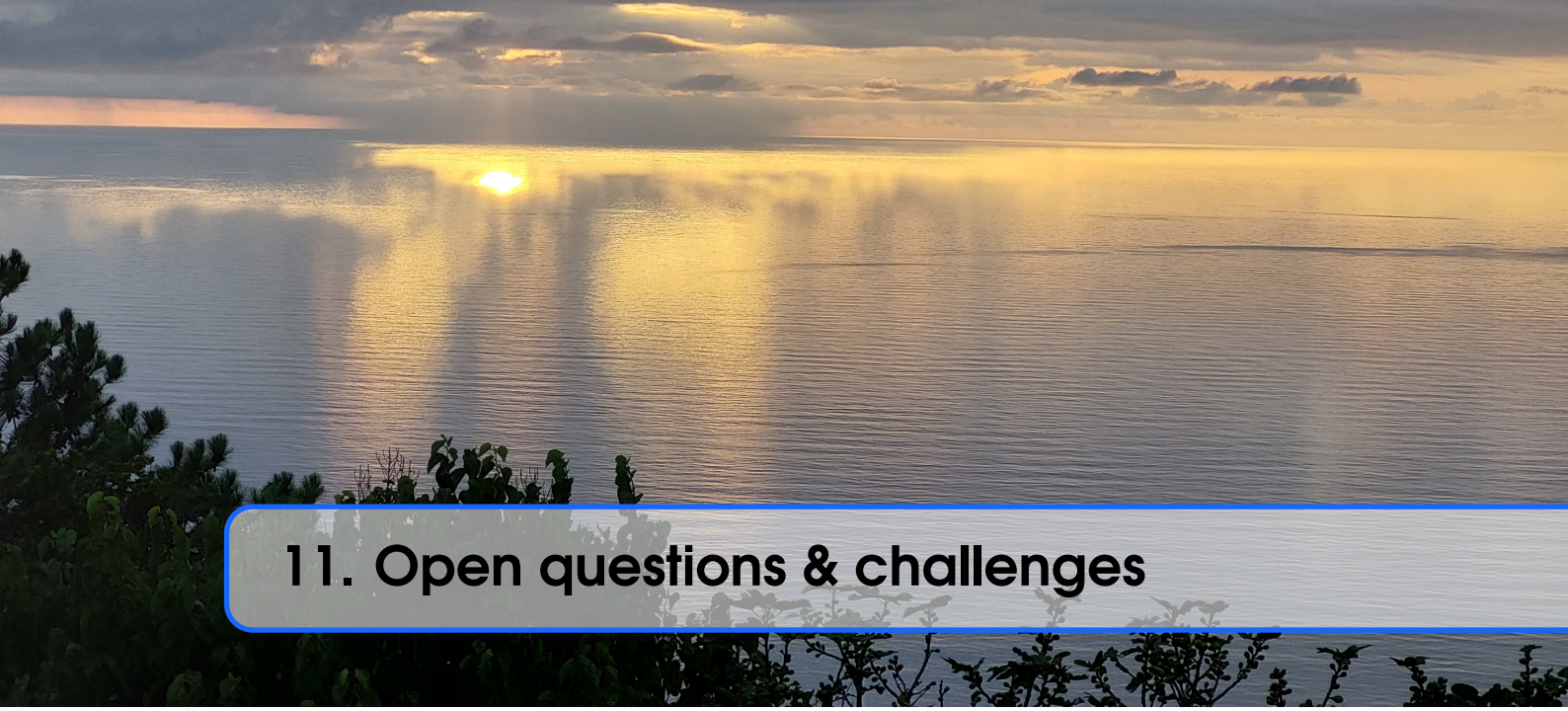

11. Open questions & challenges

Although the presented theory has been able to answer some outstanding questions around forces in physics, it is clear that many open questions still remain, which require studies:

1. §3.5 **Liénard-Wiechert fields**: Currently the deduction of the Liénard-Wiechert field equations starts with the Maxwell equations [64, 69], relying both on electric and magnetic fields. The Liénard-Wiechert field equations, as given by Eq. (3.6), only require the definition of the electric force (field). It should be possible to deduce the Liénard-Wiechert field equations from only 2 basic principles: the static electric force equation for 2 charges and the constant velocity of expansion of this force. An initial study can be found in [9] including references to previous work into this topic.

2. Chapter 4 **Electron**: what is (gravitational) model of an electron, that reconciles gravitational interaction and atomic nature (=single point charge)?

3. Chapter 4 **Anti-matter**: is still poorly understood in this new theory. It has an induced gravitational mass of opposite sign as normal mass (as it has opposite charged anti-quarks). As a result it should have inertia of opposite sign. If this is combined with the opposite electric charge, anti-matter should move in identical direction as normal mass in an external magnetic field. This is obviously not the case [56].
   However, when repeating the boxed experiment of §3.2, with matter and anti-matter inside the box, the conclusion is that the mass of matter and anti-matter is additive, as the total mass in the box is converted into energy, as $E = m c^2$.

4. §5.7 **Gravitational refractive index**: the optical refractive index can be calculated based on the Lorentz model [49, 60]. This model needs to be extended for gravity and made more quantified. Aim is to prove the gravity impact on the speed of light: Eq. (5.6). See for a possible alternative approach: footnote 1 on page 37.

5. Chapter 6 **Quantum evaluation of mass prediction from quark distributions**: the mass prediction of low-Z element nuclei, based on the semi-classical quark distribution, needs to be redone using a proper quantum mechanical methodology.

6. §7.4.3 **high velocity inertia in Hubble expanding universe**: The integral of Eq. (7.16) is still to be solved mathematically, aiming to arrive at Eq. (7.10).

7. §8.5.3 **Orbit mechanics** : still needs further analytic studies, aiming to arrive at the perihelion shift results known from General Relativity. It still puzzles me, that General Relativity gives a positive value of this shift, whereas its linearized version (as expressed by the Liénard-Wiechert forces) shows equal, but OPPOSITE values.

   It is recommended to repeat the perihelion shift calculations, first in linearized General Relativity with fully metric formulation[1], followed by a repeat of the analysis with Liénard-Wiechert forces.

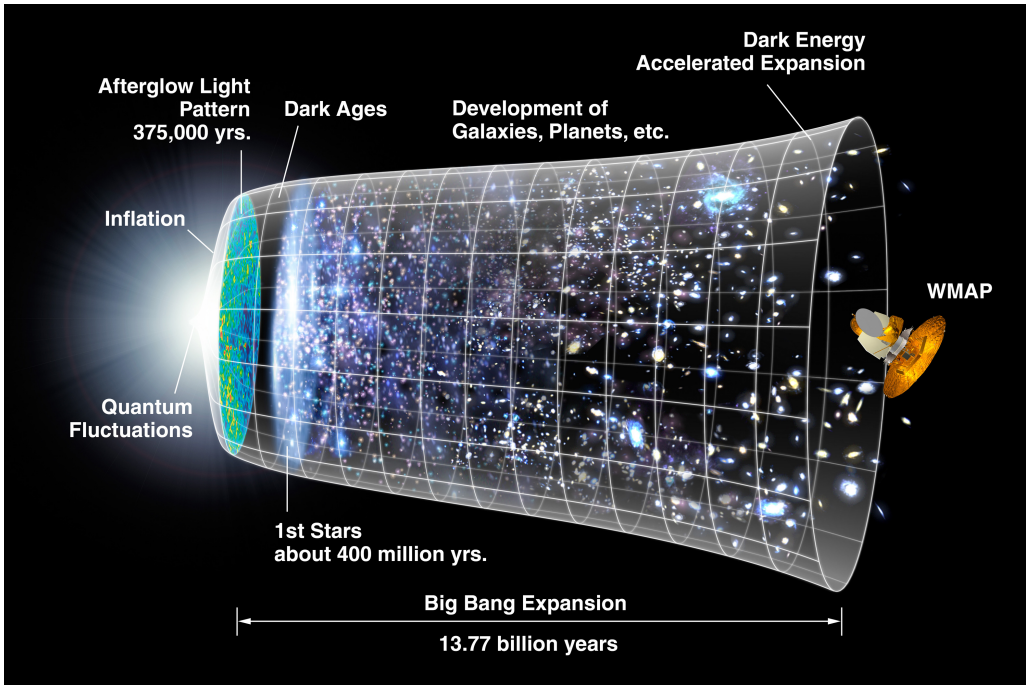

Figure 11.1: Evolution of universe [89, 39],
including the Big Bang 'afterglow light', as shown in fig. 3.11.

8. §7.3.2 **inflation & accelerated universe** : We found an acceleration term in the gravitational inertia formula Eq. (7.9) which may account for early inflation [65] and the acceleration of the universe [96, 70].

[1] It must be noted that it is claimed [68, page 446], [65, page 486] - without details - that the linearized approximation of General Relativity is not sufficiently accurate to predict the perihelion shift, although some recent efforts [47] suggest otherwise.

12. Epilog

The suggestions given in this book are based on earlier work in experimental and theoretical physics. Therefore it is clear that and old Newtonian wisdom is applicable, albeit in a slightly modified form:

If I have seen further,
it is by standing on the shoulders of giants,

but ...

I looked the other way !

Figure 12.1:
NASA James Webb [90] image of the proto-star L1527.

I hope this book stimulates new thoughts on forces in physics.

A. Equivalence principle revisited

The equivalence principle as proposed by Einstein [48, 53, 66, 69, 70] has various formulations. One of them postulates the equivalence of the results of all physical experiments for a boxed accelerated observer and a boxed observer in a gravitational (force) field, as visualized in fig. A.1. We consider the experiment of measuring time via clocks inside the boxes. As extension of the twin paradox, we want to treat the following thought experiment:

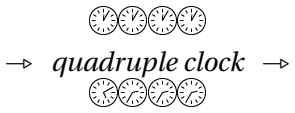

We use 4 identical clocks, initially non-rotating to the 'distant' stars, co-located in a geo-stationary orbit and synchronized. Then the clocks separate and take 4 different paths:

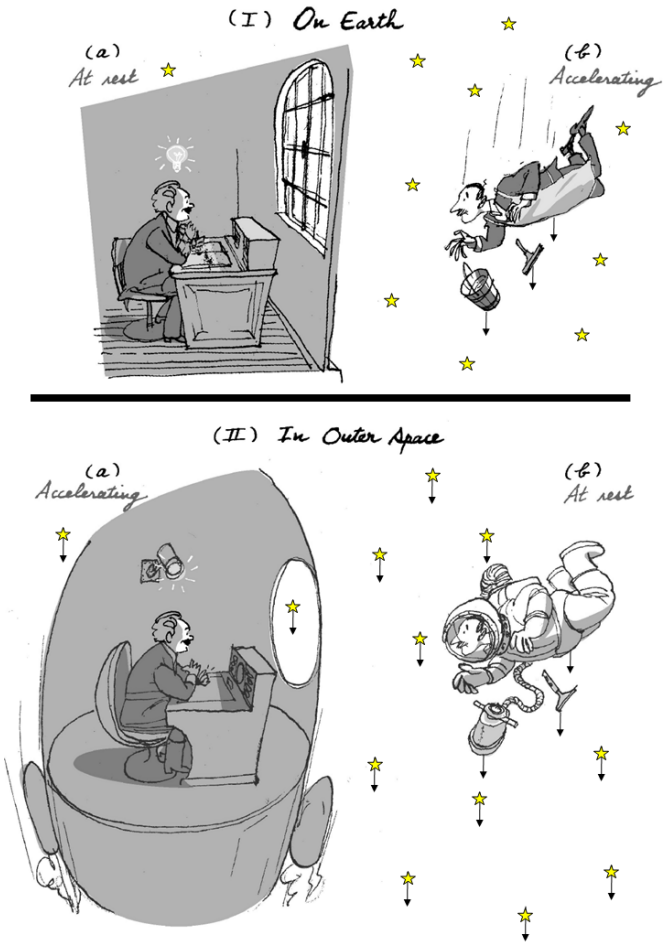

Figure A.1: Equivalence principle visualized (by L. Taudin [62]), with Machican 'fixed' stars added. The arrows indicate acceleration and velocity, as observerd by 'Einstein'.

1. remain in geo-stationary orbit.
2. remain in geo-stationary orbit, but the clock is connected to the end of a rotating rod, such that the centrifugal force that is felt, equals the gravitational force as experienced (on earth) by clock (3).
3. 'climb down' a ladder to earth, remain on earth (experiencing earth's gravity, with free fall acceleration : g $\approx$ 9.8 m/s^2) and re-climb the ladder to geo-stationary orbit, once the rocket (see below) with clock (4) returns.
4. take a ride on a (unpractically large) rocket, which has a continuous acceleration (identical to the 'ladder climbing' clock (3)). It remains accelerated for a prolonged period of time, reaching a maximum velocity (measured from earth[1]) in the order of the speed of light[2]. Then it (slowly) turns 180° to point back to the direction where it came from, while continuing to fire its forward thrusters (thus maintaining - almost - the same acceleration as clock (3) on earth). It then slows down to zero velocity compared to earth, regains velocity again towards earth and returns back to a geo-stationary orbit (after - once more - making a 180° turn), to be reunited with the other clocks

These experiments lead to various accelerations (inertial or gravitational, compared to the earth free fall acceleration constant g) and maximum velocities, with respect to earth, as summarized in the table below.

#	clock path	acceleration force: inertial or gravitational	acceleration / g	max v/c $\approx$
1	geo-stationary	none	0	0
2	geo-stationary + rotation	inertial	1	0
3	earth	gravitational	1	0
4	rocket	inertial	1	$^1/_2$

Once the rocket returns to geo-stationary orbit, and the 4 clocks are (non-rotating) co-located again, their time indications are compared. According to the equivalence principle, the clock on earth, the rotating clock in geo-stationary orbit and the clock in the rocket are equivalent, as they have experienced the same force (be it gravitational or inertial). The clock that remained, non-rotational, in geo-stationary orbit should show a different clock indication, as it experienced no force.

Note that only the clock in the rocket has actually reached high (relativistic) velocities, whereas the other accelerated clocks only reached non-relativistic velocities, compared to earth.

[1] We take earth as the center of the 'fixed' stars in Machian sense. A better definition for the velocity of the 'fixed' stars is to take the average velocity of all masses in a sphere around earth with a radius in the order of $\approx 0.01\, r_{Hubble}$ with the Hubble radius $r_{Hubble} = c/H$, where the universe become homogeneous [31]. See also chapter 7.

[2] From [99] it is known that a constant acceleration ($\vec{g}$) results in a relativistic velocity ($\vec{v}$) of magnitude: $v/c = (g\,t'/c)/\sqrt{1+(g\,t'/c)^2}$. Taking $\vec{g}$ to be the earth free fall acceleration with a magnitude of about 9.8 m/s^2, we find that the condition of $g\,t' = c \rightarrow v/c = 1/\sqrt{2}$ is reached after a (rocket) time ($t' = c/g$) of about 1 year. At these velocities the time dilation factor $\sqrt{1-(v/c)^2}$ is significant.

Now our thought experiment receives a budget cut. We go from a 4-clock experiment to a 2-clock experiment[3]

1. the geo-stationary orbit is replaced by a low-orbit space station (like ISS),
2. the rotating rod clock in geo-stationary orbit is canceled,
3. the ladder becomes an 'ordinary' rocket flying to and from ISS,
4. the (unpractical large) rocket is omitted.

Actually, long duration (> 6 months) stays in low-orbits are routine nowadays [106], without the observation of significant clock speed differences[4] between earth and ISS, in contrast to expectations from the equivalence principle. Gravity, while standing on earth, does not lead to acceleration, nor velocity, whereas an (inertial) acceleration leads to velocity, and thus time dilation, as summarized to [41, pages 599–600], [68, pages: 163-176 & 393 & 1055] :

"Velocity produces a universal time dilation, acceleration does not."

In conclusion:

The full experimental equivalence of boxed experiments
under gravity or acceleration
cannot be maintained.

Note: The 'weak' equivalence principle ('inertial mass is due to gravitational mass') has been discussed and proven in chapter 7.

[3] An even cheaper experimental setup with only earth based clocks can be defined: one clock fixed to the ground and one clock in rotation on a string. However full (force strength) equality cannot be achieved in such a setup. This experiment (5 & 6) can be easily realized by putting a clock on a rotating, flexible, device, such that it experiences only downwards forces. A spinning device that would generate an acceleration of about 5g, would result in a few weeks duriation experiment to reach significant time dilation, see footnote 2 on page 86.

#	clock path	acceleration force: inertial or gravitational	acceleration / g	max v/c ≈
5	stay put on earth	gravitational	1	0
6	stay on earth + rotation	gravitational + inertial	2 - 10	0
7	muons in cosmic radiation	negligible at nearly speed of light	≈ 0	1
8	muons in a storage ring	inertial	≫ 10.000	1

Actually executed [68, page 1055], [70, pages 66–67] experiments (7) and (8) involve spontaneously decay of relativistic fast muons. They are either created in the top layers of the atmosphere and studied on their path to earth (7), or in accelerator storage rings (8)[7]. Both experiments prove the time dilation of relativistic fast moving muons to be independent from the acceleration (force).

[4] As known from GPS satellites [2], a small time dilation between ISS and earth clocks can be expected due to gravitational time dilation in combination with Special Relativity, velocity induced, time dilation.

Figure A.2:
NASA image of collided galaxies: Bullseye [32].

B. Olber's paradox

The Olber's paradox [12, 72], [68, page 756] (*'Why is it dark at night?'*) is based on a calculation that aims to compute the total luminance of the night sky. We assume a static universe with a constant density of light emitting stars (Lum_0). As the luminance per star decreases with the distance squared ($1/r^2$), and the amount of stars increases quadratic with distance (r^2), we find for the total luminance (Lum_{tot}^{static}), for a static universe with radius r_{max}:

$$Lum_{tot}^{static} = \int_0^{r_{max}} \int_0^{\pi} \int_0^{2\pi} \frac{Lum_0}{r^2} r^2 \, Sin[\theta] d\phi d\theta dr = 4\pi \, Lum_0 \, r_{max} \tag{B.1}$$

If we take a static infinite universe ($r_{max} \to \infty$), we find an infinite luminance, which is the starting point for the Olber's paradox. However, when we introduce Hubble expansion, the situation changes dramatically, as was already shown, originally by Tolman, early 1930 [95, 33, 42]. Then, the redshift $z[r]$, see §7.8, becomes important and eq. B.1 is reformulated as (utilizing the Hubble expansion redshift Eq. (7.26):

$$\begin{aligned} Lum_{tot}^{expanding} &= \int_0^{r_{max}} \int_0^{\pi} \int_0^{2\pi} \frac{Lum_0}{(1+z[r])^n \, r^2} r^2 \, Sin[\theta] d\phi d\theta dr \\ &= 4\pi \, r_{Hubble} \, Lum_0 \int_0^{r_{max}/r_{Hubble}} e^{-n\, r/r_{Hubble}} \, d\,(r/r_{Hubble}) \end{aligned} \tag{B.2}$$

where n is a variable found in literature, that may vary from $n = 0$ representing a static universe, via $n = 2$ as shown by the original Tolman model [33, 42] (and experimental data [26]), to $n = 4$ taking into account all possible luminance reduction expansion options [95]. The integration of Eq. (B.2) is visualized in fig. B.1b. It is clear that, for a an expanding ($n > 0$) infinite universe ($r_{max} \to \infty$), we find convergence and the integral evaluates to a simple $1/n$.

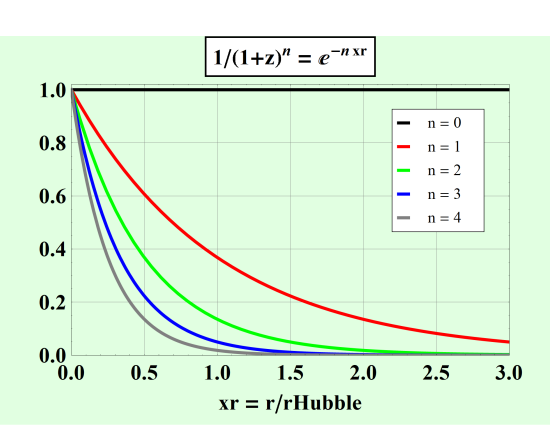

(a) Tolman luminance reduction, for various n.

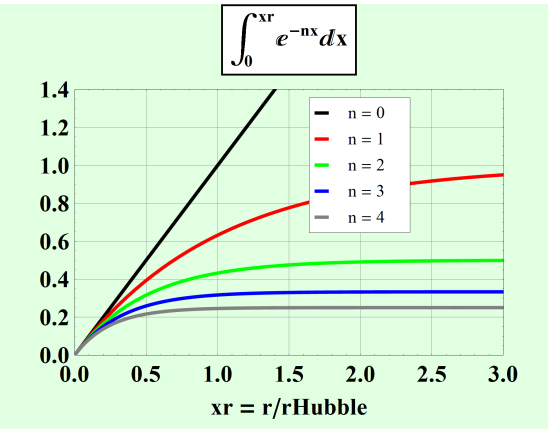

(b) Integration of Tolman function.

Figure B.1: Luminance reduction function and integral from Tolman model.

Therefore, we find that (Hubble) expansion of the universe is a sufficient explanation for solving Olber's paradox, why *'the night is dark'*.

Figure B.2:
NASA James Webb image of Stephan's Quintet.

C. Relativistic inertia increase

In this appendix we provide some computational details behind the integration of Eq. (7.9) in §7.3.2, which describes the gravitational, inertial force on an accelerated mass in relativistic movement in a static universe model. The computation has been computer assisted [85], but some intermediate steps are shown here. The gravitational Liénard-Wiechert force fields have been introduced in §7.2 and used in §7.3.2. For the static universe we put the observer (with mass m_{obs}) in the center and use spherical coordinates: $\vec{x} = (x, y, z) = (r\,Cos[\phi]\,Sin[\theta], r\,Sin[\phi]\,Sin[\theta], r\,Cos[\theta])$ (see fig. C.1a), with velocity $\vec{v} = (0, 0, v_z)$, $0 \leq v_z < c$ and acceleration $\vec{a} = (a_x, a_y, a_z)$, as shown in fig. C.1b. The definition of the velocity to be in the positive z-direction maintains generality, as we do not put constraints on the acceleration vector and we integrate over the entire (static) universe.

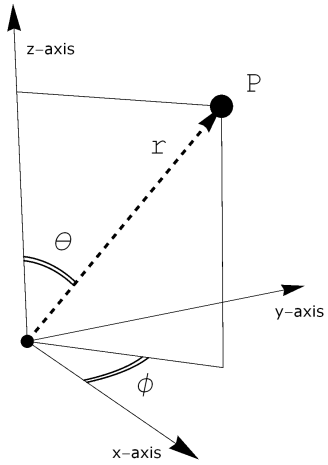

(a) Spherical coordinates definition.

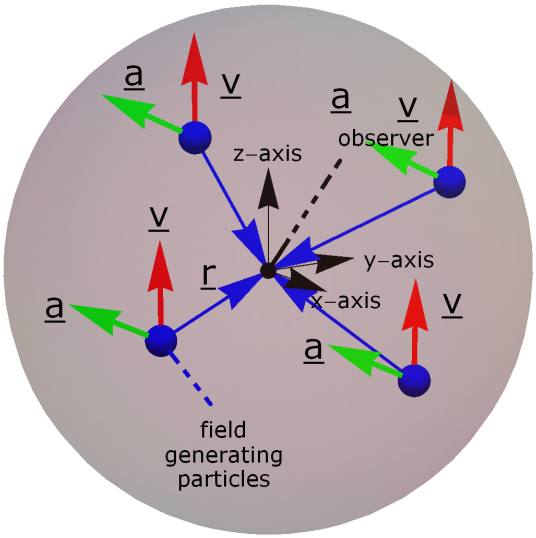

(b) Observer in the center of the static universe: all particles have identical velocity and acceleration.

Figure C.1: Spherical coordinates and the static universe in motion & acceleration.

The total force integration over all masses of the static universe amounts to:

$$\overrightarrow{F_g^{tot}} = \int^{all\ masses} \overrightarrow{F_g}\, d\,mass \tag{C.1}$$

$$= -\,m_{obs}\int_0^{r_{max}}\int_0^{\pi}\int_0^{2\pi} (\vec{E}_g^{*} + \vec{v} * \vec{B}_g^{*})\,\rho\,\frac{\sqrt{1-(v_z/c)^2}}{1+(v_z/c)\,Cos[\theta]}\,r^2\,Sin[\theta]\,d\phi\,d\theta\,dr$$

$$= m_{obs}\,G\,\rho\,\sqrt{1-(v_z/c)^2}\int^{all\ masses} (f_x, f_y, f_z)\,d\,mass$$

where r_{max} indicates the size of the universe (as seen by the observer). Also we re-used $\vec{E}_g^{*} = \vec{E}_g/m_{part}$ and $\vec{B}_g^{*} = \vec{B}_g/m_{part}$. We have taken the factors, that are constants for the (space) integration $m_{obs}\,G\,\rho\,\sqrt{1-(v_z/c)^2}$ out of the integration and find the following integrand functions in (x,y,z) directions, which include the drop of the minus sign in the 3^{rd} line of Eq. (C.1):

$$\begin{aligned} f_x = \quad & Sin[\theta]\Big(a_x\,r\,\big(8\,v_z Cos[\theta]/c + (1+(v_z/c)^2)\,(3+Cos[2\theta])\big) \\ & -4\,Cos[\phi]\,Sin[\theta]\,\big(c^2(1-(v_z/c)^2) + a_z\,r\,v_z/c + a_z\,r\,Cos[\theta]\big) \\ & -2\,(1-(v_z/c)^2)\,r\,Sin[\theta]^2\,(a_x Cos[2\phi] + a_y Sin[2\phi])\Big) \\ & /\,\Big(4\,c^2\,(1+(v_z/c)\,Cos[\theta])^4\Big) \end{aligned} \tag{C.2}$$

We find a similar integrand for the y-direction (as to be expected from symmetry considerations, around the z-axis (=velocity axis). Note some exchanges in $a_x \leftrightarrow a_y$ and $Cos[\phi] \leftrightarrow Sin[\phi]$:

$$\begin{aligned} f_y = \quad & Sin[\theta]\Big(a_y\,r\,\big(8\,v_z Cos[\theta]/c + (1+(v_z/c)^2)\,(3+Cos[2\theta])\big) \\ & -4\,Sin[\phi]\,Sin[\theta]\,\big(c^2(1-(v_z/c)^2) + a_z\,r\,v_z/c + a_z\,r\,Cos[\theta]\big) \\ & +2\,(1-(v_z/c)^2)\,r\,Sin[\theta]^2\,(a_y Cos[2\phi] - a_x Sin[2\phi])\Big) \\ & /\,\Big(4\,c^2\,(1+(v_z/c)\,Cos[\theta])^4\Big) \end{aligned} \tag{C.3}$$

For the z-direction, we find a different equation (as the velocity is in z-direction):

$$\begin{aligned} f_z = \quad & Sin[\theta]\Big(c^2\,(1-(v_z/c)^2)\,(v_z/c + Cos[\theta]) + \ldots \\ \ldots + & \frac{a_z\,r}{2}\,(1-Cos[2\theta]) - r\,Sin[\theta]\,(v_z/c + Cos[\theta])\,(a_x Cos[\phi] + a_y Sin[\phi])\Big) \\ & /\,\Big(c^2\,(1+(v_z/c)\,Cos[\theta])^4\Big) \end{aligned} \tag{C.4}$$

Now we perform a partial integration over the azimuth angle $\int_0^{2\pi} d\,\phi$ to arrive at:

$$\overrightarrow{F_g^{tot}} = m_{obs}\,G\,\rho\,\sqrt{1-(v_z/c)^2}\int_0^{r_{max}}\int_0^{\pi} (f_x^{\phi}, f_y^{\phi}, f_z^{\phi})\,d\theta\,dr \tag{C.5}$$

with:

$$\begin{aligned} f_x^{\phi}[\theta,r] &= \frac{a_x\,\pi\,r\,Sin[\theta]\,\big(8\,(v_z/c)\,Cos[\theta] + (1+(v_z/c)^2)\,(3+Cos[2\theta])\big)}{2\,c^2\,(1+(v_z/c)\,Cos[\theta])^4} \\ f_y^{\phi}[\theta,r] &= \frac{a_y\,\pi\,r\,Sin[\theta]\,\big(8\,(v_z/c)\,Cos[\theta] + (1+(v_z/c)^2)\,(3+Cos[2\theta])\big)}{2\,c^2\,(1+(v_z/c)\,Cos[\theta])^4} \\ f_z^{\phi}[\theta,r] &= \frac{2\,\pi\,Sin[\theta]\,\big(c^2\,(1-(v_z/c)^2)\,((v_z/c) + Cos[\theta]) + a_z\,r\,Sin^2[\theta]\big)}{c^2\,(1+(v_z/c)\,Cos[\theta])^4} \end{aligned} \tag{C.6}$$

Now we continue with a further integration over the polar angle $\int_0^{\pi} d\theta$:

$$\overrightarrow{F_g^{tot}} = m_{obs}\, G\rho \sqrt{1-(v_z/c)^2} \int_0^{r_{max}} (f_x^{\phi\theta}, f_y^{\phi\theta}, f_z^{\phi\theta})\, d\theta\, dr \tag{C.7}$$

with:

$$\begin{aligned} f_x^{\phi\theta}[r] &= \frac{8\pi\, a_x\, r}{3\,c^2}\, \frac{1}{1-(v_z/c)^2} \\ f_y^{\phi\theta}[r] &= \frac{8\pi\, a_y\, r}{3\,c^2}\, \frac{1}{1-(v_z/c)^2} \\ f_z^{\phi\theta}[r] &= \frac{4\pi\,(2\,a_z\, r - v_z\, c\,(1-(v_z/c)^2)}{3\,c^2}\, \frac{1}{\left(1-(v_z/c)^2\right)^2} \end{aligned} \tag{C.8}$$

Now we finish the integration by integrating of the radial coordinate of the universe $\int_0^{r_{max}} dr$. The upper integration limit r_{max} is used to obtain mathematical convergence of the integration over the radius of the sphere of the static universe. In line with §7.3, we use as maximum radius of the universe, the radius, which follows from the linear Hubble law: $v = Hr$. The (maximum possible) velocity of light is obtained for $r_{max} = c/H = r_{Hubble}$, which we will use as upper integration limit. Finally we find the results as presented in §7.3.2 and given in Eq. (7.9):

$$\begin{aligned} \overrightarrow{F_g^{tot}} &= -\, m_{obs} \int_0^{c/H} \int_0^{\pi} \int_0^{2\pi} (\vec{E}_g^{*} + \vec{v} * \vec{B}_g^{*})\, \rho\, \frac{\sqrt{1-(v_z/c)^2}}{1+(v_z/c)\,Cos[\theta]}\, r^2\, Sin[\theta]\, d\phi\, d\theta\, dr \\ &= m_{obs}\, \frac{4\pi\rho\, G}{3\,H^2} \left(\frac{a_x}{\sqrt{1-(v_z/c)^2}}, \frac{a_y}{\sqrt{1-(v_z/c)^2}}, \frac{a_z - H\, v_z\,(1-(v_z/c)^2)}{\sqrt{1-(v_z/c)^2}^3} \right) \end{aligned} \tag{C.9}$$

The importance of computer assisted mathematical analysis [85] has been made clear (at least to me).

Figure C.2: James Webb telescope [90] image of the 'Pillars of Creation' (image by NASA).

D. Inertia from expanding universe

Here we give some computational details behind the integration of Eq. (7.14) in §7.4.2, which describes the gravitational, inertial force on a, slow ($v \ll c$) moving [1] accelerated mass in an infinite Hubble expanding universe. The total force integration over all masses of the static universe amounts to:

$$\overrightarrow{F_g^{tot}} = \int^{all\ masses} \overrightarrow{F_g}\, d\,mass = m_{obs} \int^{all\ masses} (f_x, f_y, f_z)\, d\,mass \tag{D.1}$$
$$= \int_0^{\infty}\int_0^{\pi}\int_0^{2\pi} m_{obs}\,(\vec{E_g^*} + \vec{v} * \vec{B_g^*})\,\rho\; e^{-r/r_{Hubble}}\, r^2\, Sin[\theta]\, d\phi\, d\theta\, dr$$

The calculation has no symmetry condition, and therefore we expect equal results in (x,y,z) directions, for a given acceleration $\vec{a} = (a_x, a_y, a_z)$. When evaluating $\vec{E_g^*}$ and $\vec{B_g^*}$ [85], we find for f_x, f_y and f_z :

$$f_x = \frac{m_{obs}\,\rho\, G\, e^{-3r/r_{Hubble}}}{8\,c^2}\, Sin[\theta]\,. \tag{D.2}$$
$$.\Big(\quad 8\,Cosh^2[r/r_{Hubble}]\,\big(a_x\, r\, Cos^2[\theta] - a_z\, Cos[\theta]\, Cos[\phi]\, Sin[\theta] + ..$$
$$.. + Sin[\theta]\,(c^2\, Cos[\phi] + r\, Sin[\theta]\, Sin[\phi]\,(-a_y\, Cos[\phi] + a_x\, Sin[\phi]))\big) - ..$$
$$.. - 8\,Sinh^2[r/r_{Hubble}]\, c^2\, Cos[\phi]\, Sin[\theta] + ...$$
$$... + r\, Sinh[2\,r/r_{Hubble}]\,\big(3\,a_x + a_x\, Cos[2\theta] - 2\,a_z\, Cos[\phi]\, Sin[2\theta] - ..$$
$$.. - 2\, Sin^2[\theta]\,(a_x\, Cos[2\phi] + a_y\, Sin[2\phi])\big) \quad \Big)$$

$$f_y = \frac{m_{obs}\,\rho\, G\, e^{-3r/r_{Hubble}}}{8\,c^2}\, Sin[\theta]\,. \tag{D.3}$$
$$.\Big(\quad 8\,Cosh^2[r/r_{Hubble}]\,\big(a_y\, r\,\big(Cos^2[\theta] + Cos^2[\phi]\, Sin^2[\theta]\big) + ..$$
$$+ Sin[\theta]\,\big(c^2 - r\,\big(a_z\, Cos[\theta] + a_x\, Cos[\phi]\, Sin[\theta]\big)\big)\, Sin[\phi]\big) - ..$$
$$.. - 8\,c^2\, Sin[\theta]\, Sin[\phi]\, Sinh^2[r/r_{Hubble}] + ..$$
$$.. + r\, Sinh[2\,r/r_{Hubble}]\,\big(3\,a_y + a_y\, Cos[2\theta] - 2\,a_z\, Sin[2\theta]\, Sin[\phi] + ..$$
$$.. + 2\, Sin^2[\phi]\,\big(a_y\, Cos[2\phi] - a_x\, Sin[2\phi]\big)\big) \quad \Big)$$

[1] in relation to the average of nearby ($r < 0.01\ r_{Hubble}$) universe masses.

$$f_z = \frac{m_{obs}\,\rho\,G\,e^{-3r\,/\,r_{Hubble}}}{4\,c^2}\,Sin[\theta]\,. \tag{D.4}$$
$$.\Big(\quad c^2\left(3-e^{2r\,/\,r_{Hubble}}\right)Cos[\theta]+2\,e^{r\,/\,r_{Hubble}}\,Cosh[r\,/\,r_{Hubble}]\,.$$
$$.\left(c^2\,Cos[\theta]+r\left(2\,a_z\,Sin^2[\theta]-Sin[2\theta]\left(a_x\,Cos[\phi]+a_y\,Sin[\phi]\right)\right)\right)\quad\Big)$$

Similar as done in appendix C, we perform a partial integration over the azimuth angle $\int_0^{2\pi} d\,\phi$ to arrive at:

$$\overrightarrow{F_g^{tot}} = \int_0^{\infty}\int_0^{\pi}\left(f_x^{\phi}\,,\,f_y^{\phi}\,,\,f_z^{\phi}\right)d\theta\,dr \tag{D.5}$$

where we find for f_x^{ϕ}, f_y^{ϕ} and f_z^{ϕ} :

$$f_x^{\phi} = \frac{a_x\,\pi\,m_{obs}\,\rho\,G}{2\,c^2}\,r\,e^{-2r\,/\,r_{Hubble}}\,Cosh[r\,/\,r_{Hubble}]\,Sin[\theta]\,(3+Cos[2\theta]) \tag{D.6}$$

$$f_y^{\phi} = \frac{a_y\,\pi\,m_{obs}\,\rho\,G}{2\,c^2}\,r\,e^{-2r\,/\,r_{Hubble}}\,Cosh[r\,/\,r_{Hubble}]\,Sin[\theta]\,(3+Cos[2\theta]) \tag{D.7}$$

$$f_z^{\phi} = \frac{\pi\,m_{obs}\,\rho\,G}{c^2}\,e^{-3r\,/\,r_{Hubble}}\left(2\,c^2\,Cos[\theta]+a_z\,r\left(1+e^{r\,/\,r_{Hubble}}\right)Sin^2[\theta]\right) \tag{D.8}$$

As expected we regain the symmetry between f_x and f_y after the integration over the azimuth angle. After a further integration over the polar angle $\int_0^{\pi} d\,\theta$ we arrive at:

$$\overrightarrow{F_g^{tot}} = \int_0^{\infty}\left(f_x^{\phi\theta}\,,\,f_y^{\phi\theta}\,,\,f_z^{\phi\theta}\right)dr \tag{D.9}$$

where we find (as to be expected) identical formulas for $f_x^{\phi\theta}$, $f_y^{\phi\theta}$ and $f_z^{\phi\theta}$:

$$f_x^{\phi\theta} = a_x\,\frac{4\,\pi\,m_{obs}\,\rho\,G}{3\,c^2}\,r\,e^{-r\,/\,r_{Hubble}}\left(1+e^{-2r\,/\,r_{Hubble}}\right) \tag{D.10}$$

$$f_y^{\phi\theta} = a_y\,\frac{4\,\pi\,m_{obs}\,\rho\,G}{3\,c^2}\,r\,e^{-r\,/\,r_{Hubble}}\left(1+e^{-2r\,/\,r_{Hubble}}\right) \tag{D.11}$$

$$f_z^{\phi\theta} = a_z\,\frac{4\,\pi\,m_{obs}\,\rho\,G}{3\,c^2}\,r\,e^{-r\,/\,r_{Hubble}}\left(1+e^{-2r\,/\,r_{Hubble}}\right) \tag{D.12}$$

Now we define the help integration variable $x = r\,/\,r_{Hubble}$ (remembering that $r_{Hubble} = c\,/\,H$ with H being the Hubble constant) and thus $1/c^2\,r\,dr = 1/c^2 r_{Hubble}^2\,x\,dx = 1/H^2\,x\,dx$. Now we can execute the final integration to arrive at the total inertial force, due to the gravitational forces of all masses in a Hubble expanding universe:

$$\overrightarrow{F_g^{tot}} = m_{obs}\,(a_x\,,a_y\,,a_z)\,\frac{4\,\pi\,\rho\,G}{3\,H^2}\int_0^{\infty} x\,e^{-x}\,(1+e^{-2x})\,dx = m_{obs}\,\vec{a}\;\frac{40\,\pi\,\rho\,G}{27\,H^2} \tag{D.13}$$

An image of (the convergence of) the integrand was given in fig. 7.7b. We find that most inertial force is generated at distances larger than the Hubble distance. The constant $\frac{40\,\pi\,\rho\,G}{27\,H^2}$ equals a value close to unity, based on the outcome of the General Relativity Friedmann models for the universe [65, 70], in combination with WMAP [89, 39] analysis.

E. Gravito-magnetism

Gravito-magnetism has a long history [36]. Maxwell applied his electro-dynamical equations to gravity, but was baffled by the possibility of inifite negative energy (currently labeled as 'black hole'). Inspired by the Maxwellian equations for electro-dynamics, Heaviside [19] proposed a gravitational analogon, but found only very limited orbital effects.

Lense-Thirring calculated the effects for a rotating mass, based upon linearized General Relativity, but found minimal effects, confirmed to limited experimental accuracy by the Gravity-Probe-B [36] mission.

Orbit calculations with gravito-magnetism have been attempted, with mixed results [4, 84, 27, 28, 34].

In this book, we have re-used the gravito-magnetism analogon, but expressed the fields not by the Maxwell equations but by their equivalent Liénard-Wiechert formulation, as shown in chapter 7 and detailed in Eq. (7.1). Contrary to Lense-Thirring, we did not focus on a rotating sphere, but studied a - low velocity - accelerated mass filled sphere. The low velocity analysis of an accelerated - static - universe elimitates the 'magnetic' field [1] , but shows the importance of the acceleration part of the 'electric' field in the Liénard-Wiechert equation. Using the size of the entire - mass filled - universe gives a significant force effect (inertia), rather than the very smal 'frame-dragging' effects of a singular rotating mass. During the beginning of the 20th century, the size of the universe, linked to Hubble expansion was not known [68, page 758], and therefore, it is historically understandable that a gravitational analysis with such a large size was not conducted. Only by 1953 did Sciama [37] study the gravitational (inertial) impact of a large accelerated mass filled sphere.

[1] as the 'magnetic' term drops from the total force term, given the gravitational equaivalent of Eq. (3.7).

Figure E.1:
NASA James Webb image of cartwheel galaxy,
located at about 500 million lightyears from earth.

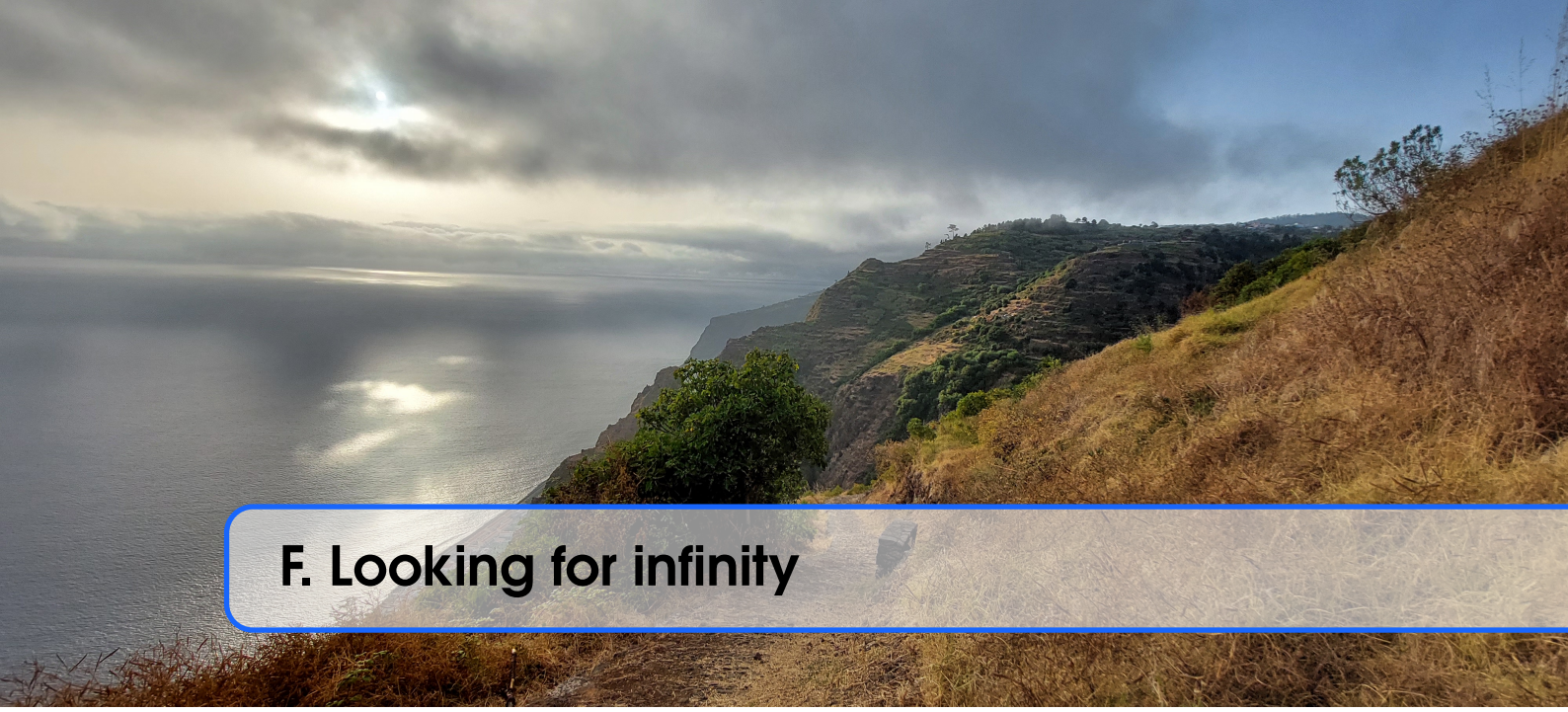

F. Looking for infinity

In this appendix we study the size of the universe, based on inertia assymetry arguments. These were originally discussed in the critique of the static university model, in §7.3.3.

Here we detail a similar asymmetry argument for the Hubble expanding universe. We will derive equations for the resulting asymmetry of inertial forces when the Hubble universe is not symmetrical on large scale [1]. To achieve this we split the result of the inertia analysis in an expanding universe, as given by Eq. (7.14), in 2 parts. The first part is a spherical symmetric force integration up to a radius: $n_{sym}\, r_{Hubble}$. The second part is an asymmetrical force integration from this distance up to infinity, with a non-complete integration over the polar angle (θ), from 0 to $\pi - \delta$. This is also shown in fig F.1. The total inertial force is then expressed as:

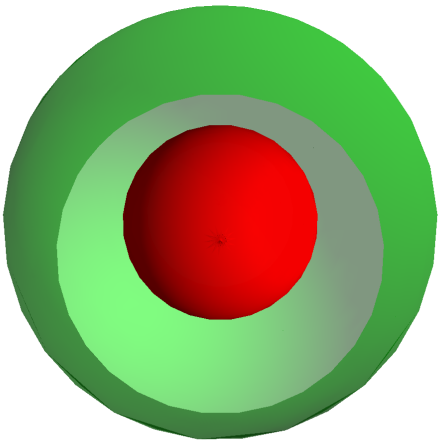

Figure F.1: Asymmetric Hubble universe: full, mass filled, sphere (up to $n_{sym}\, r_{Hubble}$) and an incomplete sphere stretching to infinity.

$$\overrightarrow{F_g^{tot}} = -\, m_{obs} \int_0^{n_{sym} r_{Hubble}} \int_0^{\pi} \int_0^{2\pi} (\vec{E_g^*} + \vec{v} * \vec{B_g^*})\, \rho\; e^{-r/r_{Hubble}}\; r^2\, Sin[\theta]\; d\phi\, d\theta\, dr - \ldots \quad \text{(F.1)}$$

$$\ldots - m_{obs} \int_{n_{sym} r_{Hubble}}^{\infty} \int_0^{\pi-\delta} \int_0^{2\pi} (\vec{E_g^*} + \vec{v} * \vec{B_g^*})\, \rho\; e^{-r/r_{Hubble}}\; r^2\, Sin[\theta]\; d\phi\, d\theta\, dr$$

$$= m_{obs} \frac{\pi\, \rho\, G}{27\, c^2} \left(a_x\, f_{xy}^{\theta_{asym}}[n_{sym}, \delta],\; a_y\, f_{xy}^{\theta_{asym}}[n_{sym}, \delta],\; f_z^{\theta_{asym}}[a_z, n_{sym}, \delta] \right)$$

[1] Note that was proven that the universe is homogeneous at length scales $r > 0.01\, r_{Hubble}$ [31].

with the function $f_{xy}^{\theta_{asym}}[n_{sym},\delta]$ and $f_z^{\theta_{asym}}[a_z,n_{sym},\delta]$ given by [85]:

$$f_{xy}^{\theta_{asym}}[n_{sym},\delta] = \frac{r_{Hubble}^2}{8}\, e^{-3n_{sym}} \ldots \qquad \text{(F.2)}$$
$$\ldots\big(\,320e^{3n_{sym}} + 9e^{2n_{sym}}(1+n_{sym})\,(-16+15Cos[\delta]+Cos[3\delta]) + \ldots$$
$$\ldots + (1+3n_{sym})\,(-16+15Cos[\delta]+Cos[3\delta])\;\big)$$

$$f_z^{\theta_{asym}}[a_z,n_{sym},\delta] = \frac{r_{Hubble}}{4}\, e^{-3n_{sym}} \ldots$$
$$\ldots\big(\,-a_z\, r_{Hubble}\,(1+3n_{sym}+9e^{2n_{sym}}(1+n_{sym})\,(-9Cos[\delta]+Cos[3\delta])\;) + \ldots$$
$$\ldots + 4\,(2a_z\, r_{Hubble}\,(-1+20e^{3n_{sym}}-3n_{sym}-9e^{2n_{sym}}(1+n_{sym})) + 9c^2(Sin[\delta])^2)\big)$$

For $\delta = 0$ we find the results from Eq. (D.13).

From Eq's. (F.1) and (F.3) we find immediately that no asymmetry forces arise in the symmetric x,y-direction, as we employ a full integration over the azymuth angle (ϕ). The force in the z-direction contains 2 parts. One part is proportional to $a_z\, r_{Hubble}$ and the other to c^2. Normally a term containing c^2 dwarfs all other terms, but not here. When evaluating $a_z\, r_{Hubble}/c^2 = a_z/(c\,H) \approx a_z\, 1.5\times 10^9$. Therefore, we can neglect the term containing c^2 in Eq. (F.3) for accelerations $|a_z| \geq |10^{-7}\, m/s^2$. This allows a simplification when taking the force ratio:

$$F_{ratio}[n_{sym},\delta] \;=\; \left(\frac{f_z^{\theta_{asym}}[a_z,n_{sym},\delta]}{a_x\, f_{xy}^{\theta_{asym}}[n_{sym},\delta]}\right) - 1 \;=\; -1 + \frac{a_z}{a_x} \ldots \qquad \text{(F.3)}$$
$$\ldots \frac{2\big(160e^{3n_{sym}} + 9e^{2n_{sym}}(1+n_{sym})(-8+9Cos[\delta]-Cos[3\delta]) + (1+3n_{sym})(-8+9Cos[\delta]-Cos[3\delta])}{320e^{3n_{sym}} + 9e^{2n_{sym}}(1+n_{sym})(-16+15Cos[\delta]+Cos[3\delta]) + (1+n_{sym})(-16+15Cos[\delta]+Cos[3\delta])}$$

$F_{ratio}[n_{sym},\delta]$ has been visualized (for $a_z/a_x = 1$) in fig. F.3a. It shows an exponential decay as function of n_{sym} and has a maximum for $\delta \approx \pi/4$. In fig. F.3a and F.3b the behavior of this function is detailed further for larger values of the homegeneous universe size $n_{sym}(*\, r_{Hubble})$. We find that a symmetric universe with a radius of $15\, r_{Hubble}$, gives a 1 ppm force asymmetry (for $\delta \approx \pi/4$). This should be detectable from Eötvös type experiments [2] [107]. If this 1ppm force asymmetry is not observed, we must conclude that the Hubble expanding universe is symmetrical up to a radius of at least $15\, r_{Hubble}$.

The alternative hypothesis, that the universe is symmetrical, but finite in size, with the earth exactly in its center, can be easily falsified. To prove this, we analyze inertia behavior of objects that are located at large distances from earth. Deep field studies [108], based upon images like fig 1, 7.8b, 7.12, E.1 and F.4 make observations at distances $> r_{Hubble}$. No evidence for inertia asymmetries in galaxy movements is known to the author. This indicates that those locations in the universe have identical inertia properties as found on earth. Therefore (under the alternative hypothesis) all these positions can also claim to have the priviliged position as the center of the universe. Thus 'every position in the universe' can claim to be its center, and thus 'there is no center of the universe'. Therefore the altenative hypothesis cannot be true, and we are lead to the conclusion of the very large (infinite?) universe as given in the previous paragraph.

[2] In fact Eötvös type experiments measure differences between gravitational mass and inertial mass. Thus asymmetries in these massses point to asymmetries in their sources: quark movements and the shape of the universe. In summary: Eötvös type experiments measure asymmetries between the smallest and largest length scales.

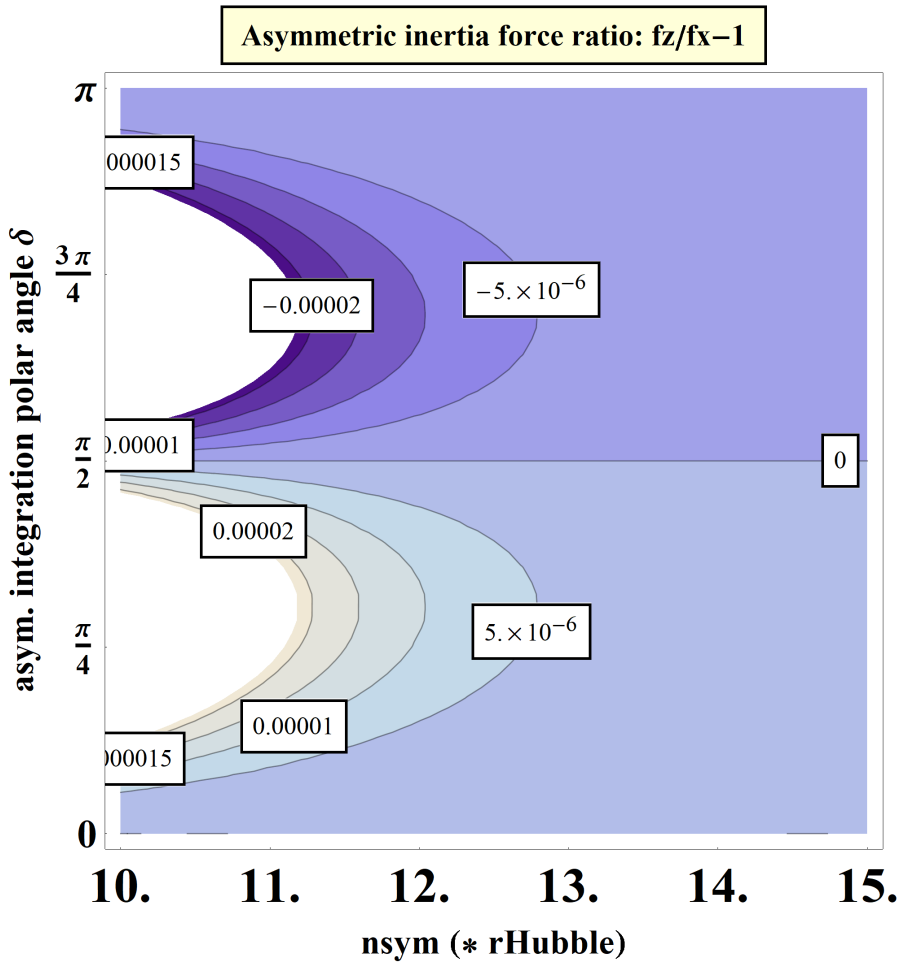

Figure F.2: Contourplot of asymmetrical inertia force.

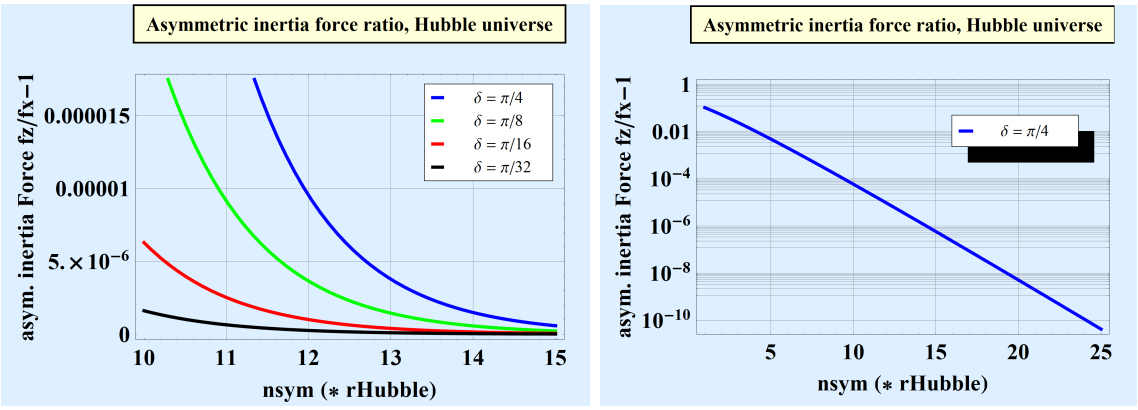

(a) Asymmetrical inertia force, for various asymmetry angles δ and symmetrical universe size ($n_{sym}\, r_{Hubble}$).

(b) Inertial asymmetry decreases exponentially with symmetrical universe size ($n_{sym}\, r_{Hubble}$).

Figure F.3: Asymetric force ratio as function of the homogeneous size of the expanding universe, expressed as $n_{sym}\, r_{Hubble}$.

Figure F.4:
NASA James Webb image of galaxy LEDA-2046648,
located at about 1 billion light years away from earth .

G. Units and notations

In this entire book, we have consistently used S.I. units [98]: seconds (s), meter (m), kilogram (kg), Ampere (A). From these elementary units, we find derived units and values for the elementary charge of the electron & proton (q_0), speed of light (c) and permittivity of vacuum (ϵ_0). These unit usages lead to the Liénard-Wiechert fields as given in Eq. (3.6) of §3.5.

In this book we have used vectors intensely as expressions for the strengths and directions for position, velocity, acceleration and force in a 3-dimensional Euclidean world, with 1 time coordinate (t). We use vectors in 3 dimensions as:

Position: $\vec{x} = (x, y, z)$
Velocity: $\vec{v} = d\vec{x}/dt = (v_x, v_y, v_z)$
Acceleration: $\vec{a} = d\vec{v}/dt = (a_x, a_y, a_z)$

The Euclidean norm of a vector is given as: $\|\vec{x}\| = \sqrt{x^2 + y^2 + z^2}$.

Spherical coordinates (See also: fig. C.1a) are given as (r, ϕ, θ) and give the vector position as: $\vec{x} = (x, y, z) = (r\,Cos[\phi]\,Sin[\theta], r\,Sin[\phi]\,Sin[\theta], r\,Cos[\theta])$.

For forces we use 2 notations: one as vector and one with an over-arrow (if long comments in the name are needed):

$$\text{Force:} \quad \vec{F} = (F_x, F_y, F_z) \qquad \text{or:} \quad \overrightarrow{F_g^{tot}}$$

For the electro-dynamical, Liénard-Wiechert, force equations, we need to use verctor dot- and cross-products, which have following properties, in flat 3D space [58, pages 601–603]:

$$\begin{aligned}
\vec{a} \bullet \vec{v} &= (a_x, a_y, a_z) \bullet (v_x, v_y, v_z) = a_x v_x + a_y v_y + a_z v_z \\
\vec{a} * \vec{v} &= (-a_z v_y + a_y v_z, a_z v_x - a_x v_z, -a_y v_x + a_x v_y) \\
\vec{x} * (\vec{v} * \vec{a}) &= (\vec{x} \bullet \vec{a})\,\vec{v} - (\vec{x} \bullet \vec{v})\,\vec{a} \\
\vec{a} \bullet (\vec{v} * \vec{x}) &= \vec{x} \bullet (\vec{a} * \vec{v}) = \vec{v} \bullet (\vec{x} * \vec{a}) \\
(\vec{a}_1 + \vec{a}_2) * \vec{r} &= \vec{a}_1 * \vec{r} + \vec{a}_2 * \vec{r} \qquad \vec{v} * \vec{v} = \vec{0}
\end{aligned} \tag{G.1}$$

Approximations for $x \ll 1$: $\sqrt[n]{1-x} \approx 1 - x/n \quad 1/\sqrt[n]{1-x} \approx 1 + x/n$

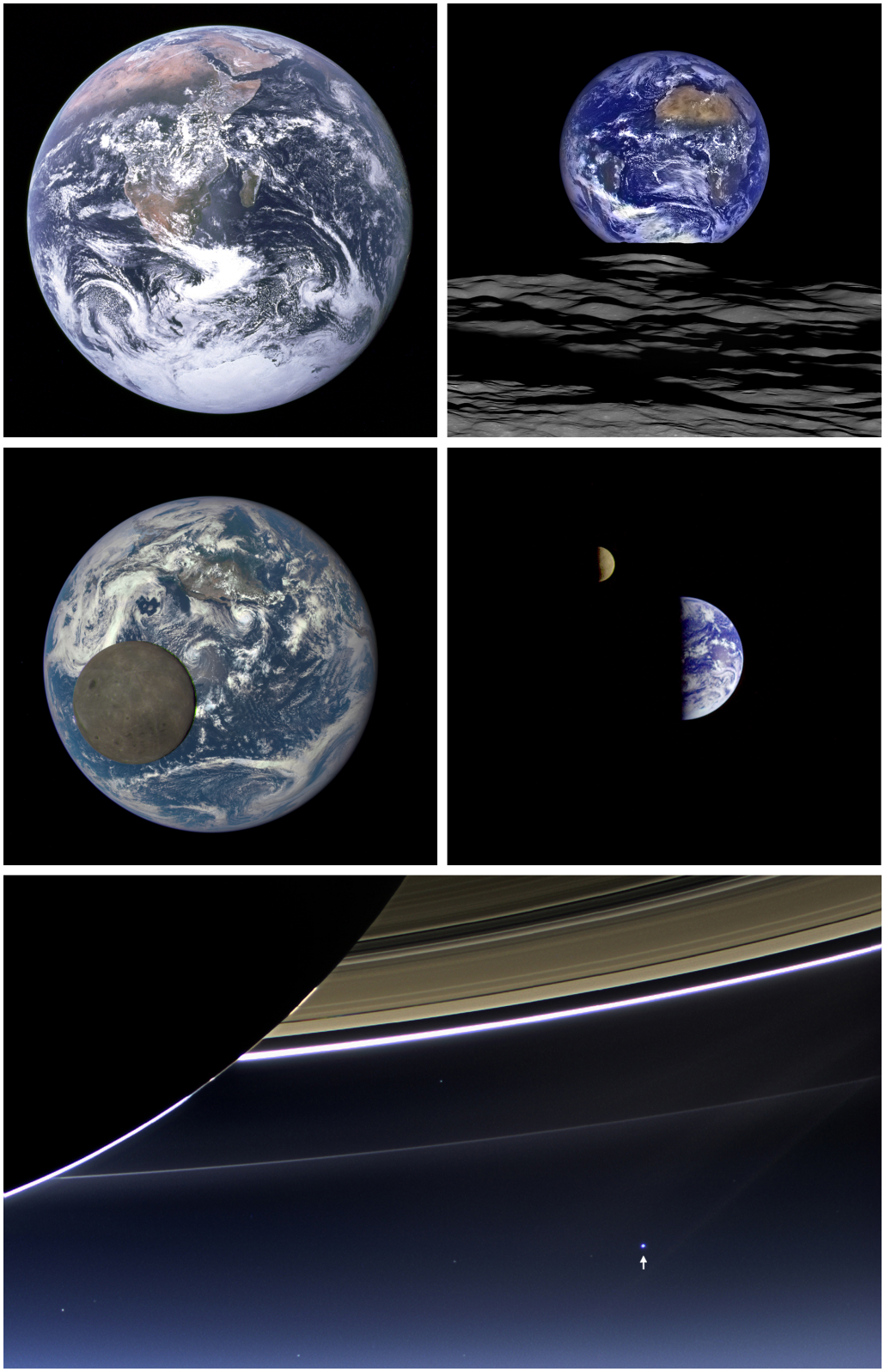

Figure G.1:
NASA image compilation of earth and moon in the solar system.

Bibliography

Articles

[1] B. P. Abbott et al. “Gravitational Waves and Gamma-Rays from a Binary Neutron Star Merger: GW170817 and GRB 170817A”. In: *The Astrophysical Journal Letters* 848:L13 (Oct. 2017). DOI: 10.3847/2041-8213/aa920c (cited on pages 9, 23, 30, 71, 76).

[2] N. Ashby. “Relativity in the Global Positioning System”. In: *Living Review Relativity* 6 (2003). DOI: 10.12942/lrr-2003-1 (cited on page 87).

[3] J. Bobin, Sureau F., and Starck J. L. “Cosmic microwave background reconstruction from WMAP and Planck PR2 data”. In: *Astronomy & Astrophysics* 591 (July 2016). DOI: 10.1051/0004-6361/201527822 (cited on pages 48, 57).

[4] S. Capozziello et al. “Relativistic orbits with gravitomagnetic corrections”. In: *Physica Scripta* 79.2 (2019). DOI: 10.1088/0031-8949/79/02/025901 (cited on pages 19, 37, 61, 63, 70, 97).

[5] J. L. Cervantes-Cota, S. Galindo-Uribarri, and G. F. Smoot. “A Brief History of Gravitational Waves”. In: *Universe* 2 (3 2016). DOI: 10.3390/universe2030022 (cited on page 71).

[6] S.D. Cheng et al. “Self-assembling behavior and interface structure in vertically aligned nanocomposite (Pr05Ba05MnO3)1-x:(CeO2)x films on (001)(La,Sr)(Al,Ta)O3 substrates”. In: *Sci Rep 10* 2348 (2020). DOI: 10.1038/s41598-020-59166-1 (cited on page 10).

[7] F. Combley and F. J. M. Farley. “g - 2 Experiments as a Test of Special Relativity”. In: *Physical Review Letters* 42.21 (1979), pages 1383–1385. DOI: 10.1103/PhysRevLett.42.1383 (cited on page 87).

[8] T. Damour. “1974: the discovery of the first binary pulsar”. In: *Classical and Quantum Gravity* 32.12 (June 2015). DOI: 10.1088/0264-9381/32/12/124009 (cited on page 71).

[9] H Dodig. “Direct derivation of Liénard Wiechert potentials, Maxwell’s equations and Lorentz force from Coulomb’s law”. In: *Mathematics 9, no3:237* (Jan. 2021). DOI: 10.3390/math9030237 (cited on pages 30, 81).

[10] A. S. Eddington. “The propagation of gravitational waves”. In: *Proceedings of the royal society A* 108 (1922), pages 268–282. DOI: 10.1098/rspa.1922.0085 (cited on pages 71, 74).

[11] A. Einstein. “Über Gravitationswellen”. In: *Sitzungsber.Preuss.Akad.Wiss.Berlin (Math.Phys.)* (Feb. 1918), pages 154–167. URL: https://adsabs.harvard.edu/pdf/1918SPAW.....154E (cited on pages 71, 74).

[12] F. R. Ellis. “Cosmology and Local Physics”. In: *New Astronomy Reviews* 46 (11 2002), pages 645–657. DOI: 10.1016/S1387-6473(02)00234-8 (cited on pages 22, 89).

[13] J. v. Engelshoven. “Study on Inertia as a Gravity Induced Property of Mass, in an Infinite Hubble Expanding Universe”. In: *Advances in Mathematical Physics* 2013.52 (Mar. 2013), pages 1–17. DOI: 10.1155/2013/801574 (cited on pages 9, 45).

[14] J. Evans et al. “Matter waves in a gravitational field: An index of refraction for massive particles in general relativity”. In: *American Journal of Physics* 69 1103 (2001). DOI: 10.1119/1.1389281 (cited on page 34).

[15] F. de Felice. “On the gravitational field acting as an optical medium”. In: *General Relativity and Graviation* 2.4 (1971), pages 347–357. DOI: 10.1007/BF00758153 (cited on page 34).

[16] G. Feng and J. Huang. “A geometric optics method for calculating light propagation in gravitational fields”. In: *Optik* 194 (Oct. 2019), page 163082. ISSN: 0030-4026. DOI: 10.1016/j.ijleo.2019.163082 (cited on page 34).

[17] D.E. Gatzia and R.D. Raimsler. “Dimensionality, symmetry and the inverse square law”. In: *Notes and Records* 75 (2020), pages 334–348. DOI: 10.1098/rsnr.2019.0044 (cited on page 13).

[18] J. Giné. “On the Origin of the Inertial Force and Gravitation”. In: *Int J Theoretical Physics 50* 2 (2011), pages 607–617. DOI: 10.1007/s10773-010-0581-1 (cited on pages 45, 46, 55).

[19] O. Heaviside. “A gravitational and electromagnetic analogy, Part 1”. In: *The Electrician* 31 (1893) (cited on pages 71, 97).

[20] R. C. Hilborn. “Gravitational waves from orbiting binaries without general relativity”. In: *American Journal of Physics* 86 (3 Mar. 2018), pages 186–197. DOI: 10.1119/1.5020984 (cited on page 71).

[21] L. Iorio. “Editorial for the Special Issue 100 Years of Chronogeometrodynamics: The Status of the Einstein’s Theory of Gravitation in Its Centennial Year”. In: *Universe* 1 (2015), pages 38–81. DOI: 10.3390/universe1010038 (cited on page 23).

[22] G. M. Koczan. “New definitions of 3D acceleration and inertial mass not violating F=MA in the Special Relativity”. In: *Results in Physics* 24 104121 (2021). DOI: 10.1016/j.rinp.2021.104121 (cited on pages 49, 60).

[23] S. M. Kopeikin. “Gravitomagnetism and the speed of gravity”. In: *International Journal of Modern Physics D* 15.3 (2006), pages 305–320. DOI: 10.1142/S0218271806007663 (cited on pages 19, 70).

[24] L. Lerner. “A simple calculation of the deflection of light in a Schwarzschild gravitational field”. In: *Am. Journ. of Physics* 65 (1997), pages 1194–1195. DOI: 10.1119/1.18757 (cited on page 36).

[25] LIGO. “The basic physics of the binary black hole merger GW150914”. In: *Annalen der Physik* 529 (Oct. 2016). DOI: 10.1002/andp.201600209 (cited on pages 71, 76).

[26] L. M. Lubin and A. Sandage. “The Tolman Surface Brightness Test for the Reality of the Expansion. IV. A Measurement of the Tolman Signal and the Luminosity Evolution of Early-Type Galaxies”. In: *The Astronomical Journal* 122 (3 2001), pages 1084–1103. DOI: 10.1086/322134 (cited on page 89).

[27] G. O. Ludwig. “Extended gravitoelectromagnetism. I. Variational formulation”. In: *The European Physical Journal Plus* 136 (2021). DOI: 10.1140/epjp/s13360-021-01367-2 (cited on page 97).

[28] G. O. Ludwig. “Extended gravitoelectromagnetism. II. Metric perturbation”. In: *The European Physical Journal Plus* 136 (2021). DOI: 10.1140/epjp/s13360-021-01452-6 (cited on page 97).

[29] H. Mutuk. “Cornell Potential: A Neural Network Approach”. In: *Advances in High Energy Physics* 2019 (2019), pages 347–357. DOI: 10.1155/2019/3105373 (cited on page 40).

[30] L. B. Okun. “The concept of mass”. In: *Sov. Phys. Usp.* 7 (1989), page 629. DOI: 10.1070/PU1989v032n07ABEH002739 (cited on pages 11, 49).

[31] B. Pandey and S. Sarkar. "Testing homogeneity of the galaxy distribution in the SDSS using Renyi entropy". In: *Journal of Cosmology and Astroparticle Physics* (July 2021). DOI: 10.1088/1475-7516/2021/07/019 (cited on pages 22, 51, 52, 86, 99).

[32] J. Pasha et al. "The Bullseye: HST, Keck/KCWI, and Dragonfly Characterization of a Giant Nine-ringed Galaxy". In: *The Astrophysical Journal Letters*, 980.1 (2025). DOI: 10.3847/2041-8213/ad9f5c (cited on page 88).

[33] F. Renzi, N. B. Hogg, and W. Giarè. "The resilience of the Etherington–Hubble relation". In: *Monthly Notices of the Royal Astronomical Society* 153 (3 2022), pages 4004–4014. DOI: 10.1093/mnras/stac1030 (cited on page 89).

[34] F. Rocha, M. Malheiro, and R. jr Marinho. "On some Aspects of Gravitomagnetism and Correction for Perihelion Advance". In: *Journal of Physics: Conference Series: XIII International Workshop on Hadron Physics* 706 (2016), pages 204–205. DOI: 10.1088/1742-6596/706/5/052014 (cited on page 97).

[35] S. Roy and A. Sen. "Study of gravitational deflection of light ray". In: *Journal of Physics: Conference Series* 1330 (Oct. 2019), page 012002. DOI: 10.1088/1742-6596/1330/1/012002 (cited on page 34).

[36] M. L. Ruggiero and D. Astesiano. "A tale of analogies: a review on gravitomagnetic effects, rotating sources, observers and all that". In: *Journal of Physics Communications* 7.11 (2023). DOI: 10.1088/2399-6528/ad08cf (cited on pages 19, 97).

[37] D. W. Sciama. "On the origin of inertia". In: *Monthly Notices of the Royal Astronomical Society* 113 (1953), pages 34–39. DOI: 10.1093/mnras/113.1.34 (cited on pages 10, 45, 46, 48, 97).

[38] I. I. Shapiro et al. "Fourth Test of General Relativity". In: *Physical Review Letters* 26.18 (May 1971), pages 1132–1135. DOI: 10.1103/PhysRevLett.26.1132 (cited on pages 33, 35).

[39] D. N. Spergel. "First Year Wilkinson Microwave Anisotropy Probe (WMAP) Observations: Determination of Cosmological Parameters". In: *The Astrophysical Journal* 148 (2003), page 175. DOI: 10.1086/377226 (cited on pages 22, 48, 57, 82, 96).

[40] H. Thirring. "Über die formale Analogie zwischen den elektromagnetischen Grundgleichungen und den Einsteinschen Gravitationsgleichungen erster Näherung". Translated by D. H. Delphenich. In: *Physikalische Zeitschrift, Leipzig* 19 (1918), pages 204–205 (cited on pages 19, 70).

[41] K. .S Thorne and T. .M. Will. "Theoretical frameworks for testing relativistic gravity. I. Foundations". In: *The Astrophysical Journal* 163 (1971), pages 595–610. DOI: 10.1086/150803 (cited on page 87).

[42] R. Tolman. "On the estimation of distances in a curved universe with a non static line element". In: *Proc. Natl. Acad. Sci.* 16 (1930), pages 511–520 (cited on page 89).

[43] P. Touboul et al. "MICROSCOPE Mission: First Results of a Space Test of the Equivalence Principle". In: *Physical Review Letters, American Physical Society* 119 (23) (2017), pages 231101-1 - 231101–7. DOI: 10.1103/PhysRevLett.119.231101 (cited on page 52).

[44] T. Treu, P. J. Marshall, and D. Clowe. "Resource Letter GL-1: Gravitational Lensing". In: *American Journal of Physics* 80 (2012), pages 753–763. DOI: 10.1119/1.4726204 (cited on page 33).

[45] A.A. Ungar. "Einstein velocity addition law and its hyperbolic geometry". In: *Int. Journal of Computers and Mathematics* 53 (2017), pages 1228–1250. DOI: 10.1016/j.camwa.2006.05.028 (cited on page 20).

[46] E. Verlinde. “On the origin of gravity and the laws of Newton”. In: *J. High Energ. Phys.* 29 (2011). DOI: 10.1007/JHEP04(2011)029 (cited on page 23).

[47] A. Yahalom. “The Weak Field Approximation of General Relativity and the Problem of Precession of the Perihelion for Mercury”. In: *Symmetry* 15 (1 2023). DOI: 10.3390/sym15010039 (cited on page 82).

Books

[48] M. Bartelmann. *General Relativity*. Heidelberg University Publishing, 2019. ISBN: 978-3-947732-59-3. URL: https://heiup.uni-heidelberg.de/catalog/book/534 (cited on pages 19, 33, 34, 36, 46, 70, 85).

[49] M. Born and E. Wolf. *Principles of Optics*. Cambridge Universtiy Press, 2019. ISBN: 978-1-108-47743-7 (cited on pages 34, 37, 81).

[50] A. S. Eddington. *Report on the Relativity Theory of Gravitation*. Minkowski Institue Press, 1920. ISBN: 978-1-927763-28-5 (cited on page 34).

[51] A. S. Eddington. *Space Time and Gravitation*. Cambridge Universtiy Press, 1920. ISBN: 978-1505496451 (cited on page 34).

[52] A. S. Eddington. *The Mathematical Theory of Relativity*. Cambridge Universtiy Press, 1923. ISBN: 978-0-521-09165-7 (cited on pages 33, 63).

[53] A. Einstein et al. *The principle of relativity [compilation of original articles]*. Dover Publications Inc., 1952. ISBN: 0-486-60081-5 (cited on pages 9–11, 15, 19, 20, 23, 32, 33, 46, 49, 51, 57, 70, 85).

[54] R. Feynman, R. B. Lighton, and M. Sands. *The Feynman Lectures on Physics, Volume I: Mechanics, Radiation & Heat*. Cambridge University Press, 1963. ISBN: 978-0-465-02493-3 (cited on page 37).

[55] N. Graneau and P. Graneau. *In the grip of the distant universe*. 1st. World Scientific Publishing Co. Pte. Ltd., 2006. ISBN: 981-256-754-2 (cited on page 45).

[56] D. A. Greenwood and W. N. Cottingham. *An introduction to: the Standard Model of Particle Physics, 2nd ed.* 2nd. Cambridge Universtiy Press, 2012. ISBN: 978-0-521-85249-4 (cited on pages 9, 12, 13, 23, 24, 81).

[57] D. J. Griffiths. *Introduction to quantum mechanics*. Prentice Hall Inc., 1995. ISBN: 0-13-124405-1 (cited on pages 9, 12, 13, 24, 39).

[58] D. J. Griffiths. *Introduction to Electrodynamics*. 4th. Pearson Education Inc., 2013. ISBN: 13: 978-0-321-85656-2 (cited on pages 14, 19, 71, 73, 74, 103).

[59] S. Hawking. *A brief history of time*. Bantam Books, 1998. ISBN: 978-0-553-10374-8 (cited on pages 23, 57).

[60] E. Hecht. *Optics*. Pearson Eductaion Ltd., 2017. ISBN: 978-1-292-09693-3 (cited on pages 37, 81).

[61] D. D. Holm. *Geometrical Mechanics*. Cambridge Universtiy Press, 2011. ISBN: 978-1848167759 (cited on page 34).

[62] M. Janssen. *’No success, like failure.’ : Einstein’s quest for General Relativity, 1907-1920*. Edited by J. Janssen and C. Lehner. Cambridge University Press, 2012, pages 167–227. ISBN: 9780521828345. DOI: 10.1017/CCO9781139024525.008 (cited on page 85).

[63] E. Kilényi. *The Eötvös experiment in its historic context*. 1st. Hungarian academy of sciences, 2019. ISBN: 978-615-5084-71-3. URL: https://real-eod.mtak.hu/8266/2/E%C3%B6tv%C3%B6s_experiment_internet.pdf (cited on pages 49, 50, 52).

[64] L. D. Landau and E. M. Lifshitz. *The Classical Theory of Fields - Vol. 2*. 4th. Elseviers, 2007. ISBN: 978-0-7506-2768-9 (cited on pages 14, 16, 19, 24, 46, 49, 50, 71, 72, 74, 76, 81).

[65] A. N. Lasenby, G. Efstathiou, and M. P. Hobson. *General Relativity*. 4th. Cambridge University Press, 2011. ISBN: 13-978-0-521-82951-9 (cited on pages 10, 11, 19, 23, 33, 35, 36, 46, 48, 49, 56, 63, 68–70, 76, 82, 96).

[66] D. F. Lawden. *Introduction to Tensor calculus, relativity and cosmology*. 3rd. Dover Publications, 2002. ISBN: 13.987-0-486-42540-5 (cited on pages 33, 45, 49, 63, 69, 85).

[67] W. Lowrie. *Fundamentals of Geophysics*. Cambridge Universtiy Press, 2007. ISBN: 0-521-85902-6. URL: https://www.academia.edu/31591629/Lowrie_Fundamentals_of_Geophysics (cited on page 9).

[68] C. W. Misner, Thorne K. S., and Wheeler J. A. *Gravitation*. W.H. Freeman and co., 1973-2017. ISBN: 07167-0334-3 (cited on pages 10, 22, 23, 33, 35, 36, 60, 63, 70, 71, 82, 87, 89, 97).

[69] R. K. Pathria. *The Theory of Relativity*. 2nd. Dover Publications, 2003. ISBN: 0-486-42819-2 (cited on pages 9–11, 14, 16, 19, 22–24, 33, 36, 45, 46, 49, 50, 53, 56, 57, 60, 63, 68, 72, 73, 76, 81, 85).

[70] W. Rindler. *Relativity*. 2nd. Oxford University Press, 2006. ISBN: 0-978-0-19-856732-5 (cited on pages 11, 19, 22, 33, 36, 37, 45, 46, 48–50, 55–57, 60, 61, 63, 68–70, 76, 82, 85, 87, 96).

[71] B. Ryden. *Introduction to Cosmology*. 1st. Addison-Wesley, 2003. ISBN: 10: 0805389121 (cited on page 57).

[72] D. W. Sicama. *The unity of the universe*. 1st edition: 1959. Dover Publications, 2009. ISBN: 978-0486472058 (cited on pages 22, 89).

[73] T. Suksumram. *Computational Mathematics and Variational Analysis; The Isometry Group of n-Dimensional Einstein Gyrogroup*. 2020, pages 505–512. ISBN: 978-3-030-44624-6. DOI: 10.1007/978-3-030-44625-3_26 (cited on page 20).

[74] J. D. Wells. *Discovery beyond the Standard Model of Elementary Particle Physics*. Springer, 2019. ISBN: 978-3030382056 (cited on pages 9, 12, 13, 23, 24).

Online

[75] M. Will Clifford. *Newtonian orbital dynamics*. University of Florida. 2013. URL: http://www.phys.ufl.edu/~cmw/Gravity-Lectures/Chapter%203.pdf (cited on page 61).

[76] G. Eichmann. *Low-energy QCD phenomenology*. University of Lisbon, Centre for Theoretical Particle Physics. 2020. URL: http://cftp.ist.utl.pt/~gernot.eichmann/2020-QCDHP/QCD-quark-models.pdf (cited on page 40).

[77] ESA. *Planck mission*. 2013. URL: https://www.cosmos.esa.int/web/planck (cited on page 22).

[78] ESO. *Orbits of stars around black hole at the heart of the Milky Way*. 2018. DOI: 10.1051/0004-6361/201833718. URL: https://www.eso.org/public/images/eso1825d/ (cited on page 59).

[79] F. Gleisner. *Three solutions to the twobody problem*. 2013. URL: https://www.diva-portal.org/smash/get/diva2:630427/FULLTEXT01.pdf (cited on page 62).

[80] R. E. Haskell. *Special Relativity and Maxwell's Equations*. Oakland University. 2003. URL: http://richardhaskell.com/files/Special%20Relativity%20and%20Maxwells%20Equations.pdf (cited on page 15).

[81] J. Henry. *Newton and Action at a Distance*. Oxford Handbooks online. 2019. DOI: 10.1093/oxfordhb/9780199930418.013.17 (cited on page 10).

[82] T. Idema. *Mechanics and Relativity*. TU Delft. 2018. DOI: https://doi.org/10.5074/t.2018.002. URL: https://textbooks.open.tudelft.nl/textbooks/catalog/book/14 (cited on page 61).

[83] A. Laschka. *Dissertation: Quark-Antiquark Potentials from QCD and Quarkonium Spectroscopy*. Technical University Munich. 2012. URL: https://mediatum.ub.tum.de/doc/1121280/1121280.pdf (cited on page 40).

[84] G. O. Ludwig. *Extended gravitoelectromagnetism. III. Mercury's perihelion advance*. Instituto Nacional de Pesquisas Espaciais. 2020. URL: http://urlib.net/8JMKD3MGP3W34R/43QQMGL (cited on page 97).

[85] *Mathematica SW*. URL: https://www.wolfram.com/mathematica/ (cited on pages 16, 17, 25, 26, 41, 48, 49, 64, 73, 76, 91, 93, 95, 100).

[86] F. Muheim. *QCD — Quantum Chromodynamics*. University of Edinburgh, School of Physics and Astronomy. 2006. URL: https://www2.ph.ed.ac.uk/~muheim/teaching/np3/lect-qcd.pdf (cited on page 40).

[87] R. Narayan and M. Bartelmann. *Lectures on Gravitational Lensing*. 1996. URL: https://arxiv.org/abs/astro-ph/9606001 (cited on page 34).

[88] NASA. *Hubble telescope mission*. 1999. URL: https://science.nasa.gov/mission/hubble/ (cited on page 22).

[89] NASA. *Wilkinson Microwave Anisotropy Probe*. 2014. URL: https://map.gsfc.nasa.gov/ (cited on pages 22, 48, 57, 82, 96).

[90] NASA. *James Webb telescope mission*. 2022. URL: https://webb.nasa.gov/ (cited on pages 6, 22, 38, 52, 58, 84, 94).

[91] The Image Team NASA. *Age & size of the universe, through the years*. 2025. URL: https://imagine.gsfc.nasa.gov/educators/programs/cosmictimes/educators/guide/age_size.html (cited on page 22).

[92] NIST. *Atomic weight isotopes*. 2014. URL: https://physics.nist.gov/cgi-bin/Compositions/stand_alone.pl (cited on pages 28, 39, 44).

[93] Nobel Prize Committee. *Nobel Prize Physics 1979: unified weak and electromagnetic interaction*. 1979. URL: https://www.nobelprize.org/prizes/physics/1979/summary/ (cited on pages 9, 23).

[94] Nobel Prize Committee. *Nobel Prize Physics 2011: accelerating universe*. 2011. URL: https://www.nobelprize.org/prizes/physics/2011/press-release/ (cited on page 49).

[95] Y. Pierseaux. *Tolman's Luminosity-Distance, Poincare's Light-Distance and Cayley-Klein's Hyperbolic Distance*. Université Libre de Bruxelles, Brussels, Belgium. 2009. URL: https://arxiv.org/abs/0907.4882 (cited on page 89).

[96] G. L. Pimentel. *Inflation: theory and observations*. 2022. URL: https://arxiv.org/abs/2203.08128 (cited on pages 49, 82).

[97] T. Potter. *QCD: Particle and Nuclear Physics*. Universtiy of Cambridge, High Energy Physics. 2021. URL: https://www.hep.phy.cam.ac.uk/~chpotter/particleandnuclearphysics/Lecture_07_QCD.pdf (cited on page 40).

[98] Bureau International des Poids et Mesures SI. *The international system of units*. Bureau International des Poids et Mesures. 2024. URL: https://www.bipm.org/documents/20126/41483022/SI-Brochure-9-EN.pdf (cited on page 103).

[99] G. F. Smoot. *Relativity*. Smoot group, Astrophysics and Cosmology, Lawrence Berkeley National Lab. 2003. URL: https://aether.lbl.gov/www/classes/p139/homework/eight.pdf (cited on page 86).

[100] *solution to Griffiths 11.24 : quadrupole radiation*. URL: https://www.physicsisbeautiful.com/resources/introduction-to-electrodynamics/problems/11.24/solutions/11.24.pdf/QVbZGoskQqd4j3wPyEsq8K/ (cited on page 71).

[101] Y. Y. Songsheng. *Solution Manual for Gravitation (MTW)*. Institute of High Energy Physics, Chinese Academy of Sciences. 2019. URL: https://dokumen.pub/solution-manual-for-gravitation-mtw-0716703440-9780716703440-9780691177793-9780716703341-9789570911336-9784621083277.html (cited on page 70).

[102] *The two body problem - PHYS103*. University of California, Santa Barbara. 2023. URL: https://web.physics.ucsb.edu/~fratus/phys103/LN/TBP.pdf (cited on page 62).

[103] Wikipedia. *Equivalence principle*. 2022. URL: https://en.wikipedia.org/wiki/Equivalence_principle (cited on page 52).

[104] Wikipedia. *Relativistic Mechanics*. 2022. URL: https://en.wikipedia.org/wiki/Relativistic_mechanics (cited on pages 49, 60).

[105] Wikipedia. *Newtonian limit of General Relativity*. 2024. URL: https://en.wikipedia.org/wiki/Newtonian_limit (cited on page 36).

[106] Wikipedia. *Timeline of longest spaceflights*. 2024. URL: https://en.wikipedia.org/wiki/Timeline_of_longest_spaceflights (cited on page 87).

[107] Wikipedia. *Eötvös experiments*. 2025. URL: https://en.wikipedia.org/wiki/E%C3%B6tv%C3%B6s%20experiment (cited on page 100).

[108] Wikipedia. *List of most distant astronomical objects*. 2025. URL: https://en.wikipedia.org/wiki/List_of_the_most_distant_astronomical_objects (cited on page 100).

[109] Wikipedia. *Two-body problem*. 2025. URL: https://en.wikipedia.org/wiki/Two-body_problem (cited on page 62).

Figure G.2:
The star cluster NGC 602 is a birthplace for new stars.
We hope this book will stimulate the birth of new ideas in phyisics.
(image by NASA/ESA)

Index

O

P

Q

R

S

T

V

W

J. van Engelshoven ⋆ ⋆ ⋆ FORCES IN PHYSICS 2025

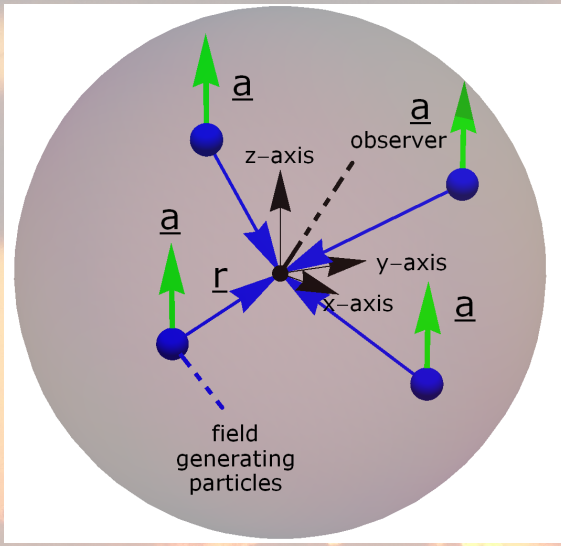

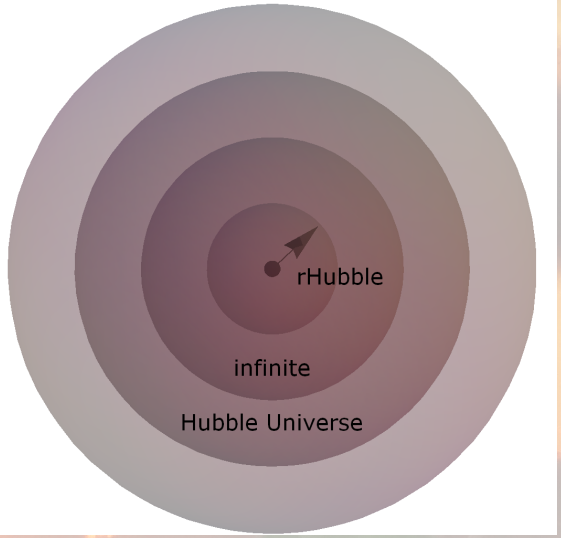

This book contains some thoughts on the origins of
gravity and **inertia**.

Based on equality of the speed of light and gravity, arguments are sought to derive gravity from electro-dynamical forces as created by the moving quarks in the nucleus: quark-gravity.

Based on suggestions by D.W. Sciama, the origin of inertia is found in gravity, including the relativistic mass increase with velocity. An infinite, Hubble expanding universe with flat space-time is found to yield finite inertia.

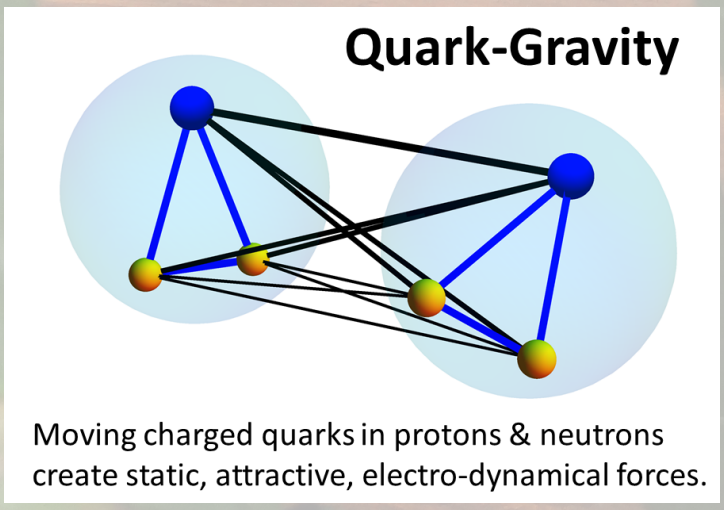

ISBN 978-989-33-7619-5